

**The recognition of lipopolysaccharides present
in Gram-negative bacteria by receptors of
the immune system**



Bander Ali Husni Khayyat

A thesis submitted for the degree of PhD in Molecular Medicine

School of Biological Sciences

University of Essex

October 2018

Acknowledgment

In the name of Allah, the Most Gracious and the Most Merciful, the peace and blessing of Allah be upon Prophet Mohammed, his family and companions. Alhamdulillah, all praises to Allah for the strengths and His blessing in completing this thesis.

I pay my gratitude to my guide, Prof. Nelson Fernández for providing the necessary infrastructure and resources to accomplish my research work. This work would not have been perfected without his guidance, support and encouragement. Under his guidance, I successfully overcame many difficulties and learned a lot. He used to review my thesis progress, give his valuable suggestions. His unflinching courage and conviction will always inspire me.

At this Juncture I think of my parents for their great efforts and unceasing prayers which enabled me to reach the present position in life. I want to express my deepest gratitude to my wife Dr. Wafa Beheiri and my sons Omar, Anas, Haitham and lovely daughter Dana for their love, understanding and their continuous support.

I thank all those who have helped me directly or indirectly in the successful completion of my thesis, Dr. Metodiev, Dr. Kamaran Karim, Dr. Alsadh, Dr. Alabdulmonem and all colleagues in the Biological department at The University of Essex. Special thanks to the Saudi Ministry of Health for the valuable opportunity. Again, I would like to thank everyone who supported and helped me during my Ph.D. study.



Abstract

Invasive bacterial infections cause severe systemic complications including a life-threatening condition known as septic shock. Sepsis results in a dysregulated systemic inflammatory immune response with systemic consequences. The function of the immune system requires efficient communication between immune cells and this is achieved partly through specific cell surface receptors, some of which are involved in bacterial recognition. One virulent pathogen that binds cell surface receptors and triggers immune cells to overproduce pro-inflammatory cytokines is gram-negative bacteria. This pathogen is covered with lipopolysaccharides (LPS), which are recognized by macrophages through the cluster of differentiation receptor 14 (CD14). CD14 functions with the co-receptor known as Toll-like receptor 4 (TLR-4), which in the presence of an accessory receptor known as myeloid differentiation 2 (MD-2) triggers immunity against gram-negative bacteria. Experiments were designed to investigate the effect of purified exogenous LPS on the expression of CD14 and TLR-4 and cytokines IL-1 β and TNF- α . In order to mimic *in vivo* responses against LPS an *in vitro* cellular model based on THP-1, a continuous cell line, was used. The cell model resembles macrophage-like cells and was previously isolated from a patient suffering from myelomonocytic leukemia. The central hypothesis for testing in this study was that blocking CD14, TLR-4 and MD-2 binding sites expressed on THP-1 cells would impair secretion of IL-1 β and TNF- α , this was indeed observed. From a mechanistic point of view, and using an improved confocal bioimaging technique it was observed that physical proximity and co-localization of CD14, TLR-4, MD2, and HMGB1 generates a receptor complex that is most likely part of the functional activation of macrophages. Future studies employing macrophages isolated from normal donors and patients suffering from septic shock would validate and yield information on the medical significance of these findings.

Table of Contents

Acknowledgment	I
Abstract	II
Table of Contents.....	III
List of tables	XI
Abbreviations	XII
1 Introduction.....	2
1.1 Immunity	2
1.2 Macrophages	3
1.3 Lipopolysaccharide (LPS).....	5
1.4 Septic shock.....	7
1.5 CD14	7
1.6 TLR-4 and MD2	8
1.7 HMGB1	10
1.8 PARP inhibitors PJ34	12
1.9 TNF α	12
1.10 IL-1 β	13
1.11 Aims of study.....	14
Chapter 2 Materials and Methods	15
2 Materials and Methods	16
2.1 Materials	16
2.1.1 Chemicals	16
2.1.2 Antibodies used.....	16
2.1.2.1 Primary Antibody.....	16
2.1.2.2 Secondary Antibody.....	16

2.1.3 Cell line	17
2.2 Methods	17
2.2.1 Cell cultures	17
2.2.2 Cryopreservation of THP-1 Cells.....	19
2.2.3 Cell viability test	19
2.2.4 Cells stimulations by LPS	19
2.2.5 THP-1 cells Differentiation	19
2.2.6 Flowcytometry	20
2.2.6.1 Experiment method	20
2.2.6.2 Antibodies concentration.....	21
2.2.7 Laser scanning confocal microscopy	21
2.2.7.1 Advantages of Confocal laser microscopy	21
2.2.7.2 Co-localisation analysis	21
2.2.7.3 Experimental Protocol	23
2.2.7.4 Image acquisition.....	25
2.2.7.5 Image processing	26
2.2.8 Preparation of total protein	27
2.2.8.1 Bradford assay	27
2.2.9 Two-Dimensional gel electrophoresis.....	28
2.2.9.1 Preparation of cell lysate	28
2.2.9.2 First dimensional gel isoelectric focusing (IEF).....	29
2.2.9.3 SDS-PAGE gel preparation.....	30
2.2.9.4 Equilibration of the IPG strips	30
2.2.9.5 Assembly and running of second dimensional gel	31
2.2.9.6 Silver staining.....	33
2.2.9.7 Gel image capture and spot analysis	33

2.2.10	Enzyme-linked immunosorbent assays (ELISA)	34
2.2.10.1	Principles of ELISA.....	34
2.2.10.2	Experimental setup.....	34
3	The interaction between CD14 and TLR-4 in presence and absence of myeloid differentiation 2 (MD2) and inhibitor PARP PJ34	37
3.1	The interaction between CD14 and TLR-4 in presence and absence of inhibitor PARP PJ34.....	37
3.1.1	Introduction.....	37
3.1.2	Antibodies concentration.....	37
3.1.3	Results	38
3.2	The Importance of myeloid differentiation MD2 to the expression of CD14 and TLR-4 in presence and absence of inhibitor PARP PJ34.	47
3.2.1	Introduction.....	47
3.2.2	Results	47
3.2.3	Conclusions	52
4	Detection of the Importance of myeloid differentiation MD2 and the effective of PARP inhibitor PJ34.....	54
4.1	Two-Dimensional gel electrophoresis to detect the Importance of myeloid differentiation MD2 and the inhibitor PARP PJ34.....	54
4.1.1	Introduction.....	54
4.1.2	Preparation of cell lysate.....	54
4.1.3	First dimensional gel isoelectric focusing.....	55
4.1.4	SDS-PAGE Gel preparation.....	55
4.1.5	Second dimensional gel running and staining.....	56
4.1.6	Gel image scan and analysis	57
4.1.7	Conclusions	69
5	Co-localisation study by using laser confocal microscope.....	71

5.1 The importance of MD2 detected by Bioimaging by confocal microscopy.....	71
5.1.1 Introduction.....	71
5.1.2 Results	72
5.2 Co-localisation of TLR-4 and MD2 with HMGB1 on the cell-surface of THP-1 cells.....	76
5.2.1 Introduction	76
5.2.2 Results.....	76
5.3 Conclusions	86
6 TNF-α and IL-1β Detection by Enzyme-linked immunosorbent assays (ELISA).....	89
6.1 Introduction.....	89
6.2 Materials and methods	90
6.3 Results	90
6.4 Conclusions	108
7 General Discussion.....	112
Reference.....	117
Appendix	126
A.1 Chemicals	126

Table of figure

<i>Figure 1-1: THP-1 cells Images by X40 light microscope.....</i>	<i>4</i>
<i>Figure 1-2: The schematic structure of LPS.....</i>	<i>6</i>
<i>Figure 1-3: Schematic of the signaling pathway when the lipopolysaccharides (LPS) detected by membrane receptor the Cluster of differentiation 14 (CD14) and interact with the receptors complex known as tool like receptor 4 (TLR-4) and myeloid differentiation 2 (MD-2).....</i>	<i>9</i>
<i>Figure 1-4: HMGB1 released from cells via multiple pathways.</i>	<i>11</i>
<i>Figure 2-1: THP-1 cells Images by X40 light microscope.....</i>	<i>18</i>
<i>Figure 3-1: The proper concentration of the CD14 and TLR-4 antibodies required to be used in flowcytometer experiment.</i>	<i>39</i>
<i>Figure 3-2: The proper concentration of the MD2 antibody.</i>	<i>40</i>
<i>Figure 3-3: The expression of CD14 in THP-1 cell lines in 2 hours stimulation with LPS and PJ34.</i>	<i>41</i>
<i>Figure 3-4: The expression of CD14 in THP-1 cell lines in 6 hours stimulation with LPS and PJ34.</i>	<i>42</i>
<i>Figure 3-5: The expression of CD14 in THP-1 cell lines in 24 hours stimulation with LPS and PJ34.</i>	<i>43</i>
<i>Figure 3-6: The expression of TLR-4 in THP-1 cell lines in 2 hours stimulation with LPS and PJ34.</i>	<i>44</i>
<i>Figure 3-7: The expression of TLR-4 in THP-1 cell lines in 6 hours stimulation with LPS and PJ34.</i>	<i>45</i>
<i>Figure 3-8: The expression of TLR-4 in THP-1 cell lines in 24 hours stimulation with LPS and PJ34.</i>	<i>46</i>
<i>Figure 3-9: The expression of CD14 in differentiated THP-1 cell lines when stimulated with LPS for 2 hours and treated by PJ34 and block the MD2.</i>	<i>48</i>
<i>Figure 3-10: The expression of TLR-4 in differentiated THP-1 cell lines when stimulated with LPS for 2 hours and treated by PJ34 and block the MD2.</i>	<i>49</i>
<i>Figure 3-11: The expression of CD14 in non-differentiated THP-1 cell lines when stimulated with LPS for 2 hours and treated by PJ34 and block the MD2.</i>	<i>50</i>

Figure 3-12: The expression of TLR-4 in non-differentiated THP-1 cell lines when stimulated with LPS for 2 hours and treated by PJ34 and block the MD2.	51
Figure 4-1: Two Dimensional gel images for twelve different conditions.	58
Figure 4-2 : The images for 3D spot graph analysed by Progenesis SameSpot software.	59
Figure 4-3 : 3D spot graph analysis using Progenesis SamSpot software.	61
Figure 4-4 : Representative 2D gel images of total cell proteins from THP-1 cells untreated and treated with PJ34 stimulate the cells by rough (EH100) and smooth (055:B5) lipopolysaccharides (LPS).	62
Figure 4-5 : The SamSpot software indicates the protein spots on gels marked by Progenesis SamSpot software as shown in numbers.	63
Figure 4-6 : 3D spot graph analysis using Progenesis SamSpot software.	64
Figure 4-7 : 3D spot graph analysis using Progenesis SamSpot software.	65
Figure 4-8 : 3D spot graph analysis using Progenesis SamSpot software.	66
Figure 4-9 : 3D spot graph analysis using Progenesis SamSpot software.	67
Figure 5-1A: Co-localisation of CD14 and TLR-4 on the THP-1 cell-surface, examined by confocal laser scanning microscopy.	73
Figure 5-2: Co-localisation analysis of CD14 and TLR-4 by Pearson's coefficient correlation using a scatter plot on THP-1 Cells.	75
Figure 5-3:Co-localisation of (a)MD2 and HMGB1 and (b)TLR-4 and HMGB1 on the cell-surface of THP-1 cells for 30 min stimulation with rough EH100 and smooth 055:B5 LPS.	77
Figure 5-4: Co-localisation of MD2 and HMGB1 on the cell-surface of THP-1 cells for 30 min stimulation with rough EH100 and smooth 055:B5 LPS.	78
Figure 5-5: Co-localisation of TLR-4 and HMGB1 on the cell-surface of THP-1 cells for 30 min stimulation with rough EH100 and smooth 055:B5 LPS.	79
Figure 5-6:Co-localisation of (a) MD2 and HMGB1 and (b) TLR-4 and HMGB1 on the cell-surface of THP-1 cells for 60 min stimulation with rough EH100 and smooth 055:B5 LPS.	80

Figure 5-7: Co-localisation of MD2 and HMGB1 on the cell-surface of THP-1 cells for 60 min stimulation with rough EH100 and smooth O55:B5 LPS.....	81
Figure 5-8: Co-localisation of TLR-4 and HMGB1 on the cell-surface of THP-1 cells for 60 min stimulation with rough EH100 and smooth O55:B5 LPS.....	82
Figure 5-9: Co-localisation of (a) MD2 and HMGB1 and (b)TLR-4 and HMGB1 on the cell-surface of THP-1 cells for 120 min stimulation with rough EH100 and smooth O55:B5 LPS.	83
Figure 5-10: Co-localisation of MD2 and HMGB1 on the cell-surface of THP-1 cells for 120 min stimulation with rough EH100 and smooth O55:B5 LPS.....	84
Figure 5-11: Co-localisation between TLR-4 and HMGB1 on the cell-surface of THP-1 cells for 120 min stimulation with rough EH100 and smooth O55:B5 LPS.	85
Figure 6-1: TNF-α level in differentiated and non-differentiated THP-1 in presence and absence of (MD2), also presence and PJ34, then stimulated with rough (EH100) and smooth (O55:B5) LPS for four hours.	92
Figure 6-2: TNF-α level in differentiated and non-differentiated THP-1 in presence and absence of PJ34 (a) and presence and absence of (MD2) (b) then stimulated with rough (EH100) and smooth (O55:B5) LPS for four hours.	93
Figure 6-3 : TNF-α level in differentiated THP-1 when TLR-4 was blocked then stimulated with (EH100) LPS (a) and stimulated with (O55:B5) (b) LPS for 30, 60, and 120 minutes.	94
Figure 6-4 : TNF-α level in differentiated THP-1 when MD2 was blocked then stimulated with (EH100) LPS (a) and stimulated with (O55:B5) LPS (b) for 30, 60, and 120 minutes.	95
Figure 6-5 : TNF-α level in differentiated THP-1 when TLR-4 and MD2 were blocked then (a)stimulated with rough LPS EH100 and (b) stimulated with smooth LPS O55:B5 for 30, 60, and 120 minutes.	96
Figure 6-6 : TNF-α level in differentiated THP-1 when TLR-4 and MD2 were blocked then (a) stimulated with EH100 and (b) stimulated with O55:B5 for 30, 60, and 120 minutes.	97
Figure 6-7: TNF-α level in differentiated and non-differentiated THP-1 cells in presence and absence of (MD2), also presence and PJ34, then stimulated with (EH100) (O55:B5) LPS for two hours.	98

Figure 6-8 : TNF-α level in differentiated and non-differentiated THP-1 in presence and absence of PJ34 then stimulated with EH100 and 055:B5 LPSs for two hours.	99
Figure 6-9: TNF-α level in differentiated and non-differentiated THP-1 cells in presence and absence of (MD2), then stimulated with EH100 and O55:B5 LPS for two hours.	100
Figure 6-10: IL-1β level in differentiated and non-differentiated THP-1 cells in presence and absence of (MD2), and (PJ34), then stimulated with EH100 and O55:B5 LPS for two hours.	101
Figure 6-11: IL-1β level in differentiated and non-differentiated THP-1 cells in presence and absence of (MD2), and (PJ34), then stimulated with EH100 and O55:B5 LPS for four hours.	102
Figure 6-12: The effect of PJ-34 on IL-1β secretion by non-differentiated and PMA differentiated THP-1 cells in presence and absence of MD2 by response to E. coli rough EH100 and smooth 055:B5 LPS.	103
Figure 6-13: The effect of PJ-34 on IL-1β secretion by non-differentiated and PMA differentiated THP-1 cells in presence and absence of MD2 by response to E. coli rough EH100 and smooth 055:B5 LPSs.	104
Figure 6-14: IL-1β level in differentiated and non-differentiated THP-1 cells in presence and absence of PJ34, then stimulated with EH100 and O55:B5 LPSs for two and four hours.	105
Figure 6-15: IL-1β level in differentiated and non-differentiated THP-1 cells in presence and absence of MD2, then stimulated with (EH100) (O55:B5) LPS for two and four hours.	106
Figure 6-16: IL-1β level in differentiated and non-differentiated THP-1 cells in presence and absence of (MD2), also presence and PJ34, then stimulated with EH100 and O55:B5 LPSs for two and four hours.	107
Figure A1: Extracellular and intracellular expression of CD14 in THP-1 cell lines.	127
Figure A2 : Extracellular and intracellular expression of TLR-4 in THP-1 cell lines.	128
Figure A3 : TNF-α Detection by (ELISA).....	129
Figure A4 : IL-1β Detection by (ELISA).....	129

Figure A5: ELISA micro plate reader	129
Figure A6 : NIKON Confocal laser microscope A1.....	129
Figure A7 : Accuri C6 Flowcytometer	129
Figure A8 BIO-RAD PROTEAN II System	129
Figure A9 : 2D gel preparation for electrophoresis system	129
Figure A 10 : Place the gels on the glass of Epson image scanner III.	129
Figure A11 : Sensitivity of instant blue and silver nitrate for the detection of 2-D gel separated polypeptide spots.....	129
Figure A12 : General Electric Healthcare Bio-sciences AB. Ettan IPG Phor3	129
Figure A 13 : Kinds of pipettes used in this study.	129

List of tables

Table 4-1: the table represent a comparison of the number of spots by Prognosis sameSpot software.....	60
Table 4-2: The 3D proteins spots analysed by the IP and molecular weight information by using expasy website, https://uniprot.org/uniprot/	68

Abbreviations

Ab	Antibody
Ag	Antigen
BSA	Bovine Serum Albumin
CD	Cluster of Differentiation
CD14	Cluster of differentiation 14
DAPI	4', 6'-diamino-2-phenylindole, dihydrochloride
DMSO	Dimethyl Sulphide
DTT	Dithiothreitol
Eliza	Enzyme-linked immunosorbent assays
FCS	Foetal Calf Serum
FITC	Fluorescein Isothiocyanate
FSC	Forward scatter channel
HMGB1	High Mobility Group Box 1
IgG	Immunoglobulin G
IL-1 β	Interlukin-1 β
KDa	Kilo Daltons
LBP	Lipopolysaccharide binding protein
LPS	Lipopolysaccharide
mCD14	Membrane cluster of differentiation 14

MD2	Myeloid Differentiation-2
MW	Molecular weight
NF- κ B	Nuclear factor kappa-light-chain-enhancer of activated B cells
NK	Natural killer
PBS	Phosphate Buffered Saline
PFA	Paraformaldehyde
PMA	Phorbol Mercyacetate Acetate
RPMI	Roswell Park Memorial Institute medium (RPMI-1640)
sCD14	Soluble cluster of differentiation 14
sd	Standard deviation
SDS	Sodium Dodecyl Sulfate
THP-1	A human monocytic cell line
TLR-4	Toll like Receptor 4
TNF- α	Tumor necrosis factor-alpha
Tween 20	Polyoxyethylene Sorbitan Monolaurat

Chapter 1 Introduction

1 Introduction

1.1 Immunity

The immune system is divided into two main parts known as innate and adaptive response systems. They are determined by speed, memory and specificity of the reaction, even though in practice there is much association between them (Crotzer and Blum, 2010; Shibutani *et al.*, 2015). The physical, chemical and microbiological barriers are usually referred to as innate immunity. However, specifically innate immunity consists of the basic elements of the immune system (neutrophils, monocytes, macrophages, complements, cytokines and acute phase proteins), which present instant host defence and protection against pathogens. Innate response is termed as the nature of the response since it can be seen even in the simplest animals. Therefore it verifies its crucial role in survival. In contrast, adaptive immunity is considered as the hallmark of the immune system of human beings and animals. The adaptive response consists of T-lymphocytes and B-lymphocytes, which are produced through antigen specific reactions. The innate immunity is quick to respond however, it can cause damage to normal cells and tissues due to the lack of specificity. Instead, adaptive immunity takes several days or even weeks to show a response, but it is highly specific. Furthermore, the adaptive immunity is highly distinct because it has memory cells and consequently, subsequent exposure leads to more various and rapid responses even though it is not immediate (Parkin and Cohen, 2001; Abbas Abul K. *et al* 2014; McMaster *et al.*, 2015; Agita and Alsagaff, 2017).

1.2 Macrophages

Innate immunity, considered as a first line of defence against microbial infectious, it depends on particular cells such as macrophages that are the first to meet pathogens during infection. Additionally, they also function in standard physiological processes, such as in the maintenance of tissue homeostasis. Macrophages are presented in several tissues, and mainly in those that function in the filtration of blood stream or lymph fluids, such as liver, spleen, lung, and lymph nodes. They differentiate between self and non-self-molecules, they affect, and destroy harmful endogenous and exogenous molecules. Macrophages have been shown to be able to bind pathogens directly, or they recognise them foreign after being coated with antibodies or complement. Macrophages express a range of germ line-encoded pattern-recognition receptors (PRRs), which can directly recognise pathogen-associated molecular patterns (PAMPs), include a variety of bacterial cell-wall components, such as lipoteichoic acid, lipopolysaccharide (LPS), and peptidoglycans. Many of these components are able to stimulate the innate immune system and the best-known example in this research is LPS. (Aderem and Ulevitch, 2000; Mukherjee, Karmakar and Babu, 2016; Cao *et al.*, 2018) The THP-1 cells differentiated by 5 ng of PMA to become macrophage-like cells, as a mature cells has the receptors on the cell surface ready to define the LPSs.

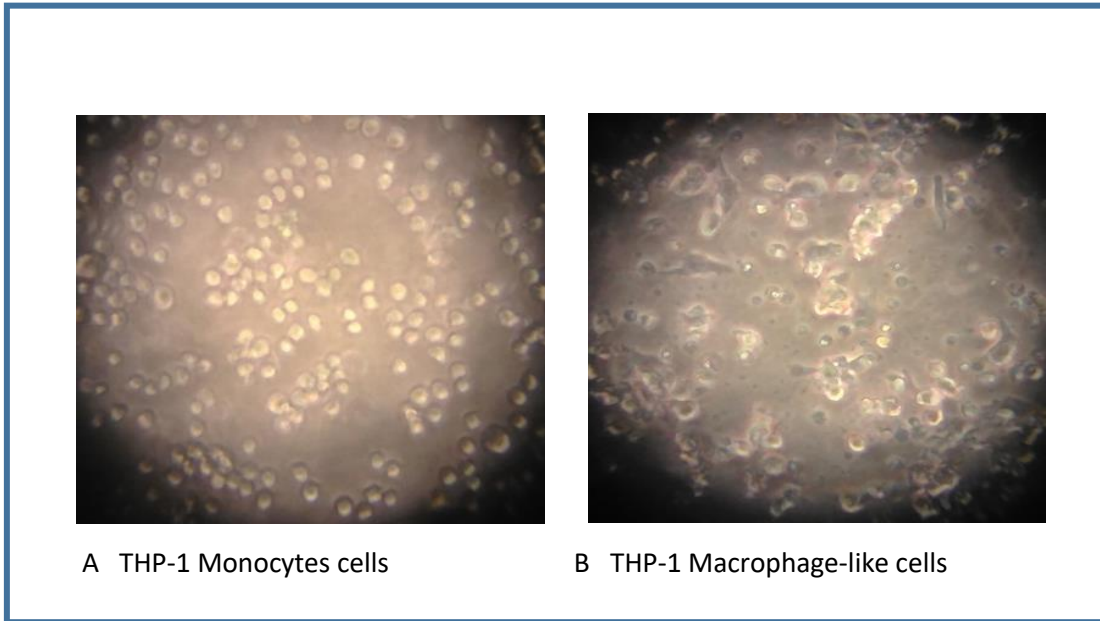


Figure 1-1: THP-1 cells Images by X40 light microscope

(A) THP-1 cells, (B) Differentiated THP-1 cells by using 5ng PMA to be macrophage-like cells. (Khayyat, B. 2015, BS, Essex University)

1.3 Lipopolysaccharide (LPS)

Gram-negative bacteria cells contain several types of LPS which release on the length of their polysaccharides. The polysaccharide core is parted into three molecules, the inner core, the outer core and O-antigen polysaccharide groups. The whole LPS named smooth LPSs. Typical LPS core structures for enteric bacterial LPSs contain from eight to twelve sugars, and the sugar at the end is always linked to the glucosamine of lipid A. Other sugars present in the core, such as glucose, galactose, and their derivatives (Caroff and Karibian, 2003; Steimle, Autenrieth and Frick, 2016).

Rough-chemotype LPSs are transformed LPS molecules are named using the size of the polysaccharide domain, from the longest as Ra, Rb, Rc, Rd, and Re correspond to the first, second, third, fourth, and fifth levels of polysaccharide chain length so by reducing domain size (Wilkinson, 1996; Anwar and Choi, 2014) We can get several rough mutants that leave LPS missing the various components of polysaccharide group (LPS-Ra to Re) by blocking steps in the LPS simulated pathway such as E. coli LPS known as LPS-Re includes lipid A linking two keto-deoxyoctulosonate (Kdo) residues (Figure 1-2). Generally, rough mutants are more sensitive to antibiotics, mutagens and detergent. They are also less infectious and more susceptible to recognition by the body immune system (Wang and Quinn, 2010; Steimle, Autenrieth and Frick, 2016). Most LPS studies to date have focused on two main facts, the structure behavior of LPS-containing membranes and interactions of LPS with relevant components of the immune system.

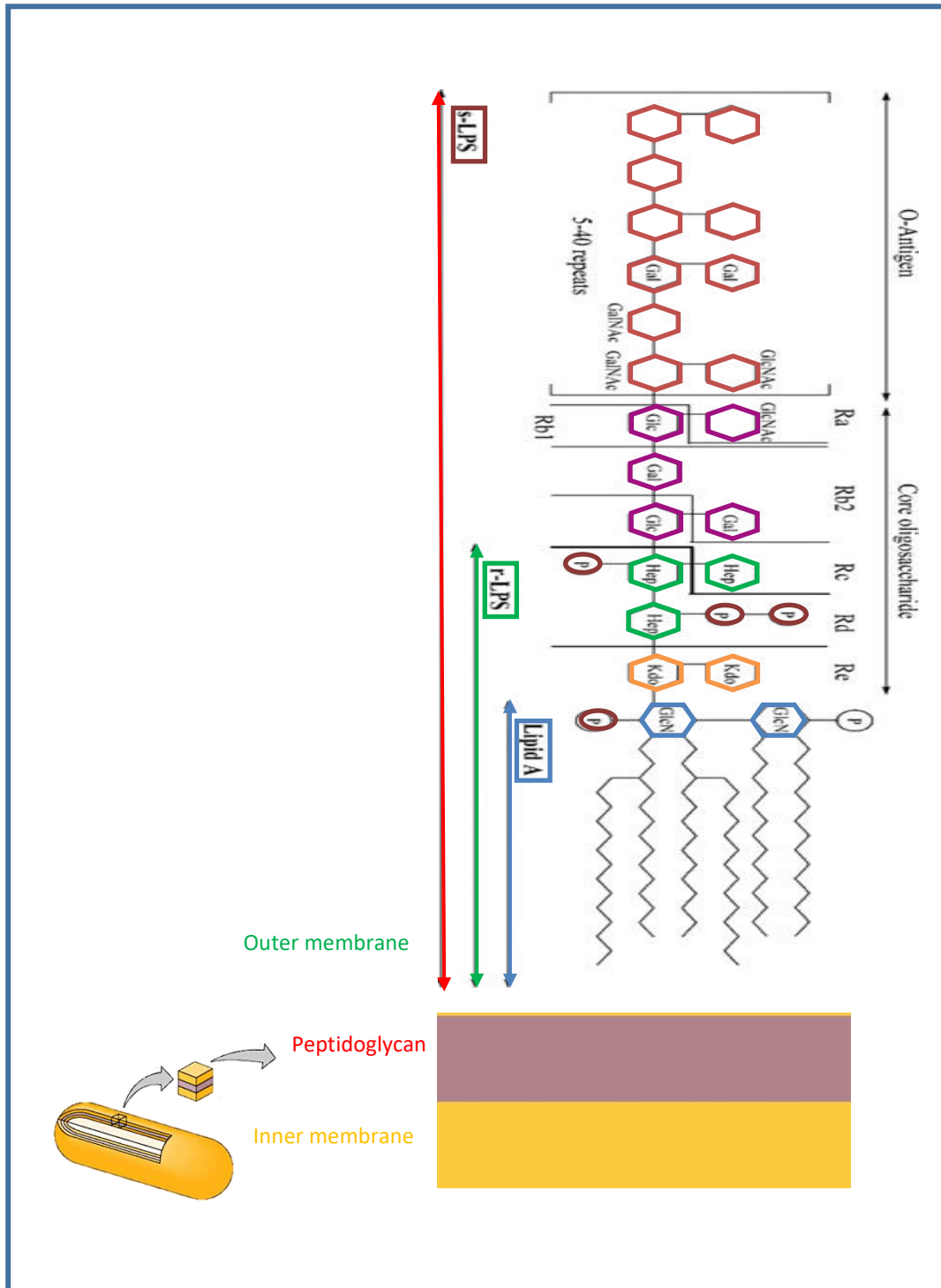


Figure 1-2: The schematic structure of LPS.

LPS is composed of three main parts: The O-antigen, the core and Lipid A, which interacts with epitopes of CD14, contains two acylated GlcNAc-P residues (GlcN). The core part consists of KDO, heptoses and galactose. The O-antigen made of repeating units of two to eight sugars.

(Source from <https://www.memorangapp.com/flashcards/73237/Microbiology>)

1.4 Septic shock

Septic shock, the most severe complication of sepsis, is a deadly disease. In the last few years, exciting advances have been made in the understanding of its pathophysiology and treatment. Pathogens, through their microbial-associated molecular patterns, activate following intracellular events in immune cells, epithelium, endothelium, and the neuroendocrine system. Proinflammatory mediators that contribute to eradication of attacking microorganisms are produced, and anti-inflammatory mediators control this response. The inflammatory response leads to damage to host tissue, and the anti-inflammatory response causes leucocyte reprogramming and changes in immunity (Schlapbach *et al.*, 2015)

The time-window for involvements is short, and treatment must promptly control the source of infection and restore haemodynamic homoeostasis. Further research is required to begin which drugs are the best. Some patients with septic shock might recovered by using medications such as corticosteroids, or activated protein C. Other therapeutic strategies are under investigation, including those that target late proinflammatory mediators, endothelium, or the neuroendocrine system (Annane, Bellissant and Cavaillon, 2005; Cecconi *et al.*, 2018).

1.5 CD14

Cluster of differentiation 14 (CD14) is a human gene.(Setoguchi *et al.*, 1989; Laganowsky *et al.*, 2014). The protein encoded by this gene is a component of the innate immune system. CD14 exists in two forms, one anchored to the membrane by a glycosylphosphatidylinositol tail (mCD14), the other is a soluble form (sCD14). CD14 acts as a co-receptor (along with the Toll-like receptor TLR 4 and MD-2) for the detection of bacterial lipopolysaccharide (LPS) (Kitchens, 2000). CD14 can bind LPS only in the presence of lipopolysaccharide-binding protein (LBP). Although LPS is

considered its main ligand, CD14 also recognizes other pathogen-associated molecular patterns such as lipoteichoic acid (Tapping, R., 2000; Stasi *et al.*, 2017).

1.6 TLR-4 and MD2

Toll-like receptors (TLRs) are a class of proteins that play a key role in the innate immune system. They are single, membrane-spanning, non-catalytic receptors usually expressed in sentinel cells such as macrophages and dendritic cells, that recognise structurally conserved molecules derived from microbes. Once these microbes have breached physical barriers such as the skin or intestinal tract mucosa, they are recognised by TLRs, which activate immune cell responses. The presence of myeloid differentiation protein-2 (MD-2) makes up the LPS receptor complex involved in the cellular recognition of and signalling by LPS (Schumann *et al.*, 1990; Murdock and Núñez, 2016). Toll-like receptor 4 is a protein that in humans is encoded by the TLR4 gene. It detects lipopolysaccharide from Gram-negative bacteria and is thus important in the activation of the innate immune system (Rock *et al.*, 1998; Shimazu *et al.*, 1999; Lu, Yeh and Ohashi, 2008; Peri and Piazza, 2012). The protein encoded by this gene is a member of the Toll-like receptor (TLR) family, which plays a fundamental role in pathogen recognition and activation of innate immunity (Figure1-3). TLRs are highly conserved from *Drosophila* to humans and share structural and functional similarities. They recognise pathogen-associated molecular patterns (PAMPs) that are expressed on infectious agents, and mediate the production of cytokines necessary for the development of effective immunity. (Medzhitov and Janeway, 1997; Shiu and Gaspari, 2017). Toll-like receptor 4 (TLR4) is associated with CD14 in inflammatory response to LPS because TLR4 is trans-membrane receptor type 1 (Singh, B. P. Chauhan, R. S. and Singhal, 2003).

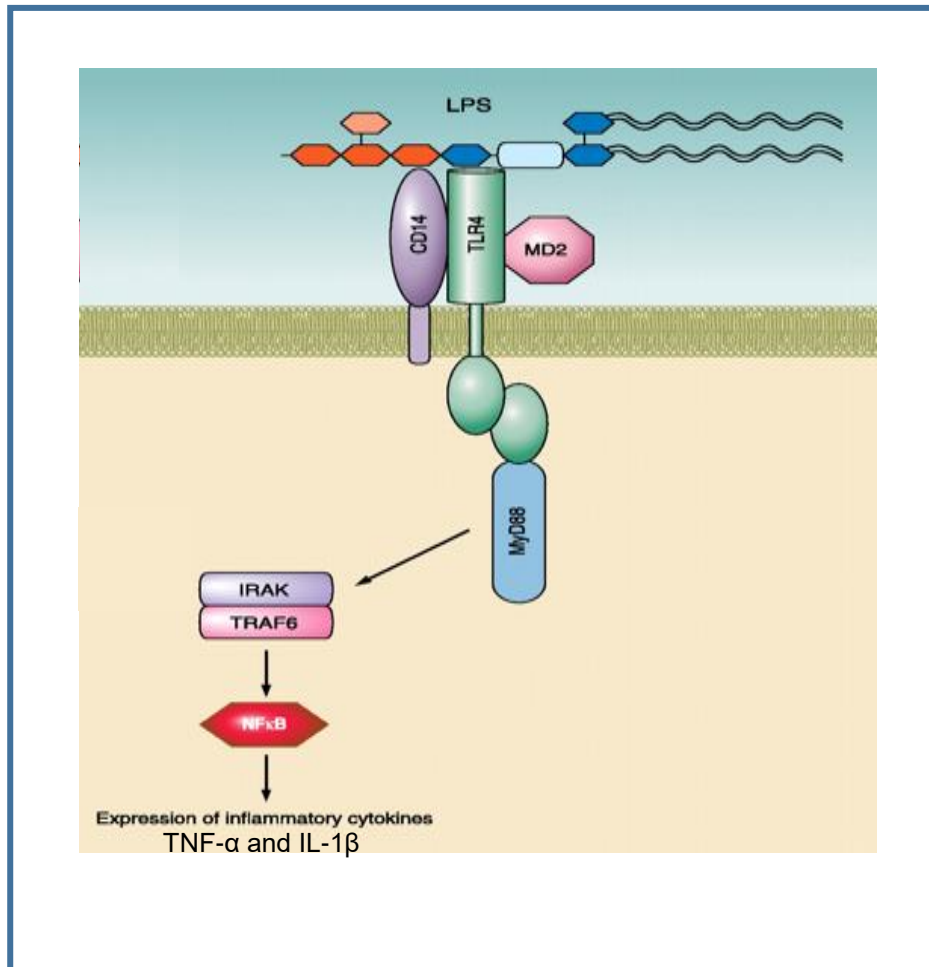


Figure 1-3: Schematic of the signaling pathway when the lipopolysaccharides (LPS) detected by membrane receptor the Cluster of differentiation 14 (CD14) and interact with the receptors complex known as tool like receptor 4 (TLR-4) and myeloid differentiation 2 (MD-2).

as shown that TLR-4 has an intracellular domain help to send the protein signals to the nuclear side to release the cytokines such as TNF-α and IL-1β.

(Source from <http://www.physiology.org/doi/abs/10.1152/physrev.00052.2009>)

1.7 HMGB1

High mobility group box 1 (HMGB1), released passively by injured or necrotic cells, acts as a pro-inflammatory cytokine and functions as a major stimulus of necrosis-induced inflammation (Scaffidi, P. *et al* 2002).

Bacterial endotoxin lipopolysaccharide (LPS) stimulates macrophages to sequentially release early tumour necrosis factor (TNF) and late HMGB1 pro-inflammatory cytokines (Chen, 2004; Zhang *et al.*, 2015). The delayed release of HMGB1 and its role as a late mediator in lethal systemic inflammation make it a potential therapeutic target. However, the molecular basis for HMGB1-induced cytokine signaling in macrophage/monocyte is poorly understood (Park *et al.*, 2004). Others have also shown that HMGB1 acts as a mediator in hepatic ischemia-reperfusion induced injury via a process that is TLR4 dependent (Tsung *et al.*, 2005; Hosakote *et al.*, 2016). However, we do not know whether TLR4 is involved in HMGB1 signaling independently or together. These points prompted us to investigate the role of TLR4 and MD2 in HMGB1 signaling in THP-1 cell lines (Figure 1-4).

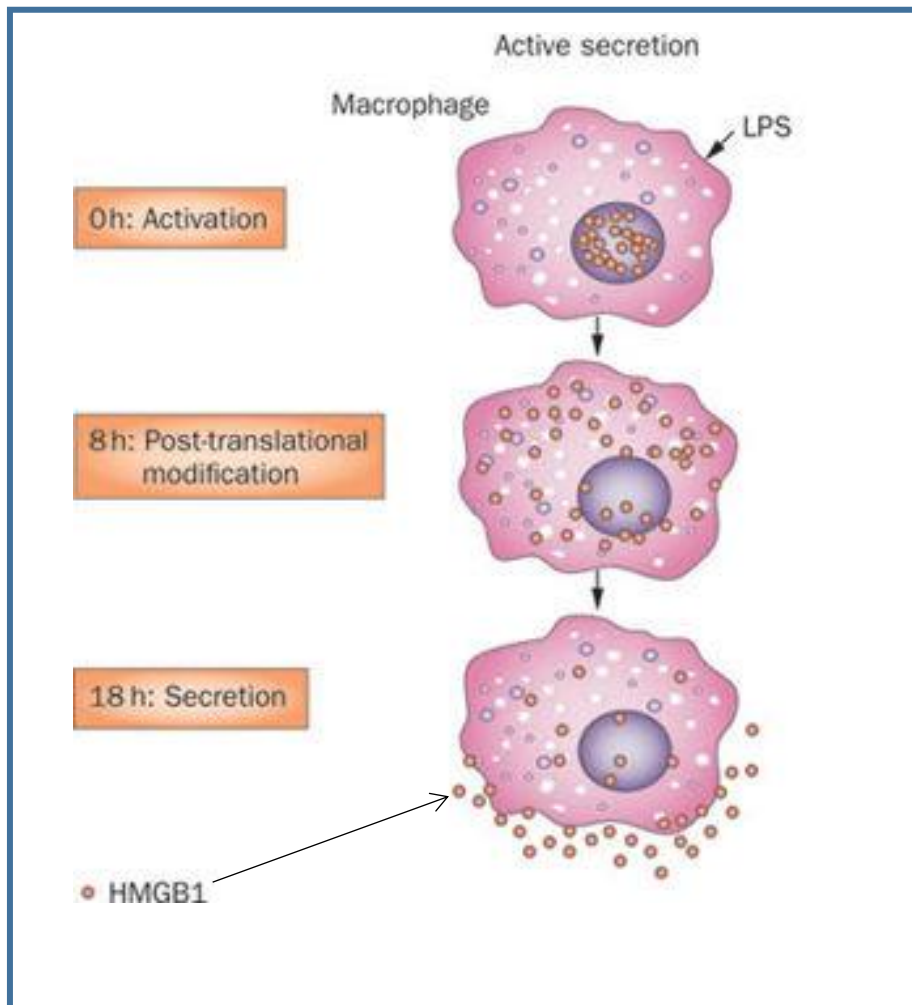


Figure 1-4: HMGB1 released from cells via multiple pathways.

This translocation can represent an active process in stimulated macrophages and is time-consuming, involving post-translational modification and eventual secretion. . During apoptosis, HMGB1 is initially retained in the nucleus but, during secondary necrosis, it can be released passively from apoptotic cells or cell fragments.(Harris *et al*, 2012)

1.8 PARP inhibitors PJ34

Scientific studies show that PARP inhibitors have anti-inflammatory effect. For example, PARP-1 plays a role in transcriptional control during CD14 activation, and identifying PARP-1 activity-dependent regulation of NF- κ B, is a novel pharmacological target in the better management of the treatment of inflammatory disorders (Szabo, 2002; Selleckchem, 2014). Evidence suggests that PARP-1-deficient mice were resistant to lethality induced by LPS, inhibitors of PARP-1 enzyme are promising tool for therapeutic intervention (Oliver *et al.*, 1999; Thorsell *et al.*, 2017). A specific PARP inhibitor, PJ34, based on a modified 6 (5H) phenanthridinone structure, increased endotoxic shock survival rate and had various anti-inflammatory effects in animal models of endotoxaemia (Scalia *et al.*, 2013). The explanation of the role of CD14 receptor – PARP enzyme correlations in innate immunity has contributed to a better molecular understanding of immunostimulatory, toxic septic processes and the pathology of atopic and Alzheimer's diseases, but has also re-activated the development of new pharmacological and immunostimulatory strategies for the prevention and therapy of infectious diseases. This research study was intended to improve our understanding of the role of innate immunity and CD14-PARP interactions in complex inflammatory diseases (Huang *et al.*, 2008; McCluskey *et al.*, 2012).

1.9 TNF α

Tumor necrosis factor alpha (TNF) is a pro-inflammatory cytokine that exhibits a wide range of biological effects. TNF is synthesised as a type II transmembrane protein (tmTNF). Upon stimulation, the TNF alpha-converting enzyme ADAM17 cleaves the extracellular domain of tmTNF, which releases the soluble TNF (sTNF). The newly

generated membrane-bound moiety of TNF is further cleaved within its intramembrane region by signal peptide peptidase-like 2b (SPPL2b), leading to the generation of an intracellular domain (ICD) of TNF. Soluble TNF signals through two distinct cell surface receptors, TNFR1 and TNFR2. Most of the biological activities of TNF are mediated through TNFR1. Upon binding to TNFR1, the ligand-bound receptor aggregates and serves as a scaffold to recruit adaptor proteins. The activated sub-membranous complex triggers cellular activation via NF κ B and mitogen-activated protein kinases or apoptosis via complex internalisation and activation of apical caspases (Poggi *et al.*, 2013; *Cytokine Frontiers*, 2014; Sedger and McDermott, 2014).

1.10 IL-1 β

IL-1 β is a member of the interleukin 1 family of cytokines. This cytokine is produced by activated macrophages as a protein, this cytokine is an important mediator of the inflammatory response, and is involved in a variety of cellular activities, including cell proliferation, differentiation, and apoptosis (NCBI, 2017). Interleukin-1 β is a pro-inflammatory cytokine that has been implicated in pain, inflammation and autoimmune conditions (Ren and Torres, 2009; Zhou *et al.*, 2014). IL-1 β known to play a role in organising the physiological changes that happen during sickness (Rachal Pugh *et al.*, 2001; Dantzer, 2004) Increased production of IL-1 β causes a number of different auto-inflammatory syndromes, most notably the monogenic conditions referred to as Cryopyrin-associated periodic syndrome (CAPS), due to mutations in the inflammasome receptor which triggers processing of IL-1 β (Masters *et al.*, 2009; LaRock *et al.*, 2016).

1.11 Aims of study

This study will address the effects of different chemotype of lipopolysaccharides to induce changes in the receptor profile and cytokine expression of THP-1 cells. This is highly relevant for understanding septic shock.

The investigation of the innate recognition receptors in LPS binding and the binding required additional proteins to induce LPS-mediated signalling such as CD14, TLR-4, MD2, and HMGB1. Using a combination of several techniques including ELISA, Flow-cytometry, confocal microscopy and proteomics.

It is hypothesised that the presence or absence of TLR-4 and MD2 will affect the signalling pathways when stimulated by rough and smooth LPS on the cytokines secretion such as TNF α and IL-1 β .

In addition, the effect of the PARP inhibitor (PJ34) on these pathways of the immune system and when stimulated by rough and smooth LPS will also be investigated.

Chapter 2 Materials and Methods

2 Materials and Methods

2.1 Materials

2.1.1 Chemicals

Chemicals used in this research include; cell culture media Roswell Park Memorial Institute medium (RPMI-1640) purchased from LONZA, Fetal Calf Serum (FCS) from Imperial Laboratories, England, Accutase from PAA, Piscataway, USA. In addition chemicals such as the endotoxins, Lipopolysaccharide (LPS) from *E. coli* serotype EH100 and 055:B5, Dimethyl Sulphide (DMSO), albumin from bovine serum, sodium carbonate, Chaps, TEMD, DDT and Iodoacetylamine, phorbol 12-myristate 13-acetate (PMA) PARP inhibitor PJ34 was purchased from Sigma Aldrich, UK. Mounting media hard set with DAPI was purchased from Victachem, UK, TNF α and IL-1 β for ELISA purchased from Ebioscience, UK. Tris Base, silver nitrate, Urea, and Glycine purchased from Fisher Scientific, UK. Acrylamide and agarose were purchased from Severn biotech, UK. IPG Buffer PH 4-7 and DeStreak, strip cover fluid purchased from GE healthcare. Immobilized pH Gradient strips (IPG) 18 cm, PH 4-7 purchased from BIORAD, UK. Instant Blue purchased from Expedition, UK.

2.1.2 Antibodies used

2.1.2.1 Primary Antibody

The vital primary antibodies used in this study include; Purified anti-human CD14 and TLR4 purchased from Biolegend, UK, Myeloid Differentiation 2 (MD2) purchased from Merck Millipore, California, US.

2.1.2.2 Secondary Antibody

Every technique has a different secondary antibody to be used, for flowcytometry technique, the antibody used is Goat anti-mouse FITC, purchased from Biolegend,

UK. In bioimaging, Alexa flour 488 (green) and Alexa flour 555 (red) Purchased from Invitrogen, UK, is applied in confocal microscopy.

2.1.3 Cell line

The main cell line, which was THP-1, used to show the significant levels of CD14 and TLR4, THP1 cells are human monocyte derived from patients with Acute Lymphocytic Leukaemia. Furthermore, we used RAJI cell line which is known as a human lymphoblastoid cells derived from a Burkitt lymphoma was used as a positive control. The cell lines were kindly provided by Professor Nelson Fernandez, Department of Biological Sciences, University of Essex, UK. Also, the cells were cultured in RPMI - 1640 medium, maintained at 37°C and 5% CO₂.

2.2 Methods

2.2.1 Cell cultures

The THP-1 cells were used to do the experiments was maintained at 37°C and 5% CO₂ in cell culture media Roswell Park Memorial Institute medium (RPMI 1640).

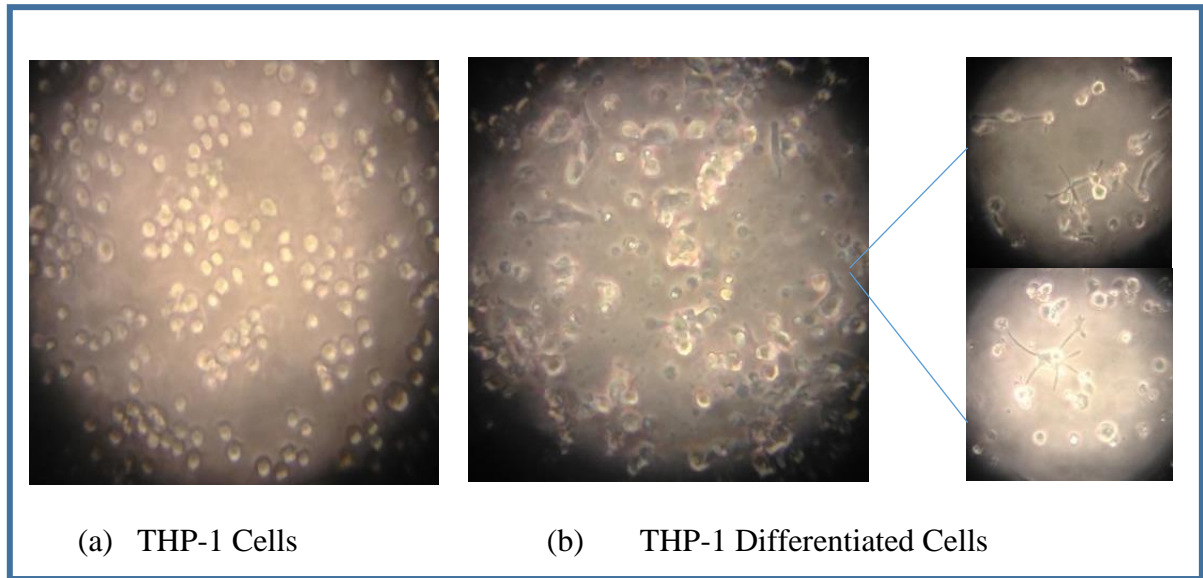


Figure 2-1: THP-1 cells Images by X40 light microscope.

(a) The THP-1 cells monocytes, (b) THP-1 differentiated cells, the cells treated by (PMA) 5 ng/ml to be to macrophage-like cells. (Khayyat, B. 2015, BS, Essex University)

2.2.2 Cryopreservation of THP-1 Cells

When the THP-1 cells were grown well and the amount become approximately 1×10^6 cells/ml, the cells were centrifuged, then prepare the freezing mixture (90% FCS and 10% Dimethyl Sulfoxide (DMSO)). Then cryotube were used by add 1 ml of the cells into each and were placed at -80°C freezer. Within 3 months should be reserved at (-196°C) in liquid nitrogen.

2.2.3 Cell viability test

The cells were washed with PBS. Applying Accutase treatment used to split the cells then the suspension was placed in a conical centrifuge tube. Then a cell suspension of 1:2 dilution in trypan blue. 10 μl of diluted cells suspension were loaded into both the haemocytometer chambers and cells were viewed under the microscope at 10x magnification. The Live cells would have the cell membranes undamaged and would reject the trypan blue dye. The dead and non-viable cells well get the dye.

2.2.4 Cells stimulations by LPS

THP-1 cells were cultured in RPMI-1640 with 10 % FCS, then stimulated with Rough (EH100) and Smooth (055:B5) LPSs at a concentration of 10 $\mu\text{g/ml}$ for period of 2, 6 and 24 hours depends on the experiments. Incubated at 37°C and 5% CO_2 . An experiments were done to approve, are the best time to stimulate the cells for 2, 6 and 24 hours for the Expression of CD14 and TLR4.

2.2.5 THP-1 cells Differentiation

To differentiate the THP-1 cells, phorbol 12-myristate 13-acetate (PMA) used in 5 ng/ml to become adhere cells which is macrophage-like cells which change the cell age to the mature with high level of receptors around the cell surface. The differentiated cells become ready after three days cultured in RPMI -1640 medium, at 37°C and 5% CO_2 (Figure 2-1).

2.2.6 Flowcytometry

Flowcytometry is a technique used to analyse and measure several properties of cells. The cells are technically tagged with a specific fluorescent probe, a fluorophore conjugated to an antibody. The cells are suspended in PBS, and the cells carrying fluid pass through a light beam. This technique use the principles of light scattering, light excitation, and the emission of fluorochrome molecules to generate specific multi-parameter data from cells. Three different parameters can be measured by photomultiplier tubes. These types of parameters are forward scatter (FSC), side scatter (SSC) and fluorescence (FL). The First advantage of the flowcytometer is the ability to evaluate a high population of cells accurately and quickly with semi quantitative results. This makes the flowcytometry technique the ideal tool for quantitative analysis of certain cellular properties, especially when the cells are a small fraction of other cell types in the cellular population. Isotype antibody was used as a negative control to evaluate the level of the positive results for other surface proteins in terms of the fluorescence intensity.

2.2.6.1 Experiment method

Untreated, LPS treated THP-1 cells and differentiated THP-1 cells were collected ($3 \times 10^5/\text{ml}$) to each sample and were washed with PBS prior to use in experiments. The cells were fixed with a 4% fixation buffer paraformaldehyde (PFA) for 20min on ice bath, the cells were then blocked with blocking buffer (0.1% BSA in PBS) to block non-specific antibody binding sites followed by washing step in PBS, All the samples were stained with suitable concentration of the anti CD14 and anti TLR4 as a primary antibody which incubated at 4°C for 60 min. The negative control (IgG1 and IgG2)

were applied to the specific samples. All samples were stained with the secondary antibody (FITC) and incubated at 4°C for 60 min, then washed by PBS to remove the extra amount of the secondary antibody and analysed using a BD Accuri 6.

2.2.6.2 Antibodies concentration

Antibodies supplied in tiny amounts, by micro litre contain nano grams (ng) of antibodies. We should deal with it in exact amount. So the first step to use them that find the proper concentration by titration experiment, which give the planned results. 1000 ng of CD14, 500 ng of TLR4 and 500 ng of MD2 were found the proper concentration of each antibodies.

2.2.7 Laser scanning confocal microscopy

2.2.7.1 Advantages of Confocal laser microscopy

Confocal laser scanning microscopy is a valuable technique that is able to produce high quality images resolution of very small objects and produce a 3D image of the cells. There are many features of confocal microscopy over the conventional microscope due to many factors; firstly the ability to control the depth of the field, secondly the reduction of background interference away from the focal plane and thirdly the ability to analyse serial sections of the cells.

2.2.7.2 Co-localisation analysis

Co-localisation analysis describes the presence of two or more types of molecules at the same physical location. Co-localisation of fluorescent signals from two or more different proteins is an indicator of their association and potential interaction. Within the context of a cell or sub-cellular protein, often the molecules are attached to the

same receptor, while in the context of digital imaging, the colours emitted by the fluorescent molecules occupy the same pixel in the image (Bolte and Cordelieres, 2006; Adler and Parmryd, 2010) Co-localisation does not refer to the likelihood that fluorochromes with similar emission spectra will appear as overlapped in the composite image. It is important to note that cross talk or “bleed-through” may occur if the emission spectra of the two fluorochromes are similar. Accurate co-localisation determination can only occur if emission spectra are sufficiently separated between fluorochromes and the correct filter sets were used during the acquisition step. To achieve this aim, red and green wavelengths are usually selected, and usually those dyes representing these wavelengths are carefully matched to the power spectrum of the illumination source to obtain maximum excitation wavelengths while still maintaining a degree of separation between the emission wavelengths.

Often, co-localisation is assessed qualitatively, for example by showing yellow areas as the overlap between dual colour fluorescence images from green and red channels. If quantitation is sought, global statistical methods to determine overlap on a pixel-per-pixel basis are commonly chosen. Measuring the co-localisation can be divided into two main methods: pixel-based and object-based. Pixel-based methods look at all pixels in an image and determine various correlations between the channels. Object-based methods first segment the images into objects, and then make some comparison between the objects in the channels (Bolte and Cordelieres, 2006; Adler and Parmryd, 2010) The Pearson correlation coefficient and Mander's overlap coefficient are the most common co-localisation measurement for pixel-based approaches. However, (Adler and Parmryd, 2010) have reported that the Pearson correlation coefficient (PCC) is superior to the Mander's overlap coefficient. The PCC is a well-established measure of correlation, originating with Galton in the

late 19th century but named after a colleague, and has range of -1 (perfect correlation) to $+1$ (perfect but negative correlation) with 0 denoting the absence of a relationship (Adler and Parmryd, 2010).

(Bolte and Cordelieres, 2006) also describe object-based approaches, which allow more spatial information to be inferred about co-localisation, helpful in determining in which subcellular compartments of the cell the stains may co-localise. Proper segmentation is very important in object-based methods, since different segmentations will give different co-localisation results. Pre-processing of the image, including filtering or illumination correction, may be necessary for proper segmentation. Once images have been properly segmented, the cells and subcellular compartments correctly identified in both channels, Bolte and Cordelieres (2006) described several methods by which to compare the co-localisation. The first was to compare the centroids of the identified objects and define co-localised objects as those whose centroids are within some specified distance (usually, less than the optical resolution of the microscope). Another method was to multiply the two channels by one another after pre-processing and then to segment the structures of interest; the result of the multiplication is composed of only pixels present in both channels. However, we applied segmentation using regional maximum detection tools followed by manual threshold. (Bolte and Cordelieres, 2006; Manders, 1997; Lachmanovich *et al.*, 2003; Rizk *et al.*, 2014; Solomon, 2017)

2.2.7.3 Experimental Protocol

Cell monolayer culture and double staining: THP-1 cell line were cultured in LabTek 8 well chambers (Thermo Fisher Scientific) at a density of 10×10^3 cells per well, or 20×10^4 cells per well cultured in 6 wells cell culture plate ready with square single

cover slips in each well, which was prepared previously with HCl and washed overnight under water stream, then ethanol 70% applied, then autoclaved at 140°C, in order to prepare the surface of the cover slips to grow the cells. Then the cells were differentiated by applying 5 ng/ml of (PMA). Afterwards, the cells were grown in RPMI 1640 supplemented with 10 % of FCS for 72 hours. For the staining procedure, all the steps were carried out at room temperature. The cells were fixed with 4% PFA (Sigma, UK) for 20 minutes on ice bath and blocked with 2% BSA (Bovine serum albumin) prepared in 1X PBS for 1 hr at room temperature. For staining, the cells were incubated with specific monoclonal antibody for 1 hr and washed three times with PBS. For the secondary antibody, anti-mouse IgG conjugated with Alexa Fluor 488 or Alexa Fluor 555 (Invitrogen, Carlsbad, CA, USA) was used for 1h. For double staining, cells were blocked again for 1h and stained with specific monoclonal antibody for 1 hr. Isotype controls were stained with only secondary antibody. Cells were then thoroughly washed and chambers were removed from the slide. Slides were rinsed in a beaker containing 1XPBS and dried. The cells were mounted with hard set mounting medium with DAPI and carefully covered with the cover slip (0.11 - 0.13 mm). Kept in the dark place at room temperature for 20-30 min until dry, and then vertically saved in slide box. Prepared slides were stored at 4°C in the dark for further analysis. The slides were then examined under a NIKON A1si laser confocal microscope using an X60 oil immersion objective (numerical aperture 1.4) and FITC filter for Alexa Fluor 488 and PE filter for Alexa Fluor 555. The images obtained were then analysed using NIS elements software (Jonkman, Brown and Cole, 2014; Kolodziejczyk *et al.*, 2015).

2.2.7.4 Image acquisition

For image acquisition, a Nikon A1si confocal microscope was used with X60 magnifying oil-immersion objective. Software used for image acquisition; NIS-Elements AR 4.13.01 (Build 916). Three-dimensional (3D) images were acquired in three channels, using one-way sequential line scans. DAPI was excited at 398.7 nm with laser power 1.6 arbitrary units, and its emission collected at 450 nm with a PMT gain of 86. Alexa Fluor 488 was excited at 488 nm with laser power 5.8, its emission collected at 525 nm with a PMT gain of 117. Alexa Fluor 555 was excited at 560.5 nm with laser power 3.7, and collected at 595 nm with a PMT gain of 98, the scan speed was $\frac{1}{4}$ frames/s (galvano scanner). The pinhole size was 35.76 μm , approximating 1.2 times the Airy disk size of the 1.4 numerical aperture (N.A) objective at 525 nm. Scanner zoom was centered on the optical axis and set to a lateral magnification of 60 nm/pixel. Axial step size was 105 nm, with 80-100 image planes per z-stack (Microscopy *et al.*, 2003).

For co-localisation study cell images were acquired using a Nikon A1R confocal microscope with a plan-apochromatic violet corrected (VC) 1.4 numerical aperture (N.A.) X 60 magnifying oil-immersion objective. Cell images were acquired in four different channels, using one-way consecutive line scans. The Alexa Fluor 488 was excited at 488 nm with laser power 7.8 Arbitrary Units (AU), its emission collected at 525/50 nm with a PMT gain of 140 AU (Green channel). The Alexa Fluor 555 signal was excited at 561 nm with laser power 2.1 AU, and collected at 595/50 nm with a PMT gain of 117 AU (Red channel). The DAPI was excited at 405nm with laser power 3.2 arbitrary units (AU), and its emission collected at 405/50 nm with a PMT gain of 118 AU. Finally, the differential interference contrast images were acquired using the transmitted light detector at a gain of 103 AU. The scan speed used was $\frac{1}{4}$ frames/s

(Galvano scanner) and no offset was used. The pinhole size was 34.5 μm , approximating 1.2 times the Airy disk size of the 1.4 N.A. objectives at 525 nm. Scanner zoom was centred on the optical axis and fixed to a lateral magnification of 55 nm/pixel and a Nyquist factor of 2.54 and 2.79 for Alexa Fluor 488) and Alexa Fluor 555 respectively. The axial step size was 140 nm, with 40-50 image planes per z-stack. Single or isolated cells with reasonable signal strength in both channels were examined to permit accurate quantitation of the flat plasma membrane and receptor distribution (Leonard *et al.*, 2017).

In order to validate a reliable co-localisation with this method, optimisation of samples were achieved with taking in account the following conditions. Saturated pixels were avoided, because it may represent lost information thus not used for quantitation. Therefore, not all the values above the dynamic range were recorded. Briefly, the smallest structure in an image, as determined by the microscope's resolution using Abbe's criterion, should be represented by at least two pixels and higher sampling, while under sampling must be avoided. Thirdly, aberrations were minimised in the imaging setup. This was done by using objectives corrected for spherical ('plan') and chromatic aberrations (achromatic, apochromatic and apochromatic violet-corrected (VC), depending on the number of colours corrected for). In addition, not bi-directional scanning, zooming in to the centre of the field of view, and separating colours in line scanning rather than full-frame mode was done as measures for reducing aberrations.(Lemcke *et al.*, 2013)

2.2.7.5 Image processing

NIS-Elements software (version 3.21.03, build 705) was used for image processing. CD14 (green) and TLR-4 (red); TLR-4 (green) and MD2 (red); TLR-4(green) and

HMGB-1 (red) channels were segmented using regional maximum detection tools followed by manual threshold. The generated binary areas were visually inspected; the overlap of the green and red channels was generated by the overlay tool, resulting in a new layer (yellow) that represents the intersection of CD14 (green) and TLR-4 (red) or TLR-4 (green) and MD2 (red) or TLR-4 (green) and HMGB-1 (red), automated volume measurement was carried out for CD14, TLR-4, MD2 and HMGB-1 and their intersection by volume measurements tool.

2.2.8 Preparation of total protein

For Lysate preparation, a pellet of 1×10^6 cells for control, untreated and treated cells were collected and washed twice in ice cold 1X PBS. Following this, 500 μ l of cell lysis mixture (Cell Lytic™ MT Reagent and Protease Inhibitor, Sigma, UK) was added. The pellet was resuspended by gentle pipetting and incubated on ice for 20 minutes. Then, the lysate was clarified by centrifugation at 15,000 rpm for 20 minutes. Finally, the protein containing supernatant was moved to a chilled test tube and the lysate was stored at -80°C for long-term use.

2.2.8.1 Bradford assay

This method was used for calculating the protein concentration in the lysate to calculate the amount of protein that should be loaded into each well before running the gel. This assay was based on the principle that when the Coomassie Blue Dye is bound to the protein in an acidic medium, a shift in absorbance occurs from 465 nm to 595 nm resulting in a colour change from brown to blue. The amount of complex now present in the solution is a measure for the protein concentration by means of an absorbance reading. Standard concentrations of BSA (Bovine Serum Albumin)

0.015, 0.031, 0.06, 0.125, 0.50, 1, and 2 mg/ml were prepared. A series of dilutions for the sample were prepared in PBS. Five microliters of the standards and samples respectively were added to the 96 well-plate. Bradford reagent was added by 250 μ l to each well and the plate was left for incubation at room temperature for 5 minutes. The Micro-titre plate reader was switched on and set up to an absorbance of 595 nm. The plate was read and results were read three times to minimise experimental error. A graph for concentration vs. absorbance was plotted on the protein concentration was found out using the $y = mx + c$ equation.

2.2.9 Two-Dimensional gel electrophoresis

2.2.9.1 Preparation of cell lysate

THP-1 cells untreated and treated by rough and smooth LPS were cultured in 100 mm cell culture dishes (Nunc, UK), and 1×10^7 cells were used per sample to make cell lysate. Cells were detached from culture dishes using accutase, counted and washed with 1X PBS as described earlier. The cell pellet was re-suspended in 1 ml of the protein extraction buffer containing 7M urea, 2M Thiourea, 4% CHAPS, 1X protease inhibitor cocktail, 20 mM DTT, 1% ampholyte, and Bensonase. All reagents were purchased from Sigma, UK. Cells were vortexed for 5 minutes at 4°C. Cell lysates were centrifuged at 20,000 rpm for 10 minutes; supernatant was collected into a clean micro-centrifuge tube and stored at -80°C for later use. The protein concentration of cell lysates was estimated using the Coo Assay (Uptima, Interchim, France) following manufacturer's instructions.

2.2.9.2 First dimensional gel isoelectric focusing (IEF)

The Immobiline dry strip gel pH 3-10NL, 17cm (GE Healthcare Bio-Sciences AB) used in this study was rehydrated in an immobiline dry strip reswelling tray. The dry strip was rehydrated for 24 hrs at room temperature in 350 µl of rehydration buffer (7M urea, 2M thiourea, 4% CHAPS, 1X protease inhibitor cocktail, 20 mM DTT, 1% ampholyte, 0.1% bromophenol blue, 0.05% SDS) containing 80 µg of sample proteins. The IPG strip was overlaid using approximately 3 ml of immobiline PlusOne dry strip cover fluid (GE Healthcare Bio-Sciences AB). After rehydration, the IPG strip was briefly rinsed with ultrapure water to remove crystallized urea.

For isoelectric focusing, the IPG-Phor was cleaned with Strip holder cleaning solution (GE Healthcare Bio-Sciences AB). The Ettan IPG Phor3 was switched on and connection with the IPG Phor3 control software was established. IPG Phor manifold was covered with 108 ml of Immobiline PlusOne dry strip cover fluid and the rehydrated strips were then placed in individual lanes of Ettan IPG strip holder (GE Healthcare Bio-Sciences AB) under the fluid using tweezers with the positive end towards the anode end of the manifold. Hydrated filter wicks were placed between the IPG strips and the electrodes. The cathodic (-ve) and the anodic (+ve) filter wick was hydrated with 150 µL DD water. The lid was closed and IPG-Phor programme was run according to the programme below.

A holding step at the end was added to so that it could be left overnight.

Step1	200 Volts	500 V	hrs
Step2	500 V	500 V	hrs
Grad3	1000 V	800 V	hrs
Grad4	10,000 V	16,500 V	hrs
Step5	10,000 V	6,200 V	hrs
Step6	200 V		24 hrs

At the end of the programme, IPG-Phor was stopped. The paper wicks were removed with tweezers and discarded. The IPG strips were placed in 10 cm a petri dish, rinsed briefly with deionized water, labelled and stored at -80°C for later use.

2.2.9.3 SDS-PAGE gel preparation

For second dimension gel electrophoresis, the PROTEAN II System (BIO-RAD, UK) was used. Glass plates were cleaned with 70% ethanol, dried, assembled with 2 mm spacers and clipped into the casting frame. Purify water was poured between the plates to check for leakage. Assemblies that leaked were taken apart and re-clipped and the process was repeated. Upon establishing a non-leaking system, the water was removed and the system was dried in situ with pressurized airflow. The gel solution 12% SDS PAGE was made with water, 1.5 M Tris-HCl and 30% acrylamide solution. These were placed in a flask and degassed for 15 minutes at ambient temperature. The TEMED, APS and SDS were added and mixed by stirring. The gel solution was poured in between glass plates, avoiding any air bubbles, to 1 cm below the lowest plate. The top of the gels was covered with overlay buffer (water saturated isopropanol 80%) and allowed to polymerise overnight. ([http://www.bio-rad.com/webroot/web/pdf/lsr/literature/Bulletin 2651.pdf](http://www.bio-rad.com/webroot/web/pdf/lsr/literature/Bulletin_2651.pdf))

2.2.9.4 Equilibration of the IPG strips

Prior to the second dimension gel run, the Immobilized pH Gradient (IPG) strips containing isoelectrically focussed proteins were equilibrated and reduced. For each strip, two vials of 10 ml aliquots of frozen equilibration buffer were thawed at room temperature. In one vial of equilibration buffer 100 mg of DTT was added while in the other 400 mg of iodo-acetamide was added and allowed to mix gently. The IPG strips

were first equilibrated in equilibration buffer containing 1% DTT, then in a buffer containing 4% iodo-acetamide for 15 min each at room temperature. The IPG strips were rinsed with 1X electrophoresis buffer before placing on second dimension gel.

2.2.9.5 Assembly and running of second dimensional gel

Agarose sealing solution was heated to liquefy. IPG strips were trimmed from each end up to 0.6 cm thus giving a final length of 16 cm. A small square of paper electrode wick (2 × 3 cm half thickness) was loaded with 10 µl of molecular weight marker and placed on the top of left hand corner of the gel. The IPG strips were placed into the wells of the 12% SDS PAGE gel with the acidic side facing the glass plate hinge and sealed with agarose solution, avoiding any air bubbles. The electrophoresis tank was filled with 1.5 L of gel running buffer. The gels with strips were removed from the casting assembly and clipped onto the core unit of the protean tank. The core unit was lifted into the tank, running buffer was added to the top of the upper buffer chamber and air bubbles were removed with a glass rod. The lid was fitted to the tank and cables were connected to the power Pac (Bio-Rad, Power Pac 1000). Electrophoresis was carried out first at 50 V for 30 minutes and then at 150 V for about 4.5 hrs or until the bromophenol red dye front had reached to the lower end (Figure 2-2). The core unit was then removed from the tank disassembled and gels were removed from the clamps. The spacers were loosened and one edge of the glass plate was lifted up with a spatula. The gel was then placed in a glass container containing gel fixing solution.(Tribbick, 2002; Janetzki and Britten, 2012)

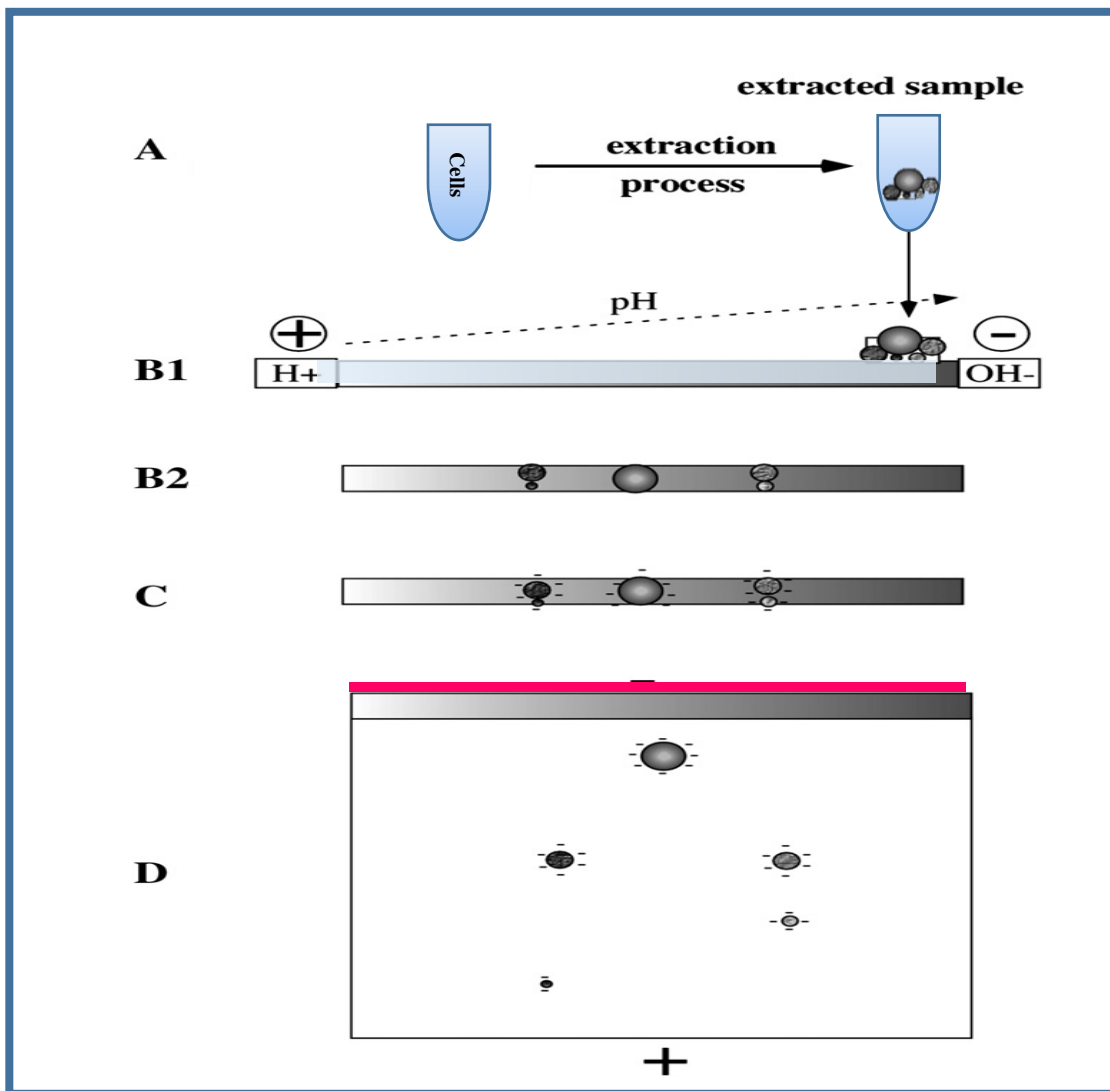


Figure 2-2: Scheme of principle of 2D gel electrophoresis.

(A) The total process start with the extraction of proteins from the biological sample to get an isoelectric focusing IEF-compatible sample. (B1) The sample is then loaded onto a pH gradient oriented with the acidic side at the anode and the basic side at the cathode. (B2) After the IEF step, the proteins have reached their pI and thus have no remaining electrical charge. (C) The strip is then equilibrated in a SDS-containing buffer, so that all proteins becomes strongly negatively charged. (D) The IEF gel is then loaded on top of a SDS PAGE gel, and the proteins are separated according to their molecular masses. After this step, the proteins are detected directly on the gel (Rabilloud *et al.* 2011).

2.2.9.6 Silver staining

For visualization of protein spots, a modified silver staining protocol was used as previously described (Yan and Chen, 2005; Ong and Mann, 2005; Geyer *et al.*, 2016). Briefly, after electrophoresis gels were fixed for half an hour in fixing solution they were sensitized for 30 minutes and washed with ultra-pure water. Staining was carried out using 2.5% silver nitrate solution for 20 minutes followed by a careful wash with ultra-pure water for a maximum of 1 min. The gels were developed for 10-15 minutes until spots appeared, and the reaction was stopped by washing with stop solution for 10 minutes. The gels were washed 3 times with ultrapure water and stored in gel preserving solution at 4°C.

2.2.9.7 Gel image capture and spot analysis

Gels were scanned using the scanner (Epson image scanner III) with LabScan 6.0 software. First, the scanner was calibrated and set to use the transparent settings at 300 dpi with the blue filter. The scanner surface was cleaned with 70% ethanol and a little purite water was poured on the surface. The gel was placed directly on the scanner, previewed and air bubbles were smoothed out if any were present. The scan area of the gel was then selected and scanned. Gel images were saved as mel and tiff files. Scanned gel images were characterised with Progenesis SameSpot software package (Nonlinear Dynamics Limited, UK).

2.2.10 Enzyme-linked immunosorbent assays (ELISA)

2.2.10.1 Principles of ELISA

This technique is one of the most common immunological assays, which highly characterized with its versatility, sensitivity and specificity and ease of automation. The coloured product formed indicated for directly proportional to the amount of antigen that bond to antibody. In this the technique, a standard curve with known concentrations of antigen of interest can be plotted in order determine the unknown antigen in experimental samples. ELISA kits ready set go supplied from E-biosciences were used to measure accurately and precisely the TNF- α , IL-1 β level produced by cells.

2.2.10.2 Experimental setup

TNF- α , IL-1 β level were measured in culture supernatants by ELISA ready set go (e-biosciences, Cambridge, UK) the manufacture protocol was followed, step by step to acquire the proper results. 96 well micro-plates were used and coated with capture antibody for overnight. The plate were aspirated and washed three times with wash buffer, then inverted and blotted on absorbent paper to remove any residual buffer. Following washing the wells blocked with 200 μ l/well of 1x assay diluent then incubated for one hour at room temperature followed by washing as previously. 100 μ l/well of diluted standard (500 pg/ml of TNF- α and 150 pg/ml of IL-1 β) were added to appropriate wells in order to plot standard curve, 2-fold serial dilution carried out and 100 μ l/well of experimental samples were added to the rest of the wells. The plate was sealed and incubated at 4 $^{\circ}$ C overnight followed by a total of 5 washes then, the detection antibody (100 μ l) diluted in 1X assay diluent was added and the plate was incubated at room temperature for another hour. Following washing, 100 μ l/well of Avidin-HRP diluted in 1X assay diluent was added into each well and the sealed plate

was incubated at room temperature for 30 minutes. Following aspiration and washing 7 times. Substrate solution (tetramethylbenzidine) added to each well and plates were incubated for 15 minutes at room temperature and the reaction was stopped by adding 50 μ l of 1M H_3PO_4 . The optical density of each well were measured at 450 nm using micro plate reader (FLUOstar OMEGA).

Chapter 3: The interaction between CD14 and TLR-4 in presence and absence of myeloid differentiation 2(MD2) and inhibitor PARP PJ34

3 The interaction between CD14 and TLR-4 in presence and absence of myeloid differentiation 2 (MD2) and inhibitor PARP PJ34

3.1 The interaction between CD14 and TLR-4 in presence and absence of inhibitor PARP PJ34

3.1.1 Introduction

In this chapter, the flow-cytometry experiments were designed to explore the effect of the PARP inhibitor (PJ34) when the THP-1 cells stimulated by lipopolysaccharides. Non-differentiated THP-1 cells and differentiated THP-1 cells were grown in RPMI 1640 supplemented with 10 % of FCS, then stimulated with rough LPS (EH100) and smooth LPS (O55: B5) in absence and presence of PARP inhibitor (PJ34). Then incubated for two, six and 24 hours and were collected (5×10^5 /ml) from each sample, then washed with PBS prior to use in experiments. The cells were fixed with a 4% fixation buffer (PFA) for 20 minutes on the ice bath. The cells were then blocked with blocking buffer (0.1% BSA in PBS) to block non-specific antibodies binding sites followed by washing step in PBS. All the samples were applied with a suitable concentration of the anti CD14 and anti TLR4 as primary antibodies, which incubated at 4°C for 60 min. The negative control (IgG1 and IgG2) were applied to the specific samples. Afterwards, all samples were applied with the secondary antibody (FITC) and incubated at 4°C for 60 min, then washed by PBS to remove the extra amount of the secondary antibody and read using BD Accuri 6 flow-cytometer.

3.1.2 Antibodies concentration

Antibodies supplied in tiny amounts by microliter, contain nano grams of antibodies. We should deal with it accurately, therefore, the first step to use them that find the suitable concentration by the titration experiment, which gives the intended results. 1000 ng of CD14, 500 ng of TLR4 and 500 ng of MD2 were found the proper concentration of each antibody (Figure 3-1, 3-2).

3.1.3 Results

The samples of the flowcytometry were read with BD Accuri 6 flowcytometer then analysed with Flo-Jo software version 8.8.6 (Tree Star Inc., Ashland, OR, USA) which downloaded as a free trial. The first step is to apply each sample tubes to the sample needle; samples run in 10,000 cells, which required for each sample, gate the area of the live cells in the dot plot graph, then open it in a histogram to show the curve of the number of events in percentage. RAJI cells used as a positive control.

The grey histogram (Figure 3-3) represents the negative control of untreated cells followed by secondary antibody Fluorescein Isothiocyanate (FITC). The red histogram represents slightly decreasing of cell surface expression of CD14 and TLR-4 on THP1 cells under treatment mentioned in 3.1.1. The result shows that two (2) hours stimulation is proper time to provide the expression of the receptors CD14 and TLR4 with the (R and S) LPS. In the other hand, the THP-1 cells treated with PJ34 is represent more expression between CD14 and TLR-4 (Figure 3-8).

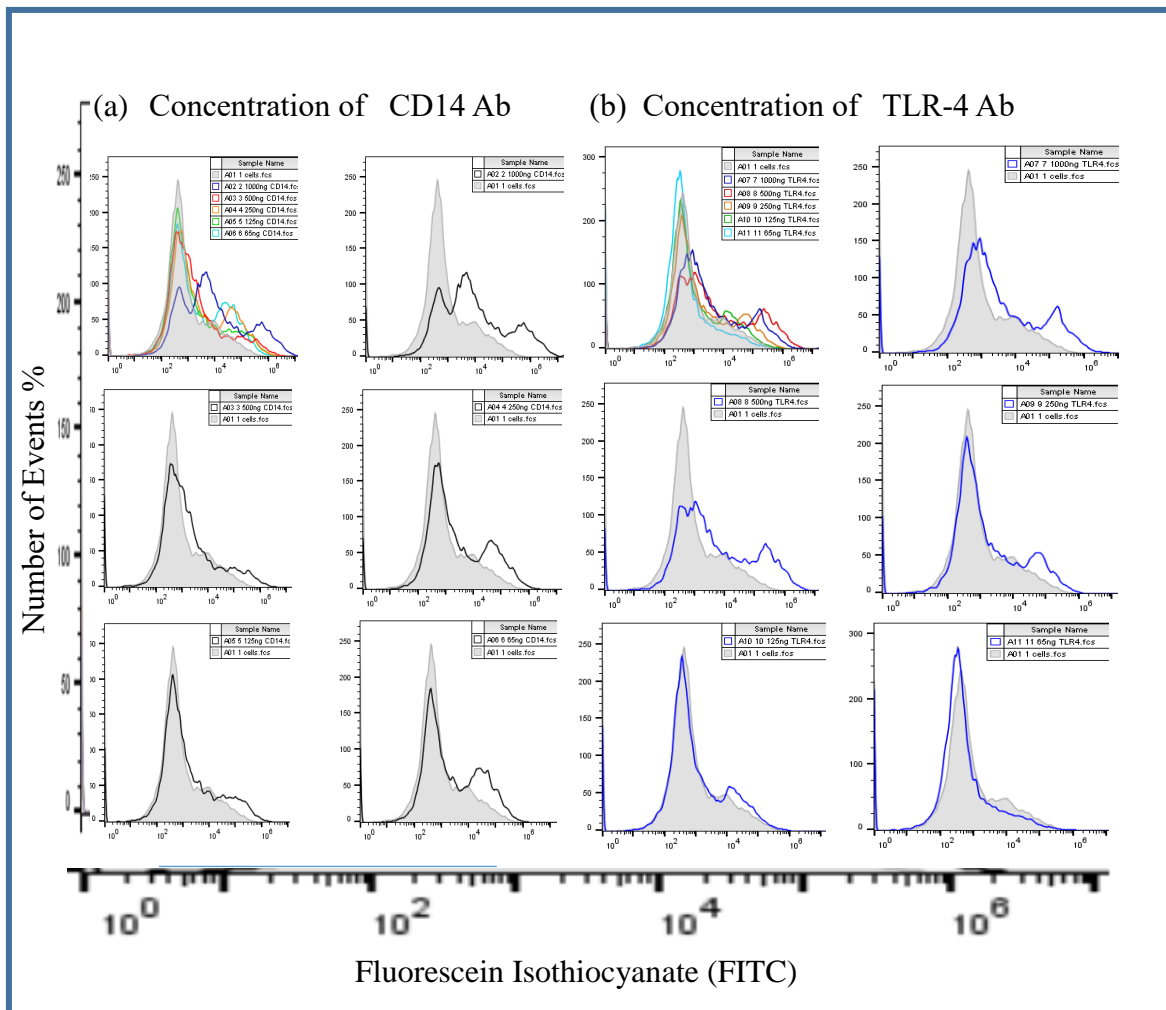


Figure 3-1: The proper concentration of the CD14 and TLR-4 antibodies required to be used in flowcytometer experiment.

(a) Concentration of CD14 Ab used 1000, 500, 250, 125 and 65 ng. The line histograms indicate that 1000 ng is the suitable titration of the antibody with 3×10^5 cells. (b) The concentration of TLR4 Ab used as 1000, 500, 250, 125 and 65 ng. We found that 500 ng are suitable titration of the antibody with 3×10^5 cells.

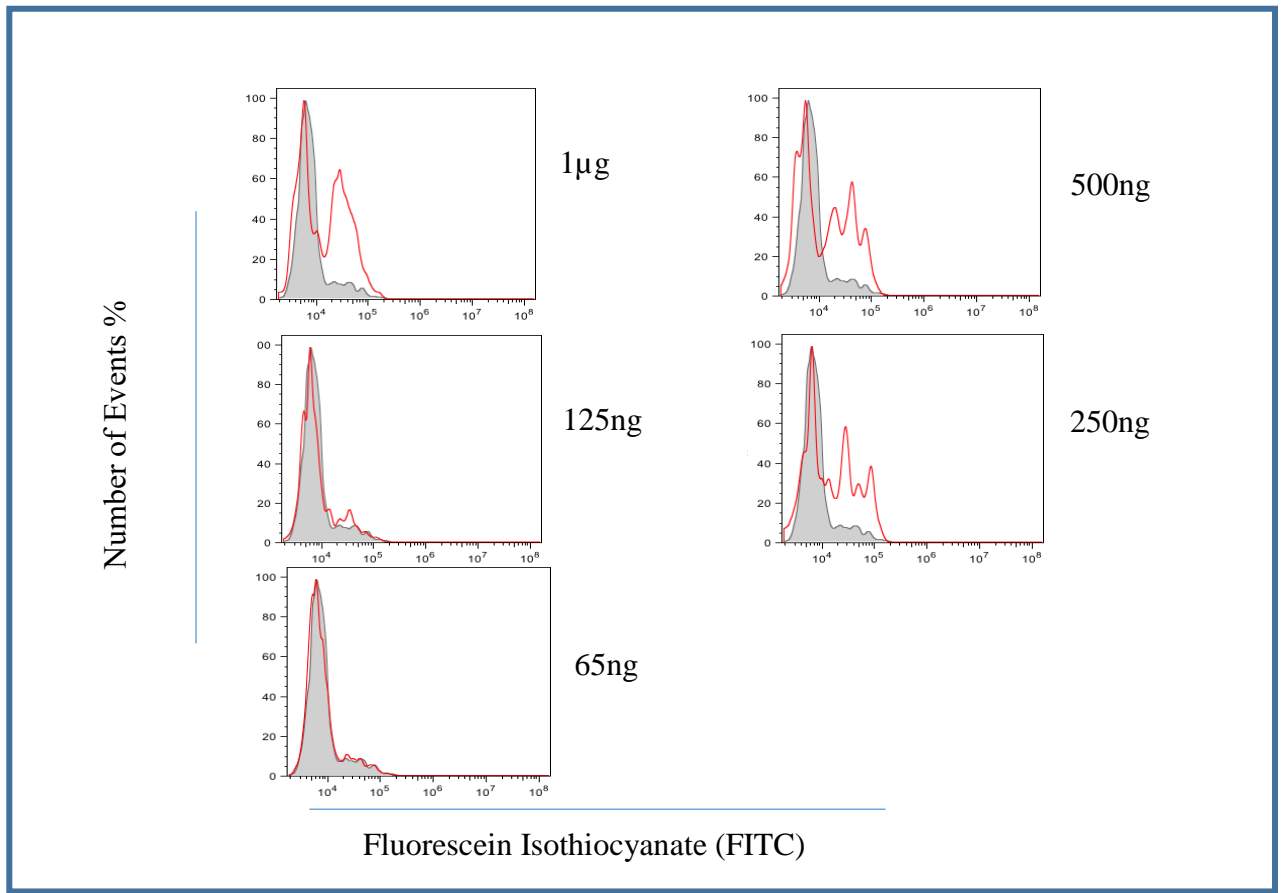


Figure 3-2: The proper concentration of the MD2 antibody.

In flowcytometer experiments, the concentration of MD2 Ab were used 1000, 500, 250, 125 and 65 ng. The suitable concentration of the antibody should be used with 3×10^5 cells is 500 ng.

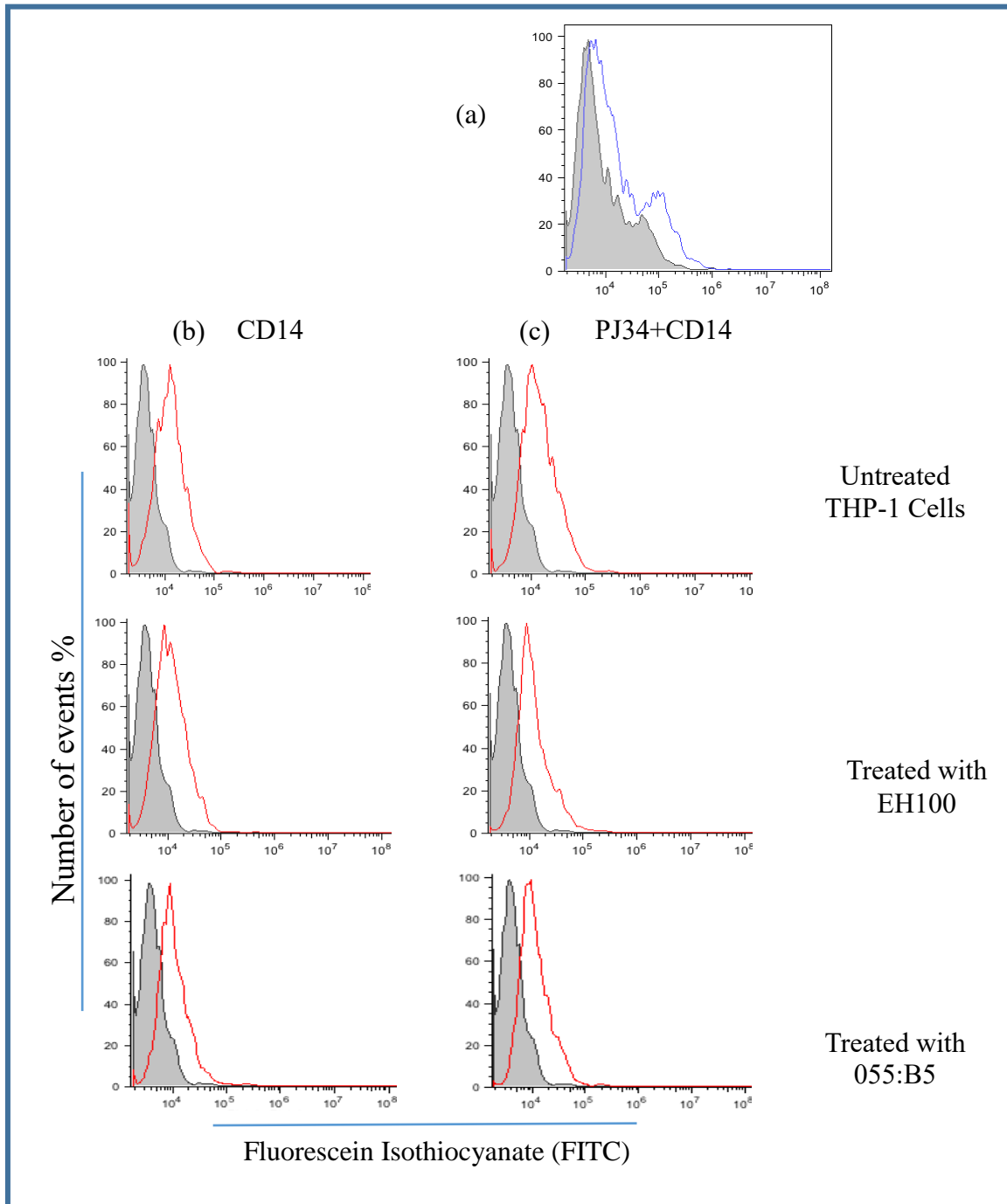


Figure 3-3: The expression of CD14 in THP-1 cell lines in 2 hours stimulation with LPS and PJ34.

(a) The expression of CD14 in RAJI cell lines as a positive control (b) 5×10^5 of THP1-1 cells were grown in RPMI 1640 supplemented with 10 % of FCS then stimulated with rough LPS EH100 and smooth LPS O55:B5 in absence and (c) presence of PARP inhibitor PJ34, then incubated for two hours. The grey histogram represents the negative control of untreated cells followed by secondary antibody Fluorescein Isothiocyanate (FITC). The red histogram represents slightly decreased of cell surface expression of CD14 on THP1 cells.

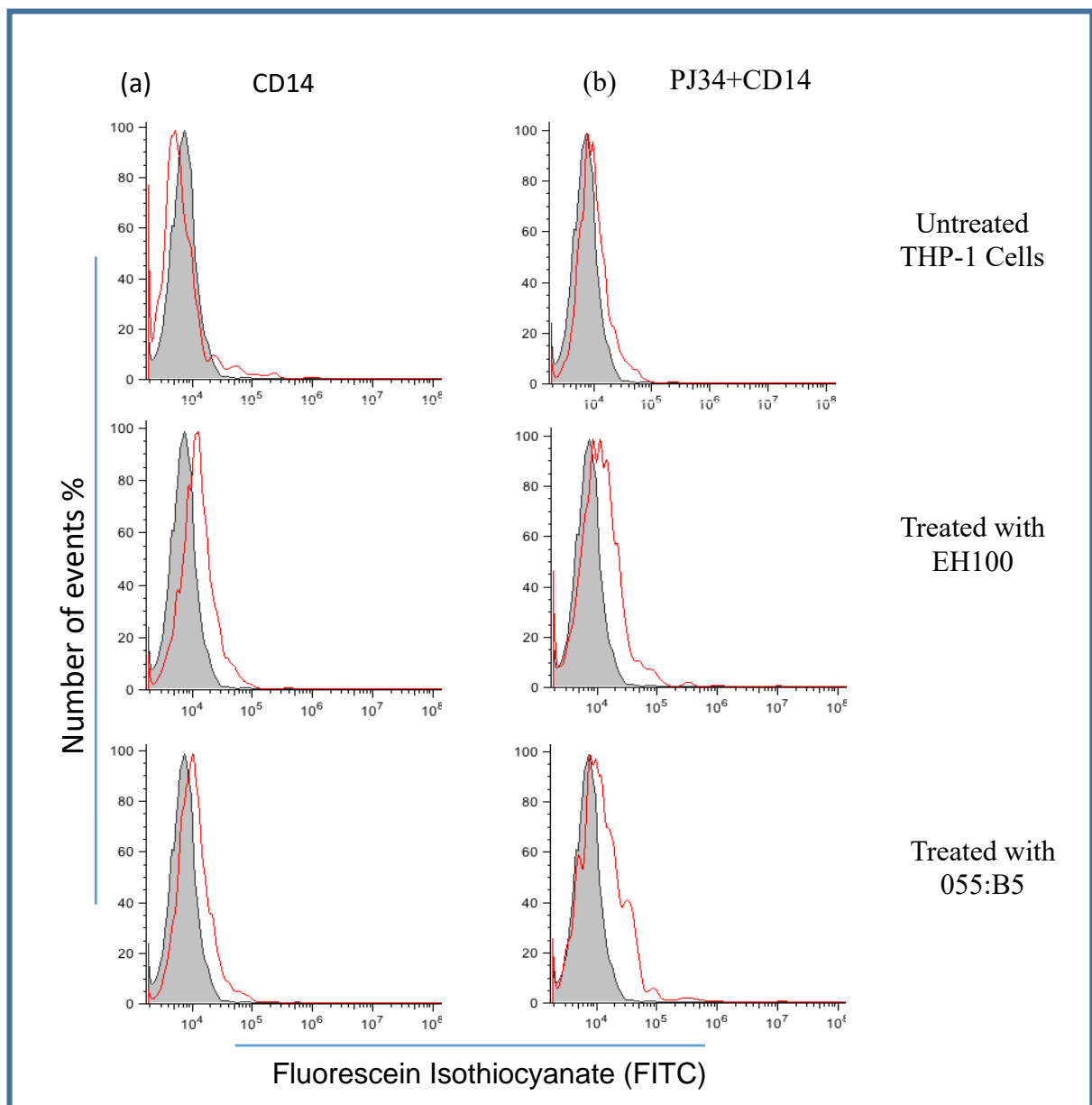


Figure 3-4: The expression of CD14 in THP-1 cell lines in 6 hours stimulation with LPS and PJ34.

5×10^5 of THP-1 cells were grown in RPMI 1640 supplemented with 10 % of FCS then stimulated with rough LPS (EH100) and smooth LPS (O55:B5) in absence (a) and presence (b) of PARP inhibitor PJ34, then incubated for **six hours**. The grey histogram represents the negative control of untreated cells followed by secondary antibody Fluorescein Isothiocyanate (FITC). The red histogram represents no significant change on cell surface expression of CD14.

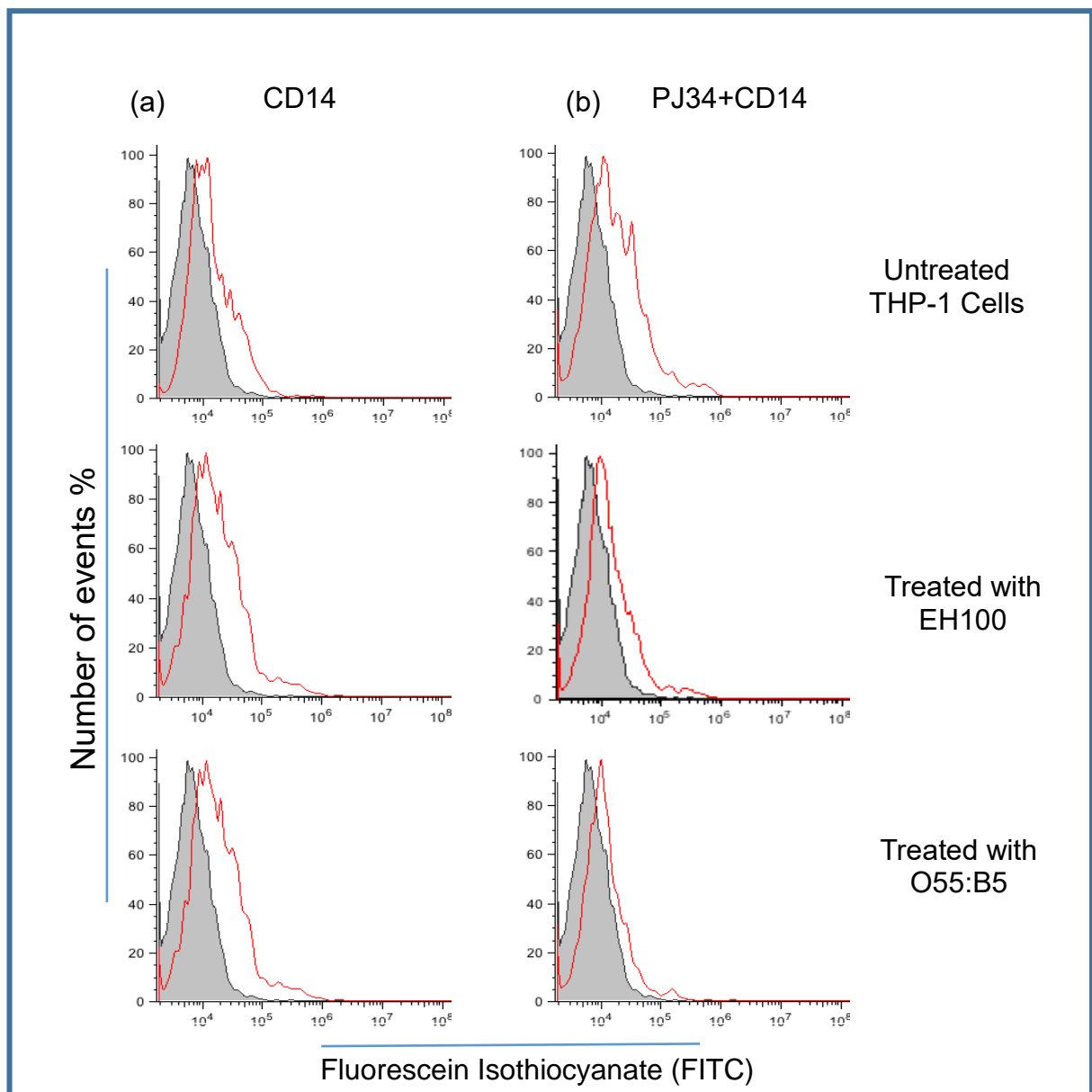


Figure 3-5: The expression of CD14 in THP-1 cell lines in 24 hours stimulation with LPS and PJ34.

(a) 5×10^5 of THP-1 cells were grown in RPMI 1640 supplemented with 10 % of FCS then stimulated with rough LPS (EH100) and smooth LPS (O55:B5) in absence (a) and presence (b) of PARP inhibitor PJ34, then incubated for **24 hours**. The grey histogram represents the negative control of untreated cells followed by secondary antibody Fluorescein Isothiocyanate (FITC). The red histogram represents no significant cell surface expression of CD14 on the THP1 cells with presence of PJ34 treated with LPSs. However, there are a significant change in cell surface expression of CD14 treated by LPSs in absence of PJ34.

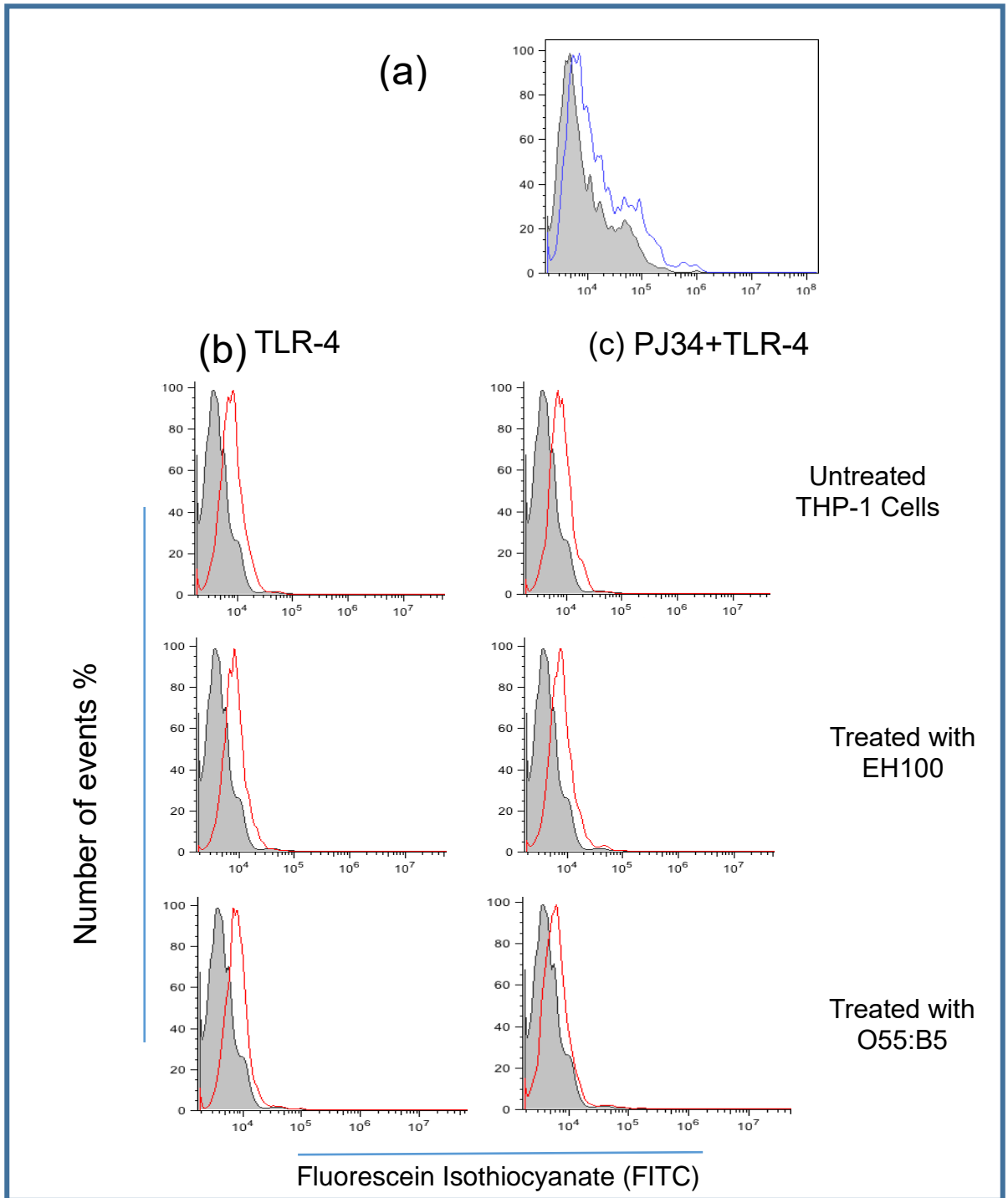


Figure 3-6: The expression of TLR-4 in THP-1 cell lines in 2 hours stimulation with LPS and PJ34.

(a) The expression of TLR-4 in RAJI cell lines as a positive control, (b) 5×10^5 of THP-1 cells were grown in RPMI 1640 supplemented with 10 % of FCS then stimulated with rough LPS (EH100) and smooth LPS (O55:B5) in absence and (c) presence of PARP inhibitor PJ34, then incubated for two hours. The grey histogram represents the negative control of untreated cells followed by secondary antibody Fluorescein Isothiocyanate (FITC). The red histogram represents weak cell surface expression of TLR-4 on THP1 cells.

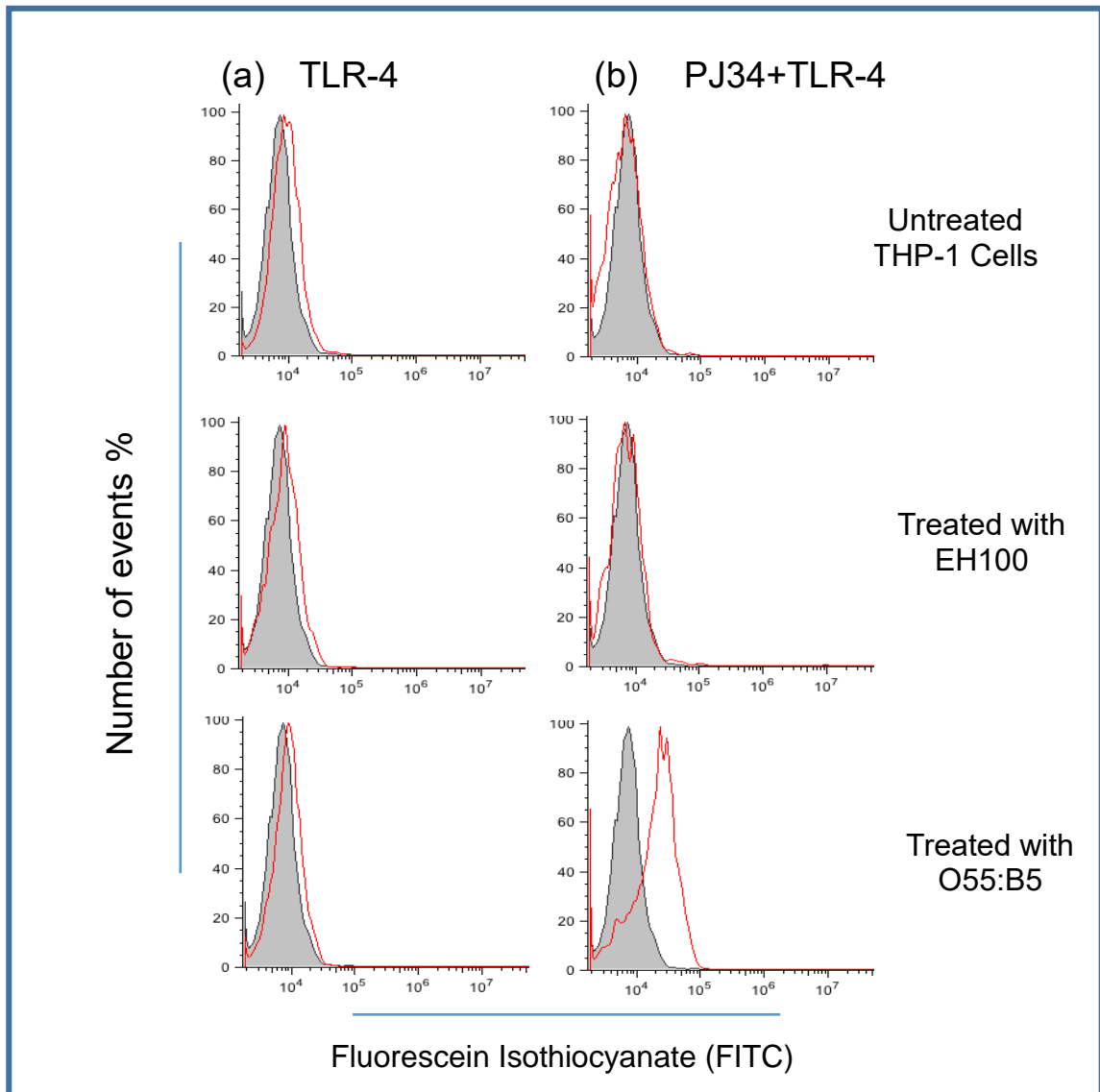


Figure 3-7: The expression of TLR-4 in THP-1 cell lines in 6 hours stimulation with LPS and PJ34.

5×10^5 of THP-1 cells were grown in RPMI 1640 supplemented with 10 % of FCS then stimulated with rough LPS (EH100) and smooth LPS (O55:B5) in absence (a) and presence (b) of PARP inhibitor PJ34, then incubated for **six hours**. The grey histogram represents the negative control of untreated cells followed by secondary antibody Fluorescein Isothiocyanate (FITC). The red histogram represents no significant change on cell surface expression of TLR-4. However, there is a significant expression on the cells treated by smooth LPS in presence of PJ34.

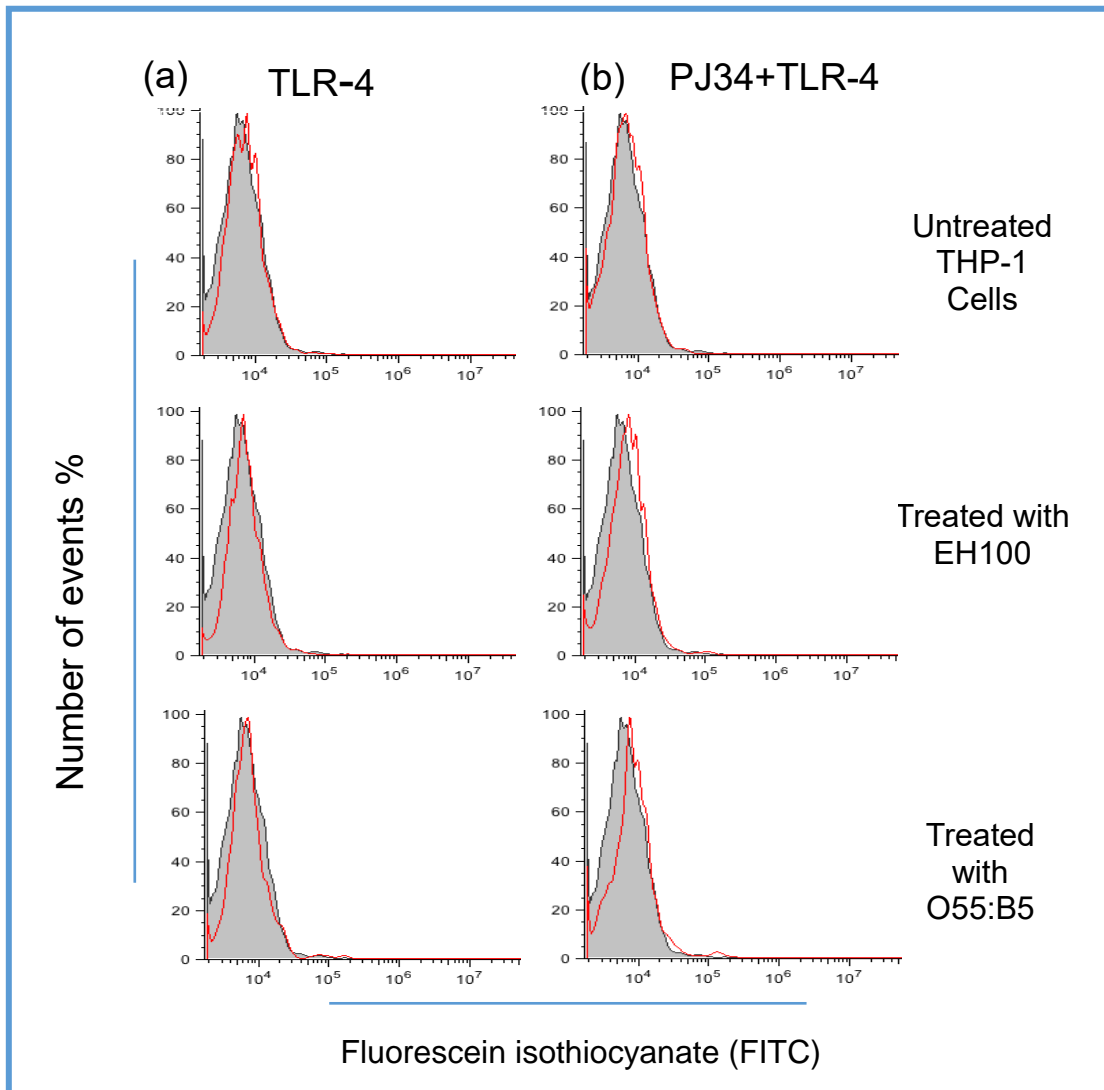


Figure 3-8: The expression of TLR-4 in THP-1 cell lines in 24 hours stimulation with LPS and PJ34.

5×10^5 of THP-1 cells were grown in RPMI 1640 supplemented with 10 % of FCS then stimulated with rough LPS (EH100) and smooth LPS (O55:B5) in absence (a) and presence (b) of PARP inhibitor PJ34, then incubated for **24 hours**. The grey histogram represents the negative control of untreated cells followed by secondary antibody Fluorescein Isothiocyanate (FITC). The red histogram represents no significant change on cell surface expression of TLR-4.

3.2 The Importance of myeloid differentiation MD2 to the expression of CD14 and TLR-4 in presence and absence of inhibitor PARP PJ34.

3.2.1 Introduction

In this chapter we designed the flow-cytometry experiments to represent the expression of CD14 and TLR-4 to explore the importance of MD2 and PJ34. In this study anti MD2 and PJ34 were used to block them in one stage of the experiment before stimulating the cells By LPS to approve whether the Importance of MD2 and PJ34. 500 ng is the best concentration of MD2 was used as the antibody used to treat the cells. The presence of myeloid differentiation protein-2 (MD-2) makes up the LPS receptor complex involved in the cellular recognition and signalling by LPS. Raji cell line was used as positive control.

3.2.2 Results

The results of the flowcytometry were read with BD Accuri 6 flowcytometer then analysed with Flo-Jo software version 8.8.6 (Tree Star Inc., Ashland, OR, USA) which downloaded as a free trial. The first step is to apply each sample tubes to the sample needle; samples run in 10,000 cells, which required for each sample, gate the area of the live cells in the dot plot graph, and then open it in a histogram to show the curve of the number of events in percentage. RAJI cells used as a positive control.

The grey histogram represents the negative control of untreated cells followed by secondary antibody Fluorescein Isothiocyanate (FITC). The blue histogram represents slightly decreased in cell surface expression of CD14 and TLR-4 on THP1 cells under treatment mentioned in 3.1.1.

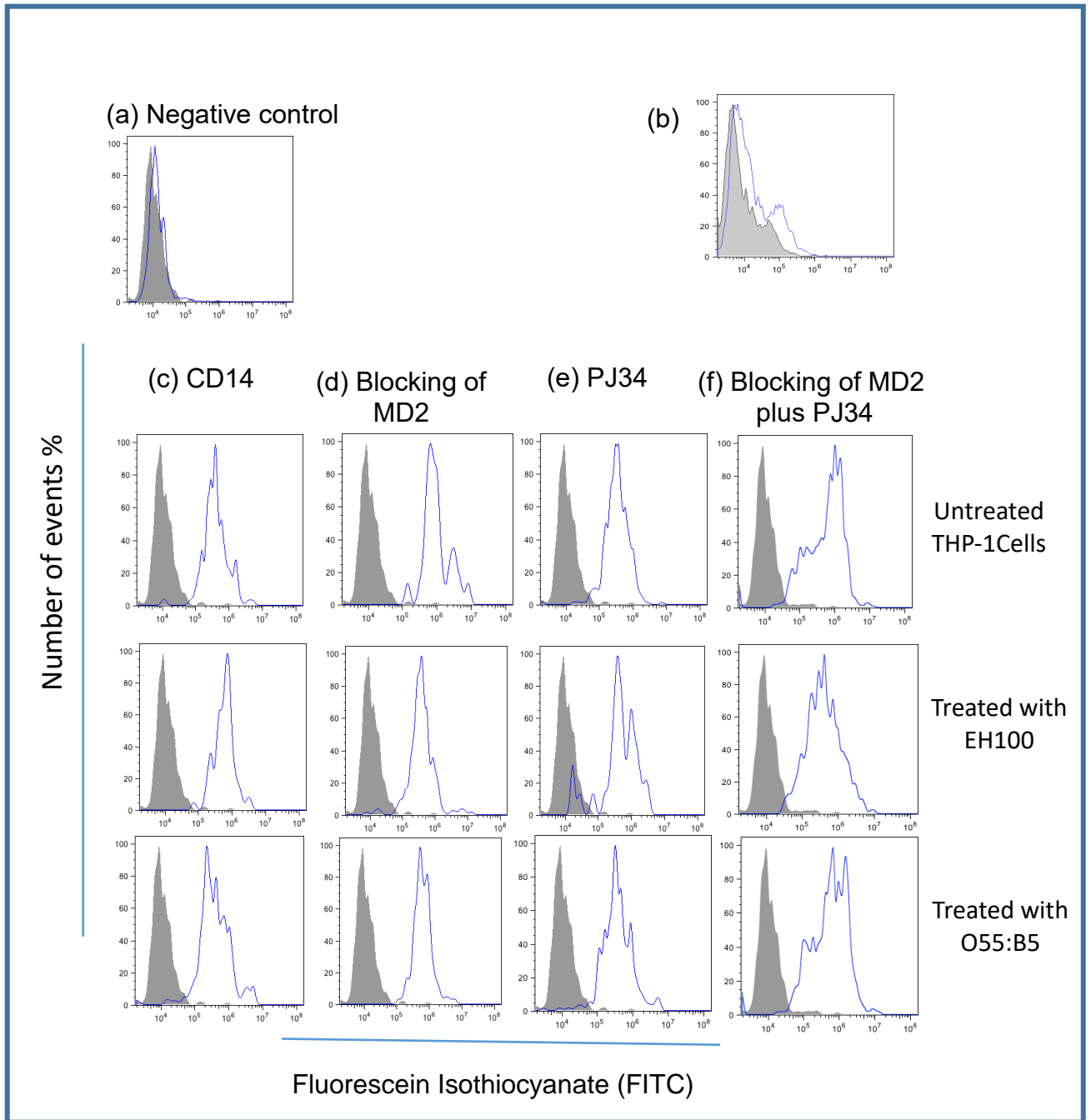


Figure 3-9: The expression of CD14 in differentiated THP-1 cell lines when stimulated with LPS for 2 hours and treated by PJ34 and block the MD2.

(a) 2×10^5 of differentiated THP1-1 cells by applying 5ng/ml of (PMA) were grown in RPMI 1640 supplemented with 10 % of FCS. The negative control, (b) The expression of CD14 in RAJI cell lines as a positive control, (c) the cells stimulated with rough LPS (EH100) and smooth LPS (O55:B5) in presence, (d) and absence (e) of Myeloid Differentiation 2 (MD2), also presence, (f) and absence PARP inhibitor PJ34, the cells incubated for two hours. The grey histogram represents the isotype untreated cells followed by secondary antibody, Fluorescein Isothiocyanate (FITC). The blue histogram represents significant changes of cell surface expression of CD14 on THP1 cells with different treatment.

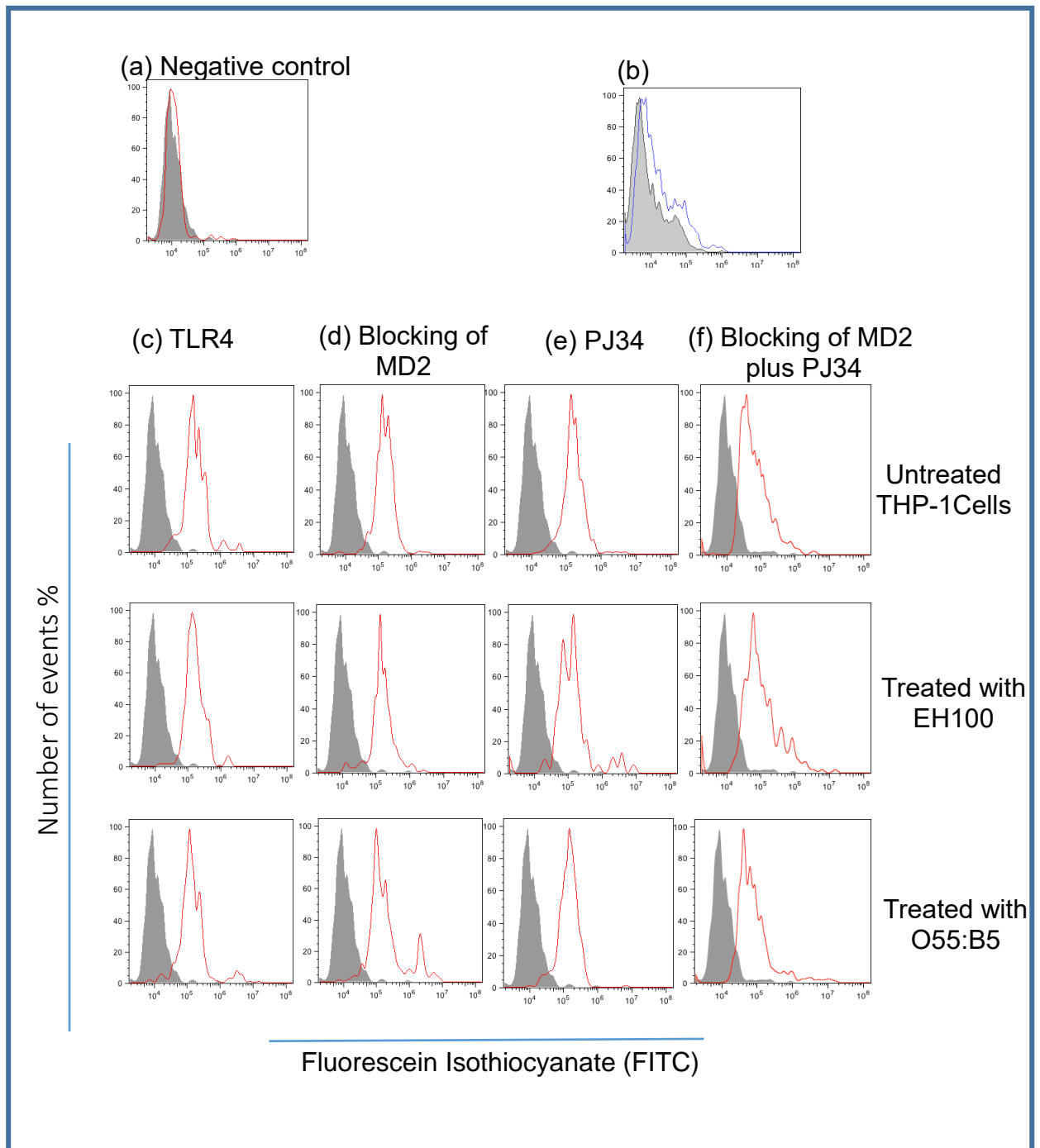


Figure 3-10: The expression of TLR-4 in differentiated THP-1 cell lines when stimulated with LPS for 2 hours and treated by PJ34 and block the MD2.

2×10^5 of differentiated THP-1 cells by applying 5ng/ml of (PMA) were grown in RPMI 1640 supplemented with 10 % of FCS. (a) The negative control, (b) The expression of TLR-4 in RAJI cell lines as a positive control, (c) the cells stimulated with rough LPS (EH100) and smooth LPS (O55:B5) in presence (d) and absence (e) of Myeloid Differentiation 2 (MD2), also presence (f) and absence (d) PARP inhibitor PJ34, the cells incubated for **two hours**. The grey histogram represents the isotype untreated cells followed by secondary antibody, Fluorescein Isothiocyanate (FITC). The red histogram represents highly significant changes of cell surface expression of TLR-4 on THP1 cells with different treatment.

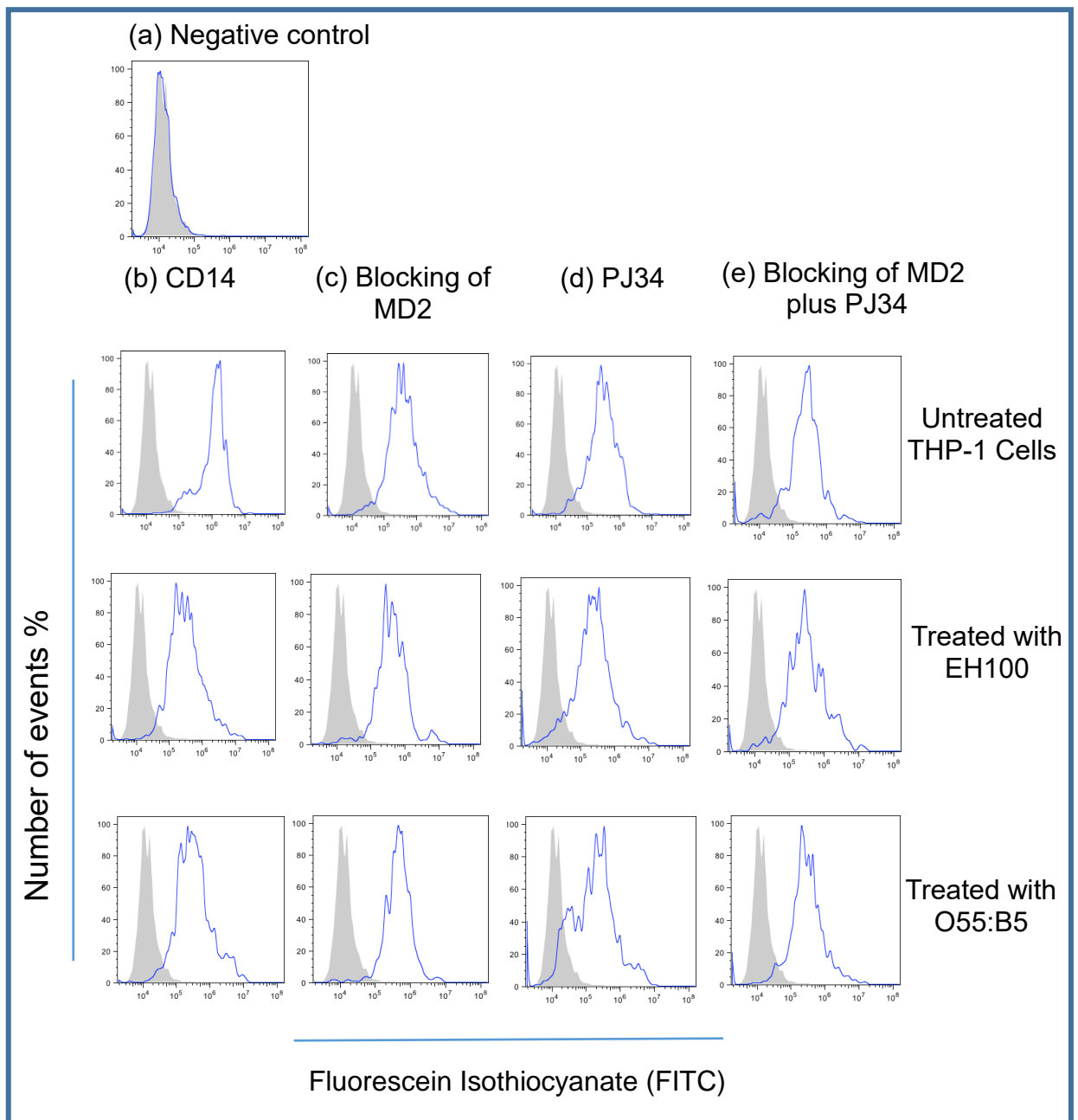


Figure 3-11: The expression of CD14 in non-differentiated THP-1 cell lines when stimulated with LPS for 2 hours and treated by PJ34 and block the MD2.

2×10^5 of THP-1 cells were grown in RPMI 1640 supplemented with 10 % of FCS. (a) The negative control, (b) normal cells with CD14 Ab. The cells stimulated and incubated for **two hours** with rough LPS (EH100) and smooth LPS (O55:B5) with (c) blocking of Myeloid Differentiation 2 (MD2), (d) with PARP inhibitor PJ34 and (e) blocking of Myeloid Differentiation 2 plus PJ34, the cells. The grey histogram represents the isotype control. Cells followed by secondary antibody, Fluorescein Isothiocyanate (FITC). The blue histogram represents significant changes of cell surface expression of CD14 on THP1 cells with the different treatment.

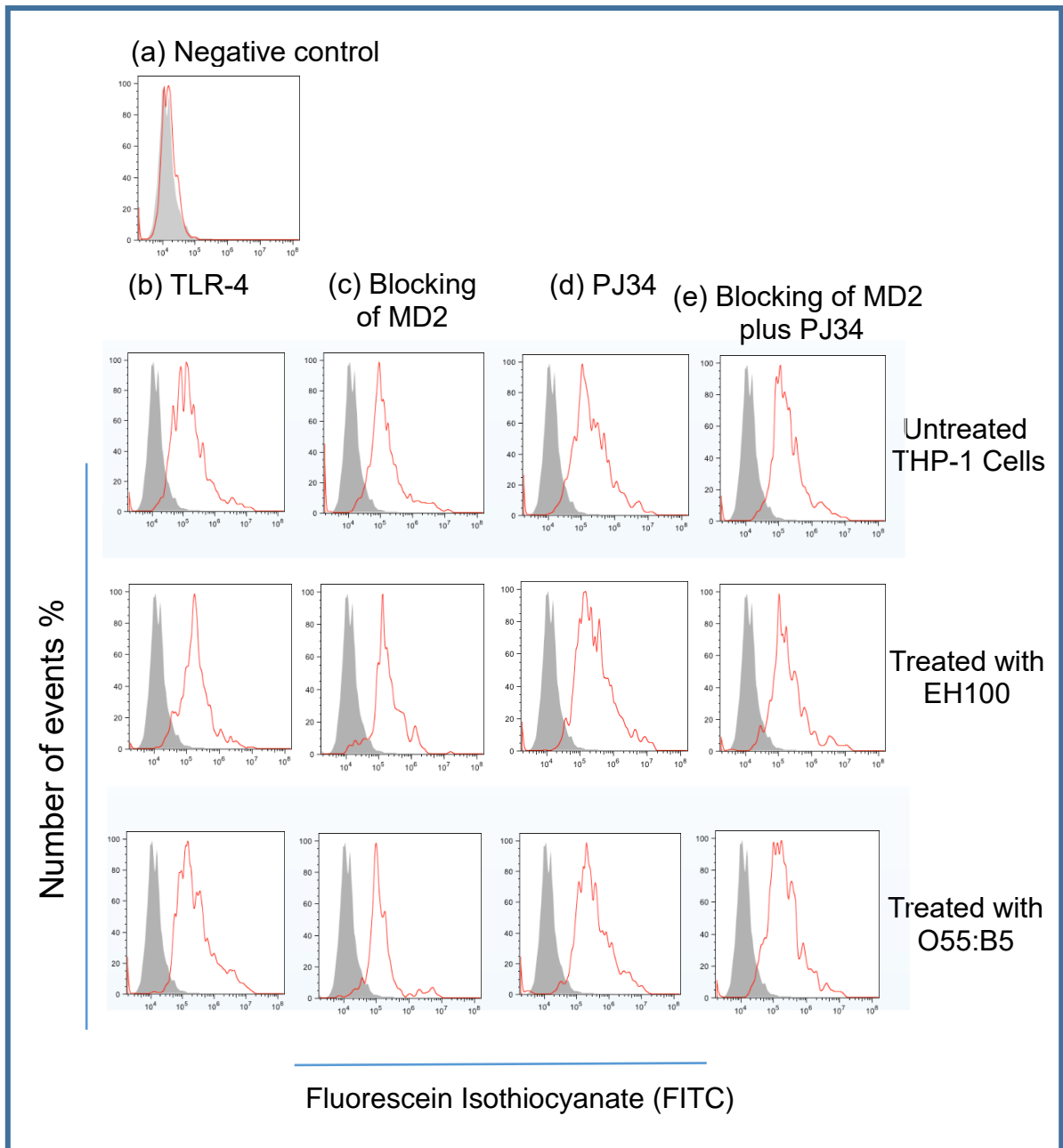


Figure 3-12: The expression of TLR-4 in non-differentiated THP-1 cell lines when stimulated with LPS for 2 hours and treated by PJ34 and block the MD2.

2×10^5 of THP-1 cells were grown in RPMI 1640 supplemented with 10 % of FCS. (a) The negative control, (b) normal cells with TLR-4 Ab. The cells stimulated and incubated for **two hours** with rough LPS (EH100) and smooth LPS (O55:B5) with (c) blocking of Myeloid Differentiation 2 (MD2), (d) adding PARP inhibitor PJ34 and (e) blocking of Myeloid Differentiation 2 plus PJ34, the cells. The grey histogram represents the isotype control. Cells followed by secondary antibody, Fluorescein Isothiocyanate (FITC). The red histogram represents significant changes of cell surface expression of TLR-4 on THP1 cells with the different treatment.

3.2.3 Conclusions

The effect of LPS known as the highest human pathogenic component is present in Gram-negative bacteria. 10 µg/ml of both rough (EH100) and smooth (055: B5) LPSs concentration was used to stimulate the THP-1 cells. Differentiated and non-differentiated THP-1 cells were treated with PARP inhibitor (PJ34) and myeloid differentiated 2 (MD2) in specific conditions and incubation time.

As represented in figures above, the results represent the expression of the receptors TLR4 with the (R and S) LPS in all conditions mentioned, and were affected more than the receptor CD14, especially on differentiated THP-1 cells, because they were macrophage-like cells (Figure 3-3), however, less effect on the non-differentiated THP-1. (Figure 3-4). It is related to MD2 the main co-receptor to TLR-4 especially when MD2 was blocked in specific samples. In the other hand, the expression on the THP-1 cells by CD14 in differentiated and non-differentiated THP-1 cells, refer this to the high amount of the mCD14 and sCD14 receptors on the surface and around the cells (Figure 3-5 to 3-6). More results represented in (Figures 3-7 to 3-8) when treat the cells with inhibitor PARP PJ34 which prevent the expression between CD14 and TLR-4. But when we block the MD2 and use the inhibitor PARP PJ34 the expression increased significantly (Figure 3-9 to 3-12).

The results conclude that the MD2 and PJ34 can be used as motivator and inhibitor of the expression of the LPS membrane complex receptors CD14 and TLR-4.

**Chapter 4 Detection of the Importance of myeloid differentiation
MD2 and the effective of PARP inhibitor PJ34.**

4 Detection of the Importance of myeloid differentiation MD2 and the effective of PARP inhibitor PJ34

4.1 Two-Dimensional gel electrophoresis to detect the Importance of myeloid differentiation MD2 and the inhibitor PARP PJ34.

4.1.1 Introduction

Two dimensional polyacrylamide gel electrophoresis is a form of gel electrophoresis in which proteins were separated and identified in two dimensions oriented at right angles to each other. In this technique, proteins were separated by two different physical properties. The first dimension, isoelectric focusing, separates proteins based on their net charge. The second dimension, SDS-PAGE, further separates the proteins by their mass. The scientist describe the 2D gel as future technique and the 3-D images for polypeptides indicate different quantitative levels of proteins and could assist in the discovery of novel proteins induced by LPS.

4.1.2 Preparation of cell lysate

Untreated and LPS treated of differentiated THP1-1 cells by applying 5 ng/ml of (PMA) were grown in RPMI 1640 supplemented with 10 % of FCS. The cells stimulated with rough LPS (EH100) and smooth LPS (O55:B5) for two hours in presence and absence of Myeloid Differentiation 2 (MD2) presence and absence PARP inhibitor PJ34 in selected dishes. To make cell lysate. Cells were detached from culture dishes using accutase, counted and washed with 1 X PBS to remove any media residue. After centrifuge the samples in 1.5 ml tubes, the cell pellet resuspended in 1 ml of the protein extraction buffer containing 7 M urea, 2 M Thiourea, 4% CHAPS, 25% Tris base. Cells were vortexed then centrifuged for 20 min on 20000 rpm at 4°C, the supernatant were collected and reserved at -80°C.

4.1.3 First dimensional gel isoelectric focusing

The dry strips gel pH 4-7, 18 cm used in this study was rehydrated in strips holder tray, which washed well special detergent to be clean from any proteins residue. The dry strip was rehydrated overnight at room temperature in 300 µl of rehydration buffer containing 50 µg of sample proteins. The IPG strip was overlaid using approximately 3 ml of dry strip cover fluid.

For isoelectric focusing, the IPG-Phor is twelve lanes as our samples, and it should be cleaned with Strip holder cleaning solution. The rehydrated strips were placed in individual lanes of Ettan IPG strip holder and covered by 108 ml of dry strip cover fluid and. The Ettan IPG Phor3 was switched on and connection with the IPG Phor3 control software. Hydrated filter wick was rehydrated with 150 µL ddH₂O were placed between the IPG strips and the electrodes, the anodic (positive) and the cathodic (negative). Run the IPG-Phor programme according to the length of the strips and left for about 19 hours. When the program stopped, the Ettan IPG Phor3 was switched off. Take off the strips individually and placed in a petri dish, labelled by the strip numbers and stored at -80°C to use in the second diminution electrophoresis.

4.1.4 SDS-PAGE Gel preparation

PROTEAN II System from Bio-Rad was used for the second dimension gel electrophoresis, glass plates were washed well, then 99% ethanol was sprayed, and kept to dry, assembled with 2 mm spacers and clipped into the casting frame. Water was filled between the plates to check if there is any leakage, the water was removed and the system was dried by pitman paper. The gel solution 12% SDS PAGE was made with water, 1.5 M Tris-HCl and 30% acrylamide solution. These were placed in a flask for 20 minutes to degas. The Ammonium persulphate and TEMED were added and mixed by stirring. The gel solution was ready to pour in between glass plates,

avoiding any air bubbles; 1 cm below the lowest plate was left. The top of the gels was covered with distilled H₂O and allowed to polymerise for at least 5 hours. The gel can be saved for One week to 10 days covered by wet tissue paper and cling film on the top of the tissue, and apply ddH₂O every 2 days to be wet until use.

Before the second dimension gel run, the IPG strips containing isoelectrically focussed proteins were equilibrated and reduced. For each strip, two vials of 10 ml aliquots of frozen equilibration buffer were thawed and used. In one vial of equilibration buffer, 100 mg of DTT while in the other one 250 mg of iodo-acetamide was added and allowed to mix gently on the rocker shaker. The IPG strips were first equilibrated in equilibration buffer containing 1% DTT for 20 min, then in a buffer 4% iodo-acetamide the same time. The IPG strips were rinsed with 1X electrophoresis buffer before placing on second dimension gel (Rogowska-Wrzesinska *et al.*, 2013).

4.1.5 Second dimensional gel running and staining

In this stage, we prepare the agarose to be used as a sealing solution, heated to be liquid. IPG strips were trimmed from the edges to be fitted to the glass length and spacer, which is about 16 cm. The plastic piece was loaded in the space between the edge of the strip and the spacer to add at the end the molecular weight protein marker with 10 µl. The electrophoresis tank was filled with 1.5 L of running buffer. The gels with strips were removed from the casting assembly and clipped onto the core unit of the protean tank. The core unit was lifted into the tank, running buffer was added to the top of the upper buffer chamber and air bubbles were removed with a glass rod. The plastic piece removed and 10 µl of the MW marker applied in the space. The lid was fitted to the tank and cables were connected to the power Pac. Electrophoresis was carried out first at 50 Volts for overnight until reached to the lower end of the gel. The core unit was then removed from the tank disassembled and gels

were removed from the clamps. The spacers were released and one edge of the glass plate was lifted up with a plastic spatula. The gel was then placed in a glass container containing Instant Blue, which recommended from the dealer for our experiment to view the spots clearly immediately, which avoid using any acids or alcohols. We apply 100 ml of the stain, but after 24 hours, the results were not satisfied, and then return to the silver stain after the gel distained.

Silver staining protocol was used, after electrophoresis gels were fixed for overnight by fixing solution, they were sensitized for 1 minute and washed with ddH₂O. Staining was carried out using 0.1% silver nitrate solution for 20 minutes followed by a careful wash with ddH₂O for a maximum of 1 min. The gels were developed until spots appeared, and the reaction was stopped by adding stop solution. The gels were washed 3 times with ddH₂O and saved in gel preserving solution at 4°C.

4.1.6 Gel image scan and analysis

By using Epson image scanner III, Gels were scanned with LabScan 6.0 software. Firstly, the scanner was calibrated and set to use the transparent settings at 300 dpi with the blue filter. The scanner surface was cleaned with 70% ethanol. The gel was placed directly on the scanner, previewed and air bubbles were smoothed out. The scan area of the gel was selected and scanned. Gel images were saved as (tiff) and (mel) format files. Scanned gel images were categorised with SameSpot software (Figure 4-1).

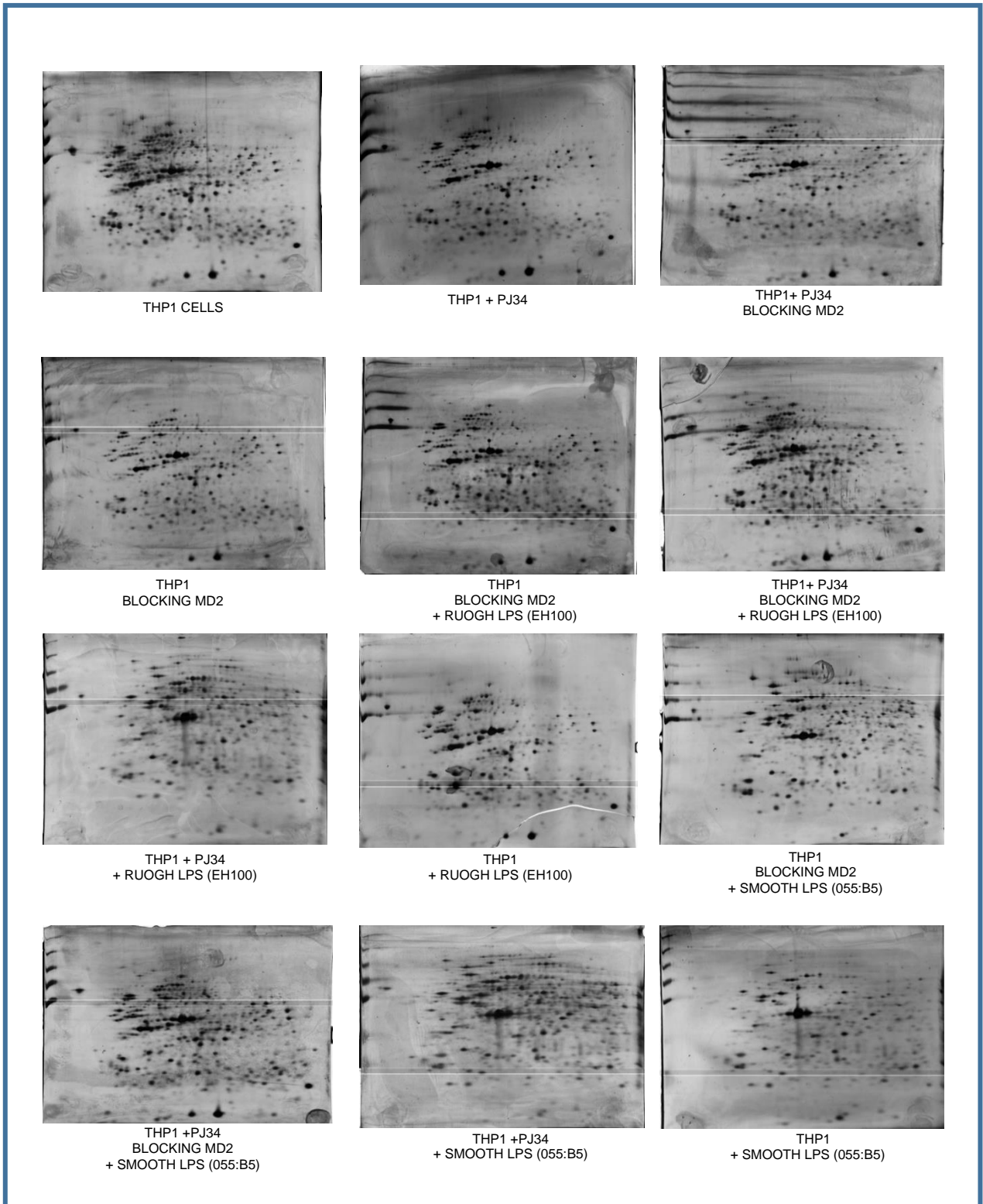


Figure 4-1: Two Dimensional gel images for twelve different conditions.

The images represent two Dimensional gels taken by Epson image scanner III for twelve gels, with different conditions appear the spots detection.

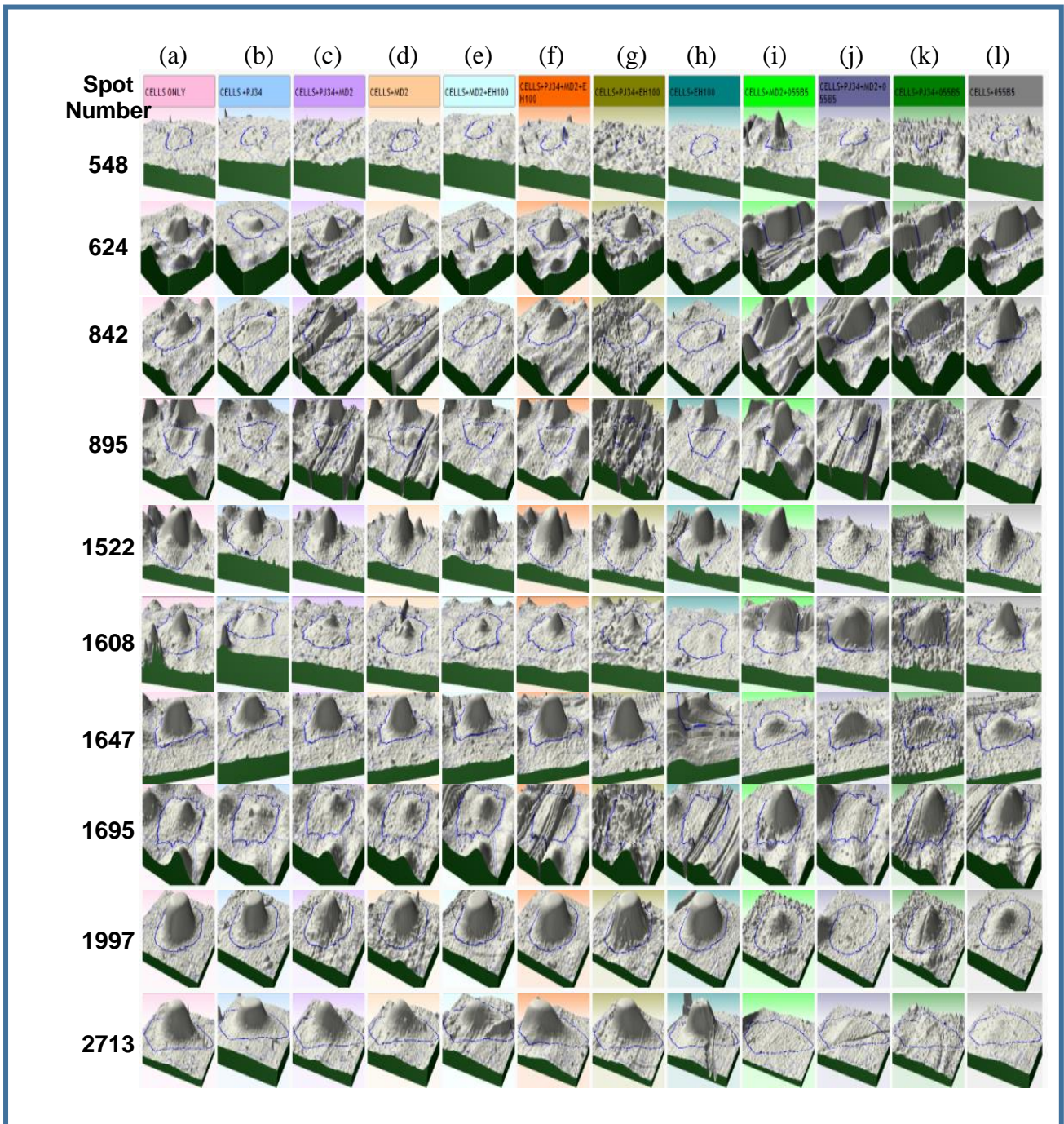


Figure 4-2 : The images for 3D spot graph analysed by Progenesis SameSpot software.

Three-dimensional spot graph showing the difference between 10 spots as the treatment done on THP-1 cells which stimulated with rough LPS EH100 and smooth LPS O55:B5 in presence and absence of Myeloid Differentiation 2 (MD2), also presence and absence PARP inhibitor PJ34, which represent a significant changes with different conditions, some spots disappeared, and some significantly highlighted. The conditions in order:

(a) THP-1, (b) THP-1+PJ34, (c) THP-1+PJ34+MD2, (d) THP-1+MD2, (e) THP-1+MD2+EH100, (f) THP-1+PJ34+MD2+EH100, (g) THP-1+PJ34+EH100, (h) THP-1+EH100, (i) THP-1+MD2+O55:B5, (j) THP-1+PJ34+MD2+O55:B5, (k) THP-1+PJ34+O55:B5, (l) THP-1+O55:B5.

Spot Number	THP1 CELLS as a reference	THP1 + PJ34	THP1+ PJ34 BLOCKING MD2	THP1 BLOCKING MD2	THP1 BLOCKING MD2 + RUOGH LPS EH100	THP1+ PJ34 BLOCKING MD2 + RUOGH LPS EH100	THP1 + PJ34 + RUOGH LPS EH100	THP1 + PJ34 + RUOGH LPS EH100	THP1 BLOCKING MD2 + SMOOTH LPS 055:B5	THP1 +PJ34 BLOCKING MD2 + SMOOTH LPS 055:B5	THP1 +PJ34 + SMOOTH LPS 055:B5	THP1 +PJ34 + SMOOTH LPS 055:B5
548	-	-	-	-	-	-	-	-	+	-	-	-
624	+++	+	++	++	++	++	++	+	++++	++++	++++	++++
842	+	-	+	-	-	+	-	-	+++	+++	+++	+++
895	-	-	-	-	-	-	-	-	+++	++	++	++
1522	+++	++	+++	+++	+++	+++	+++	+++	+++	+	+	++
1608	++	-	+	+	+	+	+	-	+++	+++	+++	+++
1647	+++	+++	+++	+++	+++	+++	++++	+++	+	++	+	+
1695	+	-	+	+	+	+	-	-	+++	-	+++	+++
1997	++++	++++	+++	++++	++++	++++	++++	++++	+	-	+	+
2713	++++	++++	+++	+++	+++	++++	++++	++++	-	-	-	-

Table 4-1 : The table represent a comparison of the number of spots by Prognosis sameSpot software

The THP1-1 cells stimulated with rough LPS EH100 and smooth LPS O55:B5 in presence and absence of Myeloid Differentiation 2 (MD2), also presence and absence PARP inhibitor PJ34 A plus sign (+) indicates the presence of spots or increase of spot size as the conditions used. A minus sign (-) indicates the absence of spots.

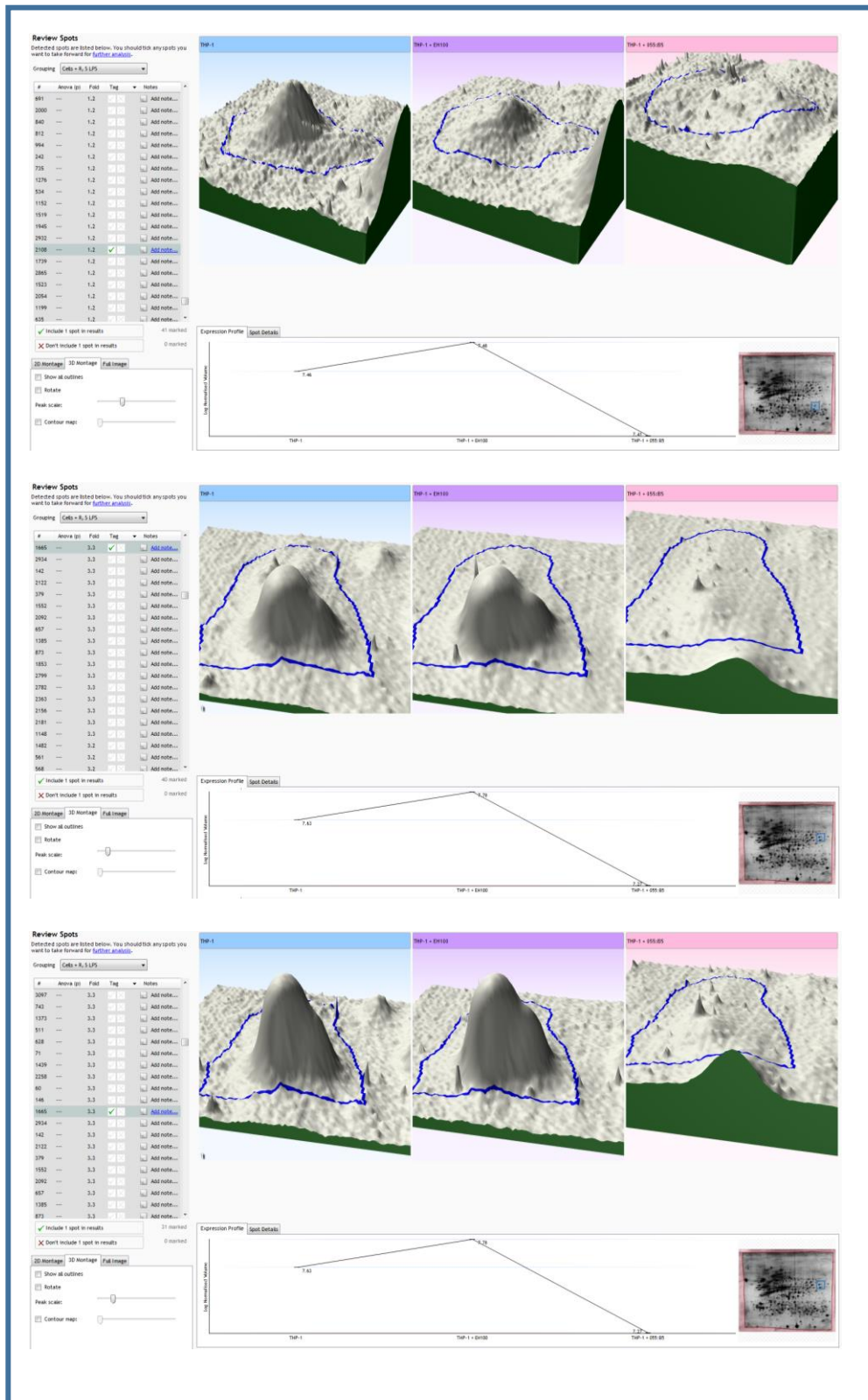


Figure 4-3 : 3D spot graph analysis using Progenesis SamSpot software.

Three-dimensional spot graph represent the difference between untreated THP-1 cells (control) and treated cells with rough (EH100) and smooth (055:B5) lipopolysaccharides (LPS). The images represent the significant effect of (055:B5) in in three different spots in the gel 2108, 1665, 2934.

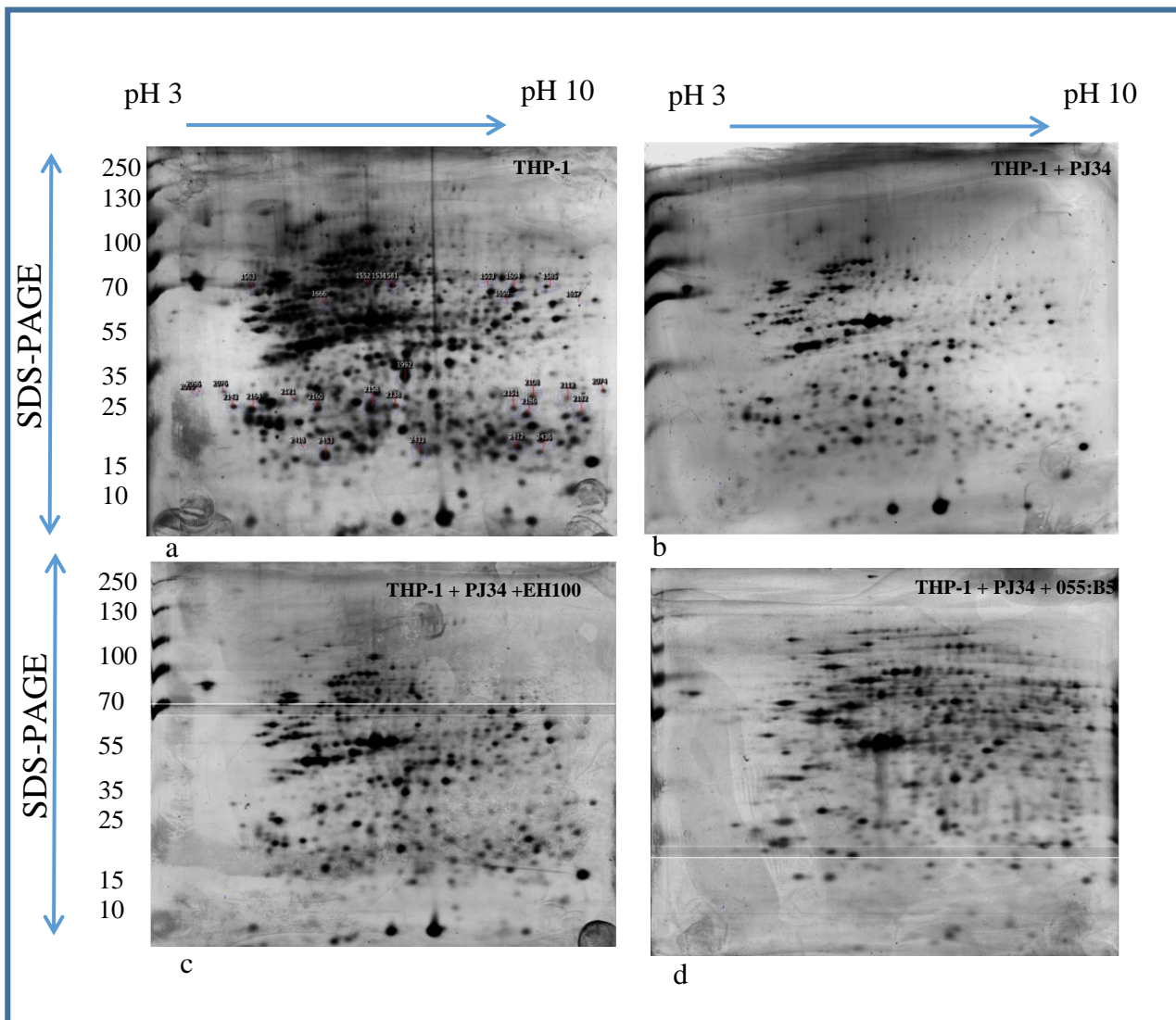


Figure 4-4 : Representative 2D gel images of total cell proteins from THP-1 cells untreated and treated with PJ34 stimulate the cells by rough (EH100) and smooth (055:B5) lipopolysaccharides (LPS).

(a)Control (untreated) THP-1 cells only, in 10% FCS RPMI medium. (b) THP-1 cells treated with 100 ng/ml PJ34. (c) THP-1 cells treated with 100 ng/ml PJ34 and stimulated with Rough LPS (EH100). (d) THP-1 cells treated with 100 ng/ml PJ34 and stimulated with Smooth LPS (055:B5). (a) Selected protein spots in four gels were marked by Progenesis SamSpot software as shown in numbers.

All incubations were for 24 hrs. In the first dimension, 50 µg total soluble protein was separated on immobiline IPG strips (18 cm, pH 3-10 NL). Isoelectric focussing was performed using the IPG Phor unit. The second dimension was performed on 12% SDS-PAGE gels, with image analysis carried out using Progenesis SameSpot software. M-Molecular mass standards are shown on the left side.

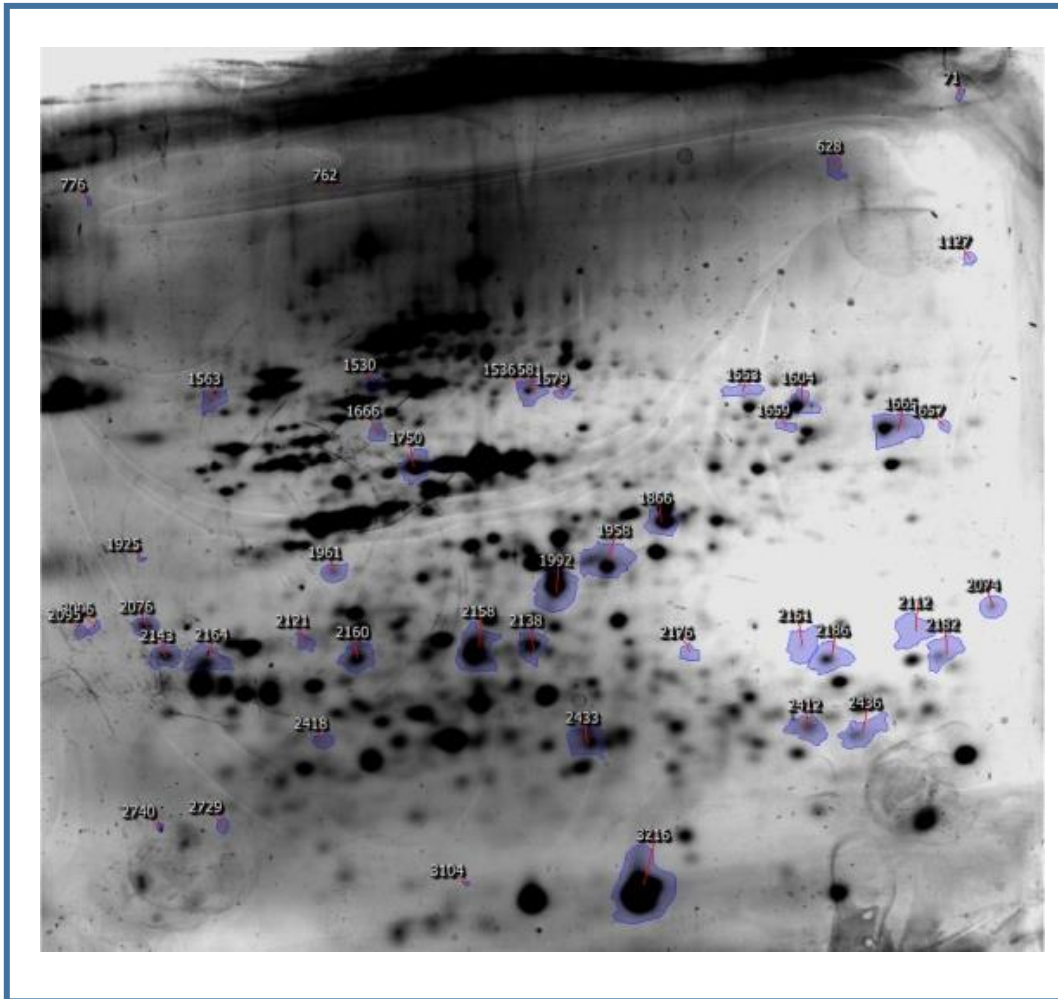


Figure 4-5 : The SamSpot software indicates the protein spots on gels marked by Progenesis SamSpot software as shown in numbers.

In the twelve conditions gels, the proteins spots marked with numbers to be easy compared with each other's, if we need more analysis.

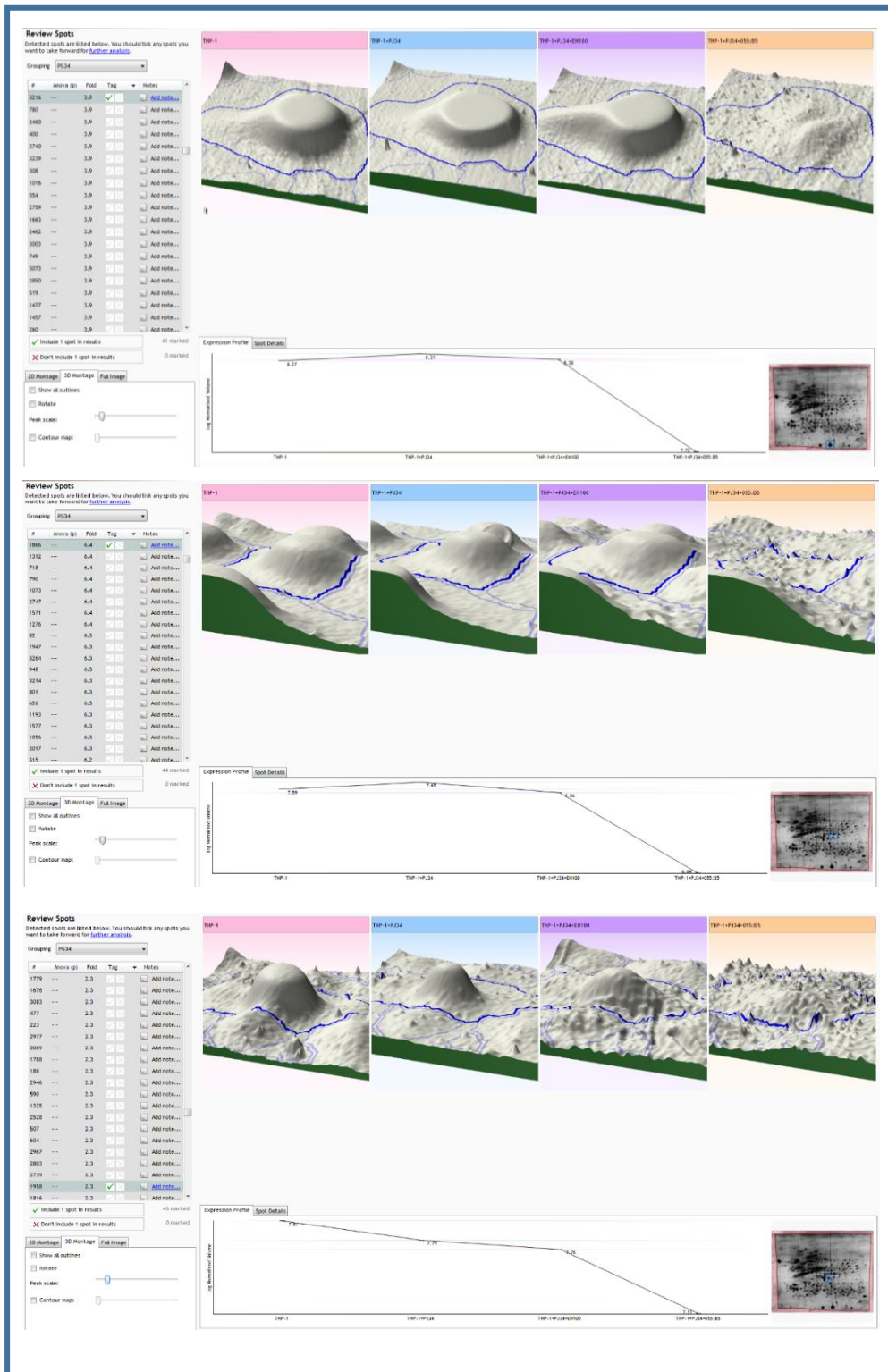


Figure 4-6 : 3D spot graph analysis using Progenesis SamSpot software.

Three dimensional spot graph represent the difference between untreated THP-1 cells (control) and treated with inhibitor PARP (PJ34) and after stimulate the cells by rough (EH100) and smooth (055:B5) lipopolysaccharides (LPS) for the spots number 3216, 1866, 1958. The images represent the significant effect of (055:B5).

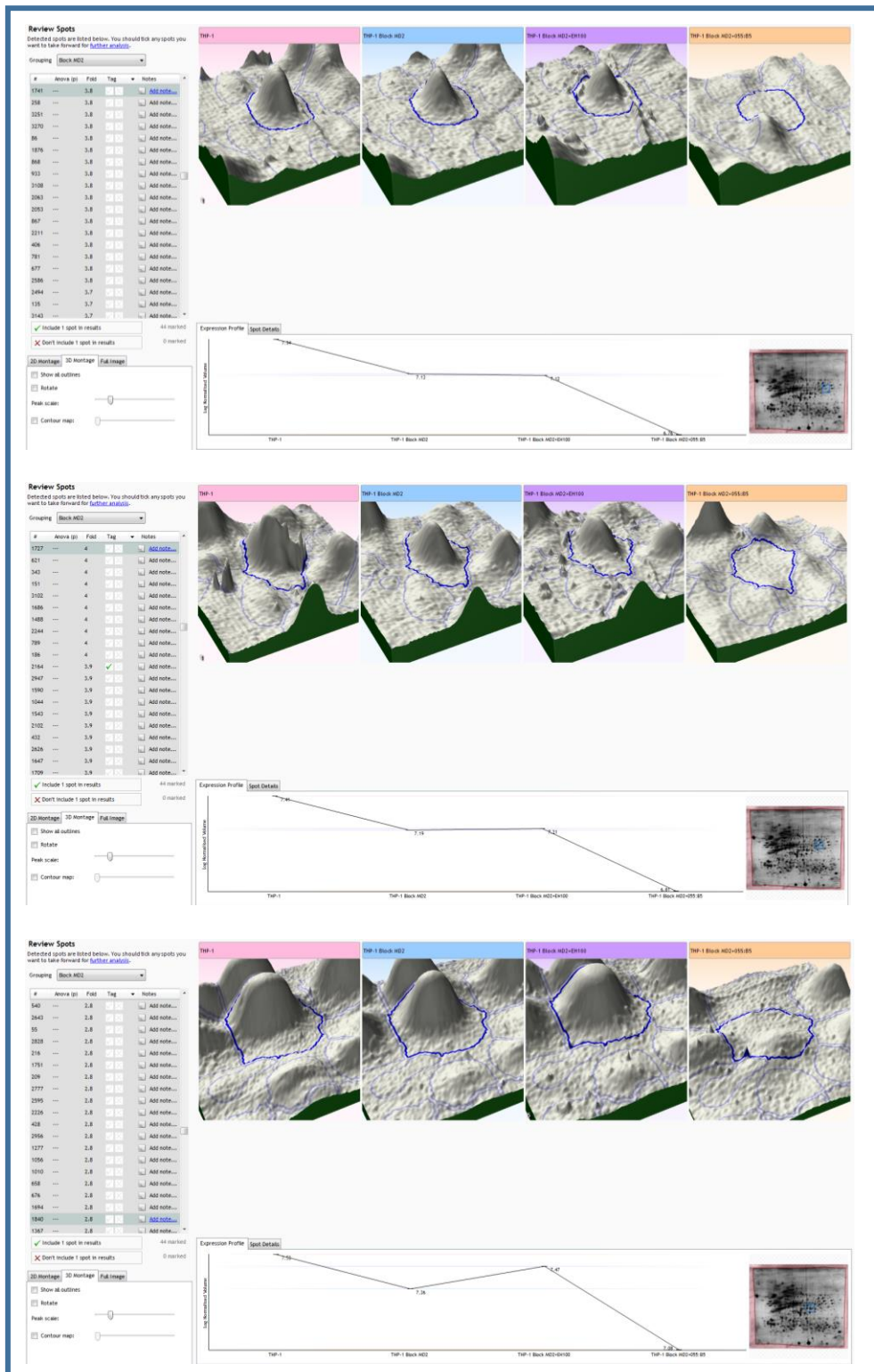


Figure 4-7 : 3D spot graph analysis using Progenesis SamSpot software.

Three-dimensional spot graph represent the difference between untreated THP-1 cells (control) and MD2 was blocked, in the case of stimulate the cells by rough (EH100) and smooth (055:B5) lipopolysaccharides (LPS). The images represent a significant effect of (055:B5) in three different spots in the gel 1741, 2164, 1840.

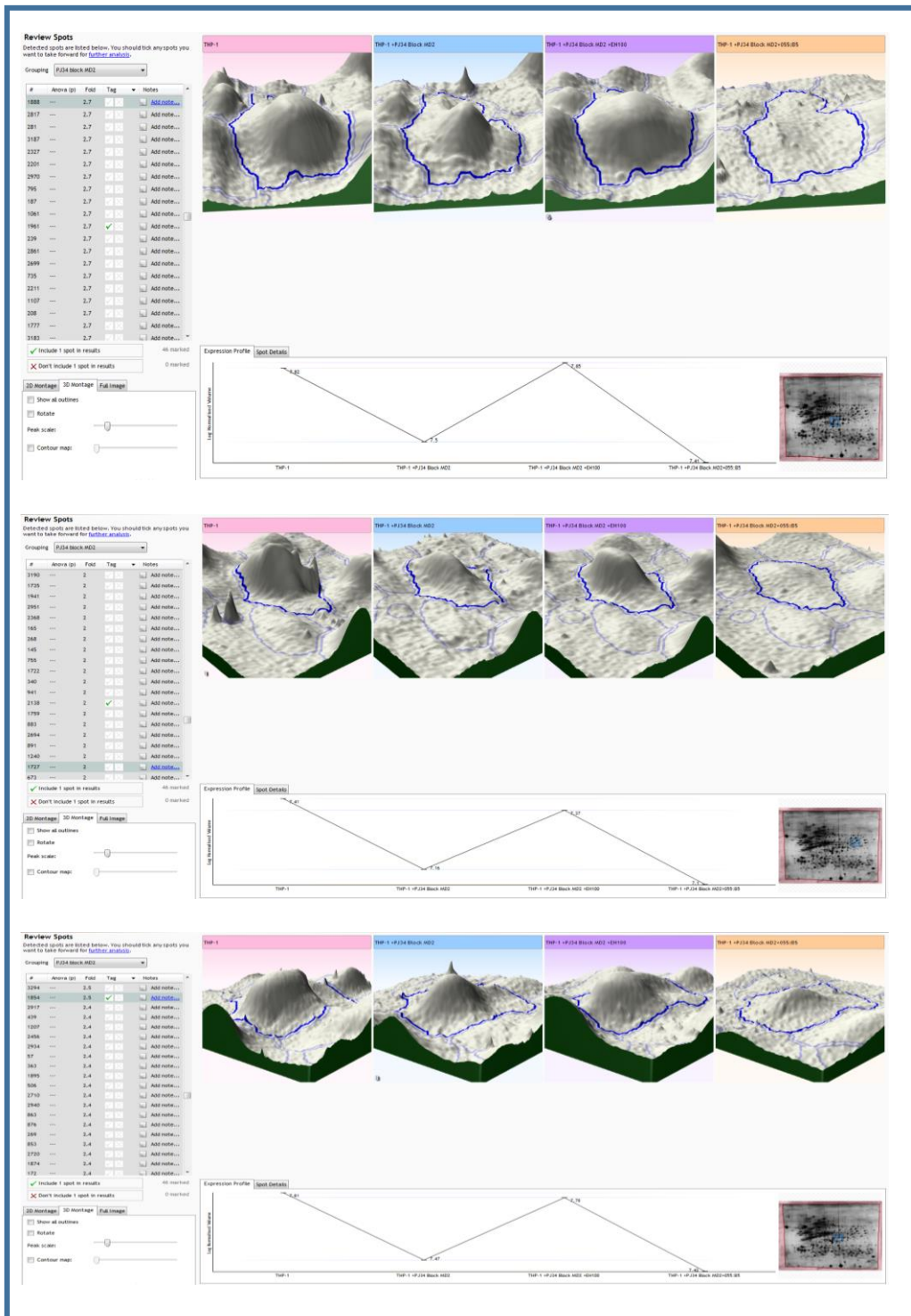


Figure 4-8 : 3D spot graph analysis using Progenesis SamSpot software.

Three-dimensional spot graph represent the difference between untreated THP-1 cells (control) and treated cells with PARP inhibitor (PJ34) when MD2 was blocked, in the case of stimulate the cells by rough(EH100) and smooth(055:B5) lipopolysaccharides (LPS). The images represent the significant effect of (055:B5) in three different spots in the gel 1961, 2138, 1854.

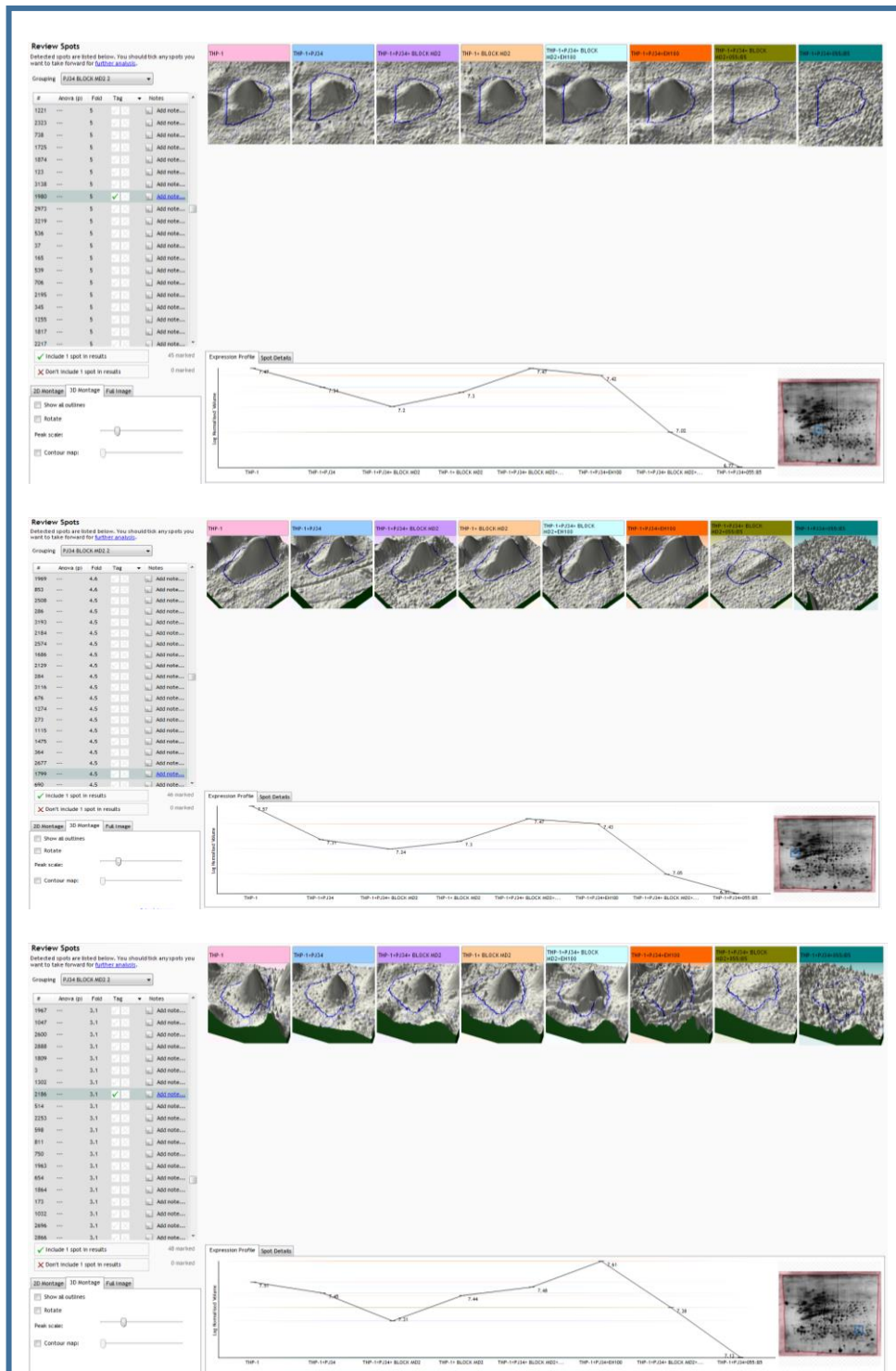


Figure 4-9 : 3D spot graph analysis using Progenesis SamSpot software.

Three-dimensional spot graph represent the difference between untreated THP-1 cells (control) and treated cells with PARP inhibitor (PJ34) when MD2 was blocked, in the case of stimulate the cells by rough (EH100) and smooth(055:B5) lipopolysaccharides (LPS). The images represent the significant effect of (055:B5) in three different spots in the gel 1980, 1799, 2186. The images represent the significant similarity in most of the spots and clearly effect of the samples treated with (055:B5).

Spot number	842	Function
Protein found	Transcription termination factor 2	DsDNA-dependent ATPase which acts as a transcription termination factor by coupling ATP hydrolysis with removal of RNA polymerase II from the DNA template. May contribute to mitotic transcription repression. May also be involved in pre-mRNA splicing.
Gene	TTF2	
Subcellular location	Nucleus	
pI range	8.5- 8.7	
MW range Dalton	130,000-+0.2%	
Spot number	1695	
Protein found	Pre-mRNA-processing factor 19	Ubiquitin-protein ligase which is a core component of several complexes mainly involved pre-mRNA splicing and DNA repair. Required for pre-mRNA splicing as component of the spliceosome.
Gene	PRPF19	
Subcellular location	Nucleus Cytoskeleton Cytoplasm	
pI range	6 - 6.1	
MW range Dalton	55,000 -+0.2%	
Spot number	2713	
Protein found	Diamine acetyltransferase	Ubiquitin-protein ligase which is a core component of several complexes mainly involved pre-mRNA splicing and DNA repair. Required for pre-mRNA splicing as component of the spliceosome.
Gene	SAT1	
Subcellular location	Cytoplasm	
pI range	5 - 5.2	
MW range Dalton	20,000 -+0.2%	

Table 4-2 : The 3D proteins spots analysed by the IP and molecular weight information by using EXpasY software website, <https://uniprot.org/uniprot/>

This software helps the researchers to identify the proteins by downloading digital information to represent the closest information needed about the protein detected.

4.1.7 Conclusions

The twelve conditions of 2-D gels were analysed by loading them in Progenesis SameSpot software, exposing a huge number of polypeptides expressed with presence and absence of MD2 and PARP inhibitor (PJ34), all done when THP-1 cells stimulated by rough (EH100) and smooth (055:B5) LPS for 24 hours. Some spots were not presented in samples stimulated with smooth (055:B5), even the one treated by PJ-34 for 30 minutes, which indicated that the smooth LPS is more effective than the rough LPS, especially in this study. In addition, we found that PJ-34 PARP inhibitor imparts a protective effect, allowing sustained cell survival after LPS was targeted. Further study of the polypeptide proteins found to be differentially expressed is now necessary in order to establish their role in sepsis, and to assess the role of PJ-34 in cell survival during LPS-induced toxemia.

By searching and comparing different spots in the gel, then found the similar one, the three dimensional spot graphs analysis represent clearly the significant effect of the smooth LPS 055:B5 in the expression profile. This technique inspires the researcher to explore the protein in those spots by using the mass spectrometry test or the digital one through the proteins data base website such as ExPASy (Table 4-2).

**Chapter 5 Co-localisation study by using laser confocal
microscope**

5 Co-localisation study by using laser confocal microscope

5.1 The importance of MD2 detected by Bioimaging by confocal microscopy

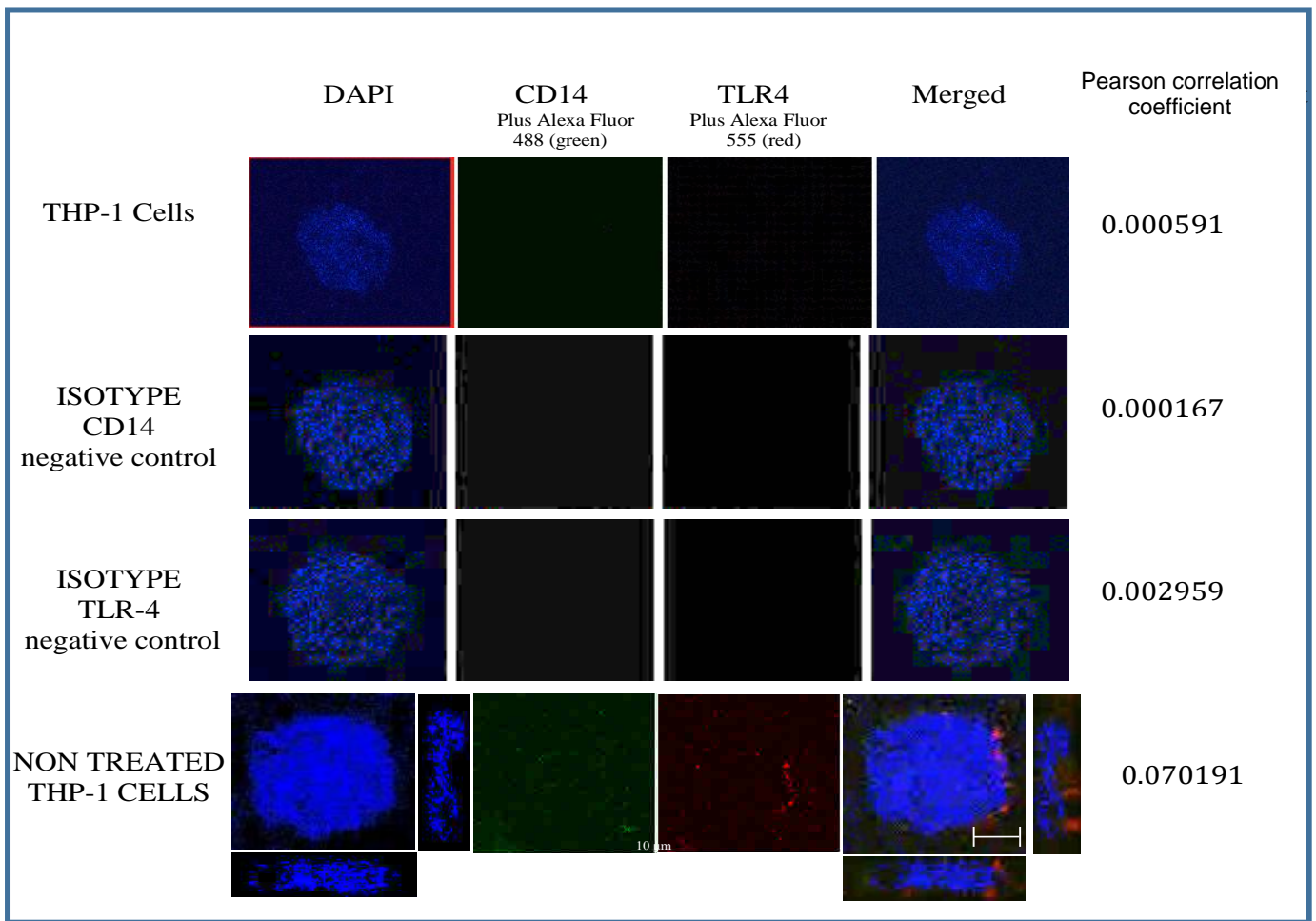
5.1.1 Introduction

The confocal laser scanning microscopy is a scientific technique to show a high resolution cells images, in two and three dimensions. Nikon A1si confocal microscope was used. Co-localisation of fluorescent signals from two or more different proteins is an indicator of their association and potential interaction the co-localisation measures by Pearson correlation coefficient is one of the most common co-localisation measurement methods.

THP-1 cells were cultured on cover slips, sized 2 cm² and 0.13 thickness at a density of 25 x10³ cells per well for 72 hours after treated by 5 ng of PMA to be macrophage-like cells as a mature cells. We investigate the importance of Myeloid Differentiation2 (MD2) interacts between CD14 and TLR-4 when treated by rough EH100 and smooth 055:B5 lipopolysaccharides. The cells washed and stained as the samples coverslips with isotype control, mouse IgG1 as primary antibody with Alexa Fluor 488 and mouse IgG2 as primary antibody with Alexa Fluor 555 secondary antibodies, visualised by using green 488 nm and red 555 nm wavelength lasers to measure non-specific antibody binding. Blue colour shows 4', 6-diamidino-2-phenylindole (DAPI). DAPI stained cell's nuclei. Red and Green shows merged image. Co-localisation of CD14 and TLR4 on the cell-surface of THP-1 cells are shown in treated cells.

5.1.2 Results

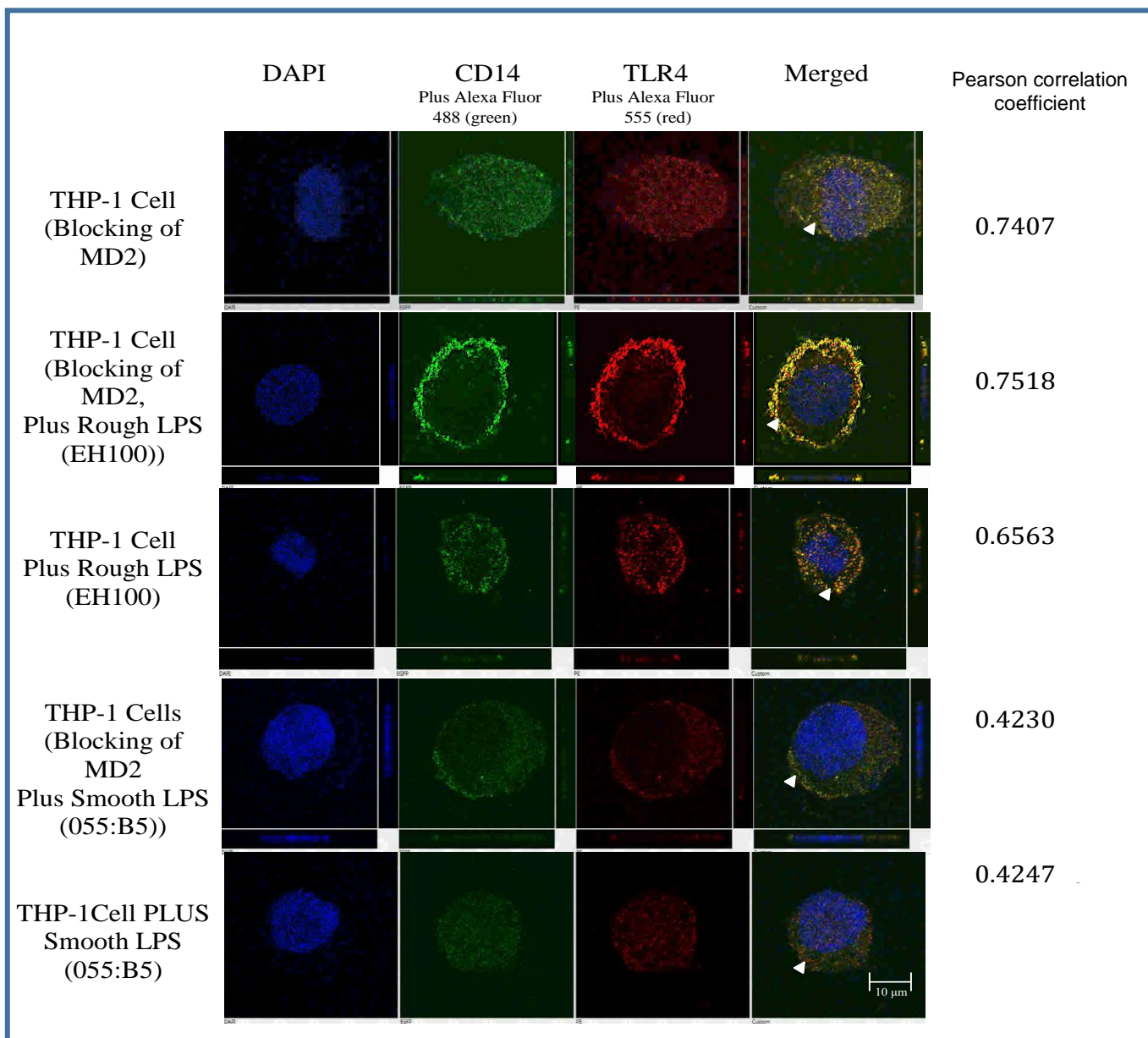
NIS-Elements software (version 3.21.03) was used for image processing. CD14 (green) and TLR4 (red) channels were segmented using regional maximum detection tools followed by manual threshold. The generated binary areas were visually inspected; the overlap of the green and red channels was generated by the overlay tool, resulting in a new layer (orange or yellow) as shown at (Figure 5-1B) that represents the crossing of CD14 and TLR4. The automated volume measurement was carried out for them and their crossing. The description of the figures is followed in the legends,



A

Figure 5-1A: Co-localisation of CD14 and TLR-4 on the THP-1 cell-surface, examined by confocal laser scanning microscopy

THP-1 cells were cultured on cover slips 2 cm² and 0.13 thickness at a density of 10 x10⁴ cells per well for 72h. We investigate whether the importance of Myeloid Differentiation2 (MD2) to interact between CD14 and TLR-4 treated by rough EH100 and smooth 055:B5 lipopolysaccharides. (A) Shows Isotype representing cells stained with isotype control, mouse IgG1 primary and Alexa Fluor 488 and mouse IgG2 primary and Alexa Fluor 555 secondary antibodies, visualised by using green 488 nm and red 555 nm wavelength lasers to measure non-specific antibody binding. Blue colour shows 4', 6-diamidino-2-phenylindole (DAPI). DAPI stained cell's nuclei. Red and Green shows merged image. Co-localisation of CD14 and TLR4 on the cell-surface of THP-1 cells is shown in treated cells.



B

Figure 5-1B: Co-localisation of CD14 and TLR-4 on the THP-1 cell-surface, examined by confocal laser scanning microscopy

THP-1 cells were cultured on cover slips 2 cm² and 0.13 thickness at a density of 10 x10⁴ cells per well for 72h. We investigate whether the importance of Myeloid Differentiation2 (MD2) to interact between CD14 and TLR-4 treated by rough EH100 and smooth 055:B5 lipopolysaccharides.

[B] Co-localisation of CD14 and TLR4 on the cell-surface of THP-1 cells is shown THP-1 cells were double stained with CD14 primary antibody labelled with Alexa Fluor 488 (green) and with TLR-4 primary antibody labelled with Alexa Fluor 555 (red). Co-localisation is shown as Yellow/orange, fluorescence shows the potential co-localisation of two antigens which are the result of merging green and red channels, highly co-localised area of CD14 and TLR-4 is shown in specific slides which will be analysed by another application.

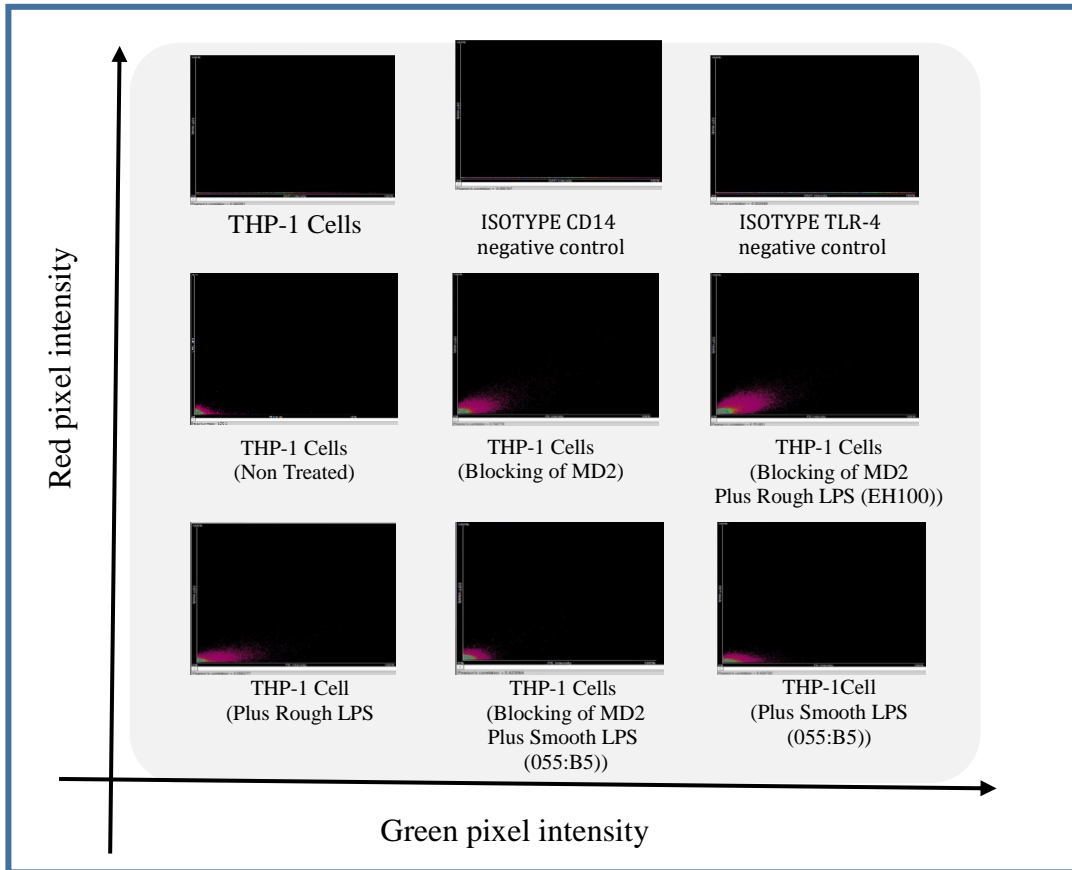


Figure 5-2: Co-localisation analysis of CD14 and TLR-4 by Pearson's coefficient correlation using a scatter plot on THP-1 Cells.

Each pixel in the image was plotted in the scatter diagram based on its intensity level in each channel. The colour in the scatterplot signifies the number of pixels plotted in that region. Green intensity is shown on the x-axis and red intensity is shown on the y-axis. The Pearson's correlation coefficient (PCC) was calculated based on different images and indicates Co-localisation of CD14 and TLR-4 on THP-1 cells.

5.2 Co-localisation of TLR-4 and MD2 with HMGB1 on the cell-surface of THP-1 cells.

5.2.1 Introduction

To demonstrate the cellular relation between the HMGB1 and the TLR-4 or MD2 in case of infection with rough and smooth LPS, THP-1 cells were cultured on square cover slips 2 cm², at a density of 10 x10⁴ cells per well for 72h. We investigate whether the importance of Myeloid Differentiation2 (MD2), (TLR-4) and (HMGB1) treated for **(30, 60, and 120 min)** with rough EH100 and smooth 055:B5 lipopolysaccharides. Isotype representing cells stained with isotype control mouse IgG1 primary and Alexa Fluor 488 and Alexa Fluor 555 secondary antibodies, visualised by using green 488 nm and red 555 nm wavelength lasers to measure non-specific antibody binding. Blue colour shows 4', 6-diamidino-2-phenylindole (DAPI). DAPI stained cell's nuclei. Red and Green shows merged image. Co-localisation of TLR4 and HMGB1, MD2 and HMGB1 on the cell-surface of THP-1 cells are shown. THP-1 cells were double stained with TLR-4, MD2 primary antibodies labelled with Alexa Fluor 488 (green) and with HMGB1 secondary antibody labelled with Alexa Fluor 555 (red).

5.2.2 Results

NIS-Elements software (version 3.21.03) was used for image processing. TLR-4, MD2 (green), and HMGB1 (red) channels were segmented using regional maximum detection tools followed by manual threshold. The generated binary areas were visually inspected, the overlap of the green and red channels was generated by the overlay tool, resulting in a new layer (orange or yellow) as shown at (Figure 5-1, 5-2) that represents the crossing of (TLR4 and HMGB1) also the crossing of (MD2 and HMGB1). The automated volume measurement was carried out for them and their crossing.

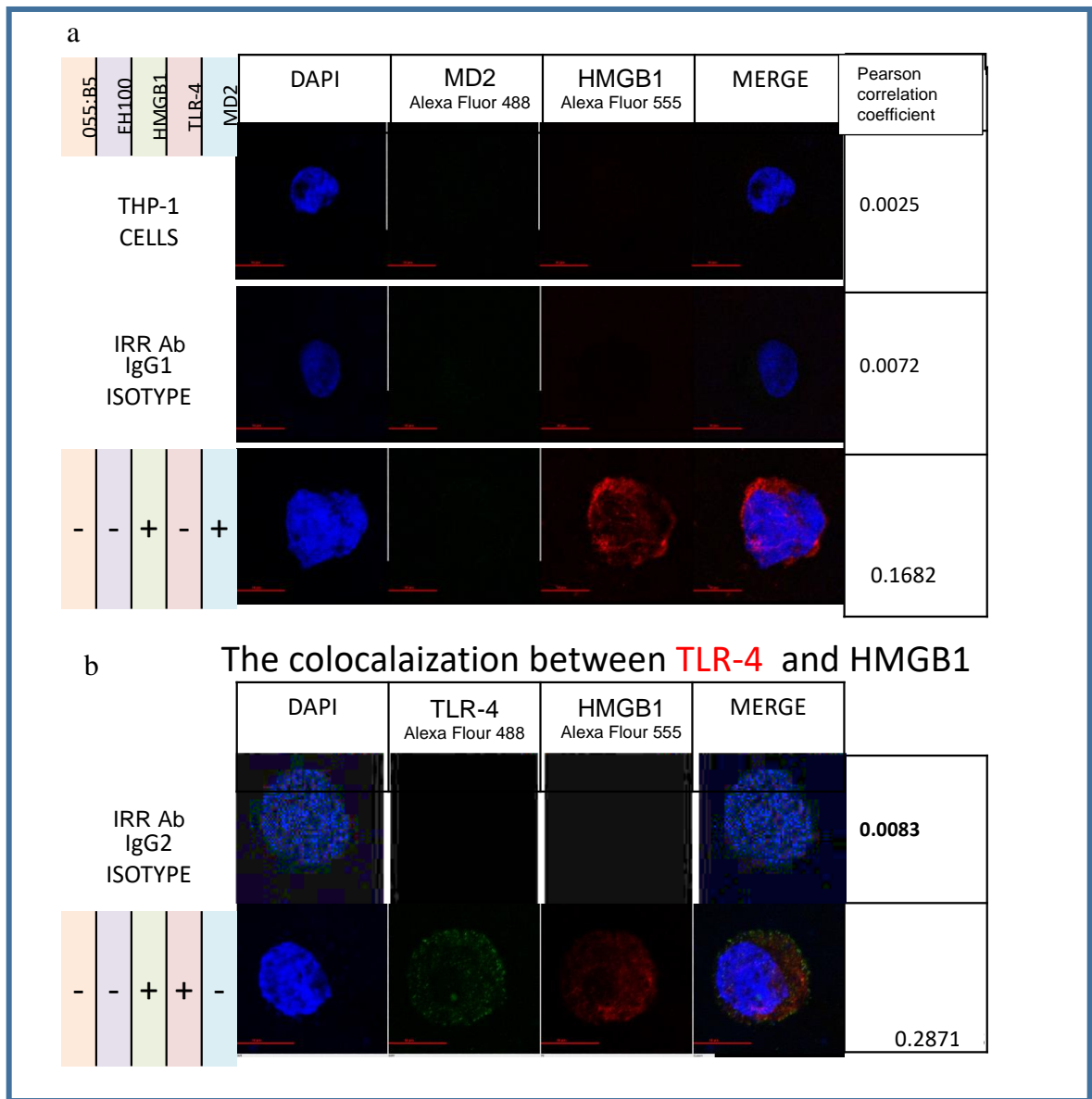


Figure 5-3: Co-localisation of (a) MD2 and HMGB1 and (b) TLR-4 and HMGB1 on the cell-surface of THP-1 cells for 30 min stimulation with rough EH100 and smooth 055:B5 LPS.

THP-1 cells were cultured on square cover slips 2 cm² at a density of 10 x10⁴ cells per well for 72h. We investigate whether the importance of Myeloid Differentiation2 (MD2), (TLR-4) and (HMGB1) treated for (30 min) by rough EH100 and smooth 055:B5 lipopolysaccharides. Isotype representing cells stained with isotype control mouse IgG1 primary and Alexa Fluor 488 and Alexa Fluor 555 secondary antibodies, visualised by using green 488 nm and red 555 nm wavelength lasers to measure non-specific antibody binding. Blue colour shows 4', 6-diamidino-2-phenylindole (DAPI). DAPI stained cell's nuclei. Red and Green shows merged image. Co-localisation of TLR4 and HMGB1, MD2 and HMGB1 on the cell-surface of THP-1 cells is shown. THP-1 cells were double stained with TLR-4, MD2 primary antibodies labelled with Alexa Fluor 488 (green) and with HMGB1 secondary antibody labelled with Alexa Fluor 555 (red). Co-localisation is shown as Yellow/orange, fluorescence shows the potential co-localisation of two antigens which are the result of merging green and red channels, (a) and (b) shown a controls with no co-localisation as isotype and some co-localised area of TLR4 and HMGB1, MD2 and HMGB1 is shown in specific slides.

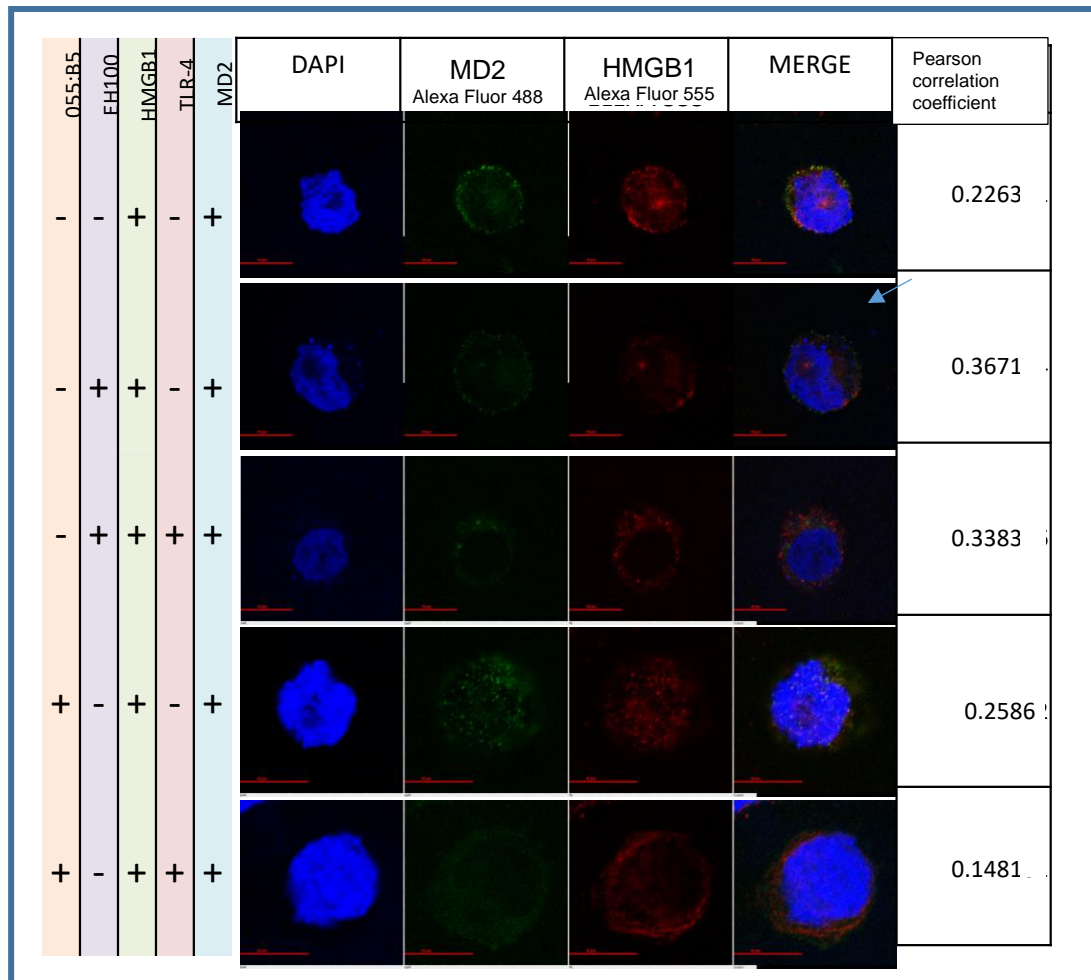


Figure 5-4: Co-localisation of MD2 and HMGB1 on the cell-surface of THP-1 cells for 30 min stimulation with rough EH100 and smooth 055:B5 LPS.

THP-1 cells were cultured on square cover slips 2 cm² at a density of 10 x10⁴ cells per well for 72h. We investigate whether the importance of Myeloid Differentiation2 (MD2) and (HMGB1) in presence and absence of (TLR-4) when treated for (30 min) by rough EH100 and smooth 055:B5 lipopolysaccharides. Isotype representing cells stained with isotype control mouse IgG1 primary and Alexa Fluor 488 and Alexa Fluor 555 secondary antibodies, visualised by using green 488 nm and red 555 nm wavelength lasers to measure non-specific antibody binding. Blue colour shows 4',6-diamidino-2-phenylindole (DAPI). DAPI stained cell's nuclei. Red and Green shows merged image. Co-localisation of TLR4 and HMGB1, MD2 and HMGB1 on the cell-surface of THP-1 cells are shown. THP-1 cells were double stained with MD2 antibody labelled with Alexa Fluor 488 (green) and with HMGB1 antibody labelled with Alexa Fluor 555 (red). Co-localisation is shown as Yellow/orange; fluorescence shows the potential co-localisation of two antigens, which are the result of merging green and red channels, the images above shown different levels of co-localisation area of MD2 and HMGB1.

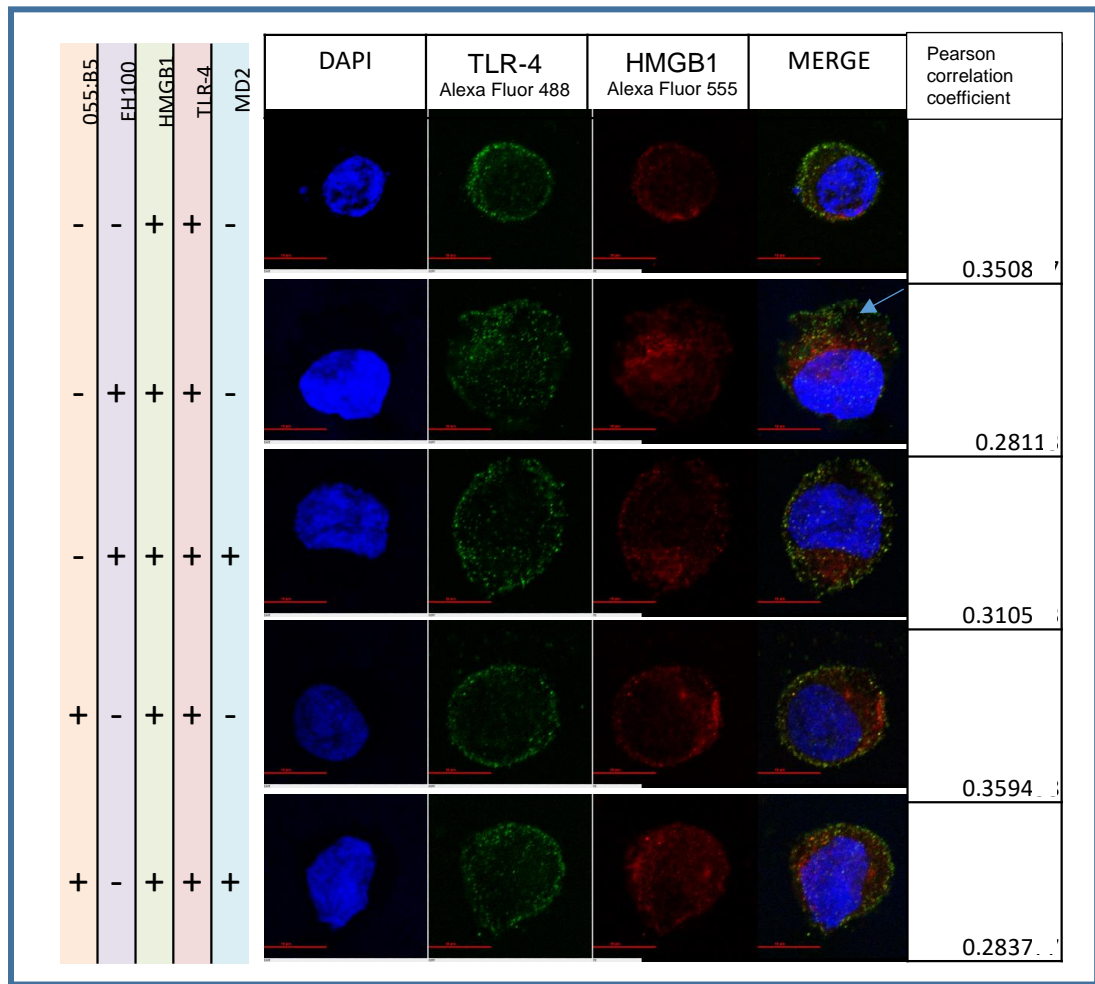


Figure 5-5: Co-localisation of TLR-4 and HMGB1 on the cell-surface of THP-1 cells for 30 min stimulation with rough EH100 and smooth 055:B5 LPS.

THP-1 cells were cultured on square cover slips 2 cm² at a density of 10 x 10⁴ cells per well for 72h. We investigate whether the (TLR-4) and (HMGB1) in presence and absence of (MD2) treated for **30 min** by rough EH100 and smooth 055:B5 lipopolysaccharides. Isotype representing cells stained with isotype control mouse IgG1 primary and Alexa Fluor 488 and Alexa Fluor 555 secondary antibodies, visualised by using green 488 nm and red 555 nm wavelength lasers to measure non-specific antibody binding. Blue colour shows 4', 6-diamidino-2-phenylindole (DAPI). DAPI stained cell's nuclei. Red and Green shows merged image. Co-localisation of TLR-4 and HMGB1 on the cell-surface of THP-1 cells are shown. THP-1 cells were double stained with TLR-4 antibody labelled with Alexa Fluor 488 (green) and with HMGB1 antibody labelled with Alexa Fluor 555 (red). Co-localisation is shown as Yellow/orange; fluorescence shows the potential co-localisation of two antigens, which are the result of merging green and red channels, the images above shown different levels of co-localisation area of MD2 and HMGB1.

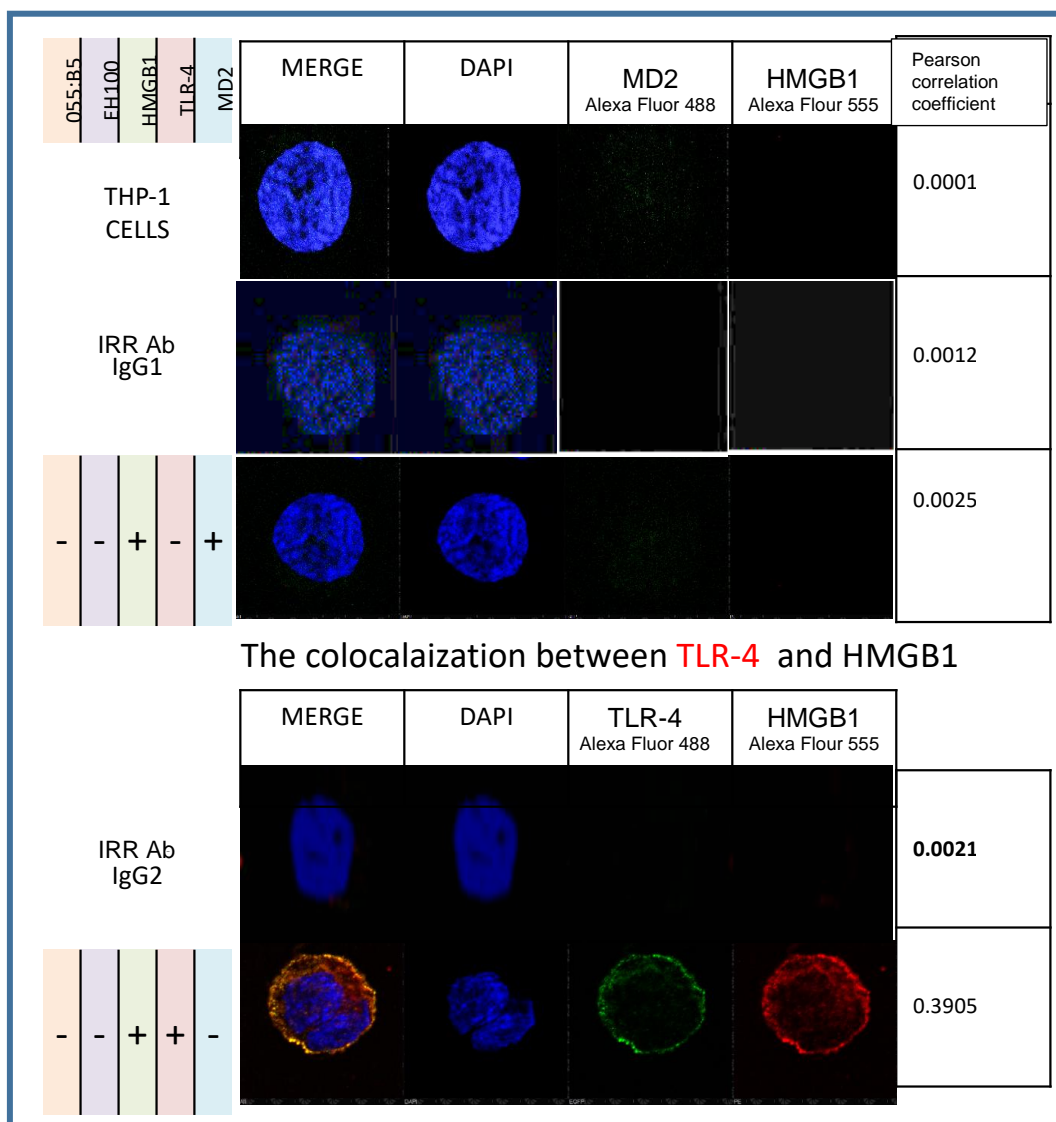


Figure 5-6: Co-localisation of (a) MD2 and HMGB1 and (b) TLR-4 and HMGB1 on the cell-surface of THP-1 cells for 60 min stimulation with rough EH100 and smooth 055:B5 LPS.

THP-1 cells were cultured on square cover slips 2 cm² at a density of 10 x10⁴ cells per well for 72h. We investigate whether the importance of Myeloid Differentiation2 (MD2), (TLR-4) and (HMGB1) treated for **60 min** by rough EH100 and smooth 055:B5 lipopolysaccharides. Isotype representing cells stained with isotype control mouse IgG1 primary and Alexa Fluor 488 and Alexa Fluor 555 secondary antibodies, visualised by using green 488 nm and red 555 nm wavelength lasers to measure non-specific antibody binding. Blue colour shows 4', 6-diamidino-2-phenylindole (DAPI). DAPI stained cell's nuclei. Red and Green shows merged image. Co-localisation of TLR4 and HMGB1, MD2 and HMGB1 on the cell-surface of THP-1 cells are shown. THP-1 cells were double stained with TLR-4, MD2 primary antibodies labelled with Alexa Fluor 488 (green) and with HMGB1 secondary antibody labelled with Alexa Fluor 555 (red). Co-localisation is shown as Yellow/orange, fluorescence shows the potential co-localisation of two antigens which are the result of merging green and red channels, (a) and (b) shown a controls with no co-localisation as isotype and some co-localised area of TLR4 and HMGB1, MD2 and HMGB1 is shown in specific slides.

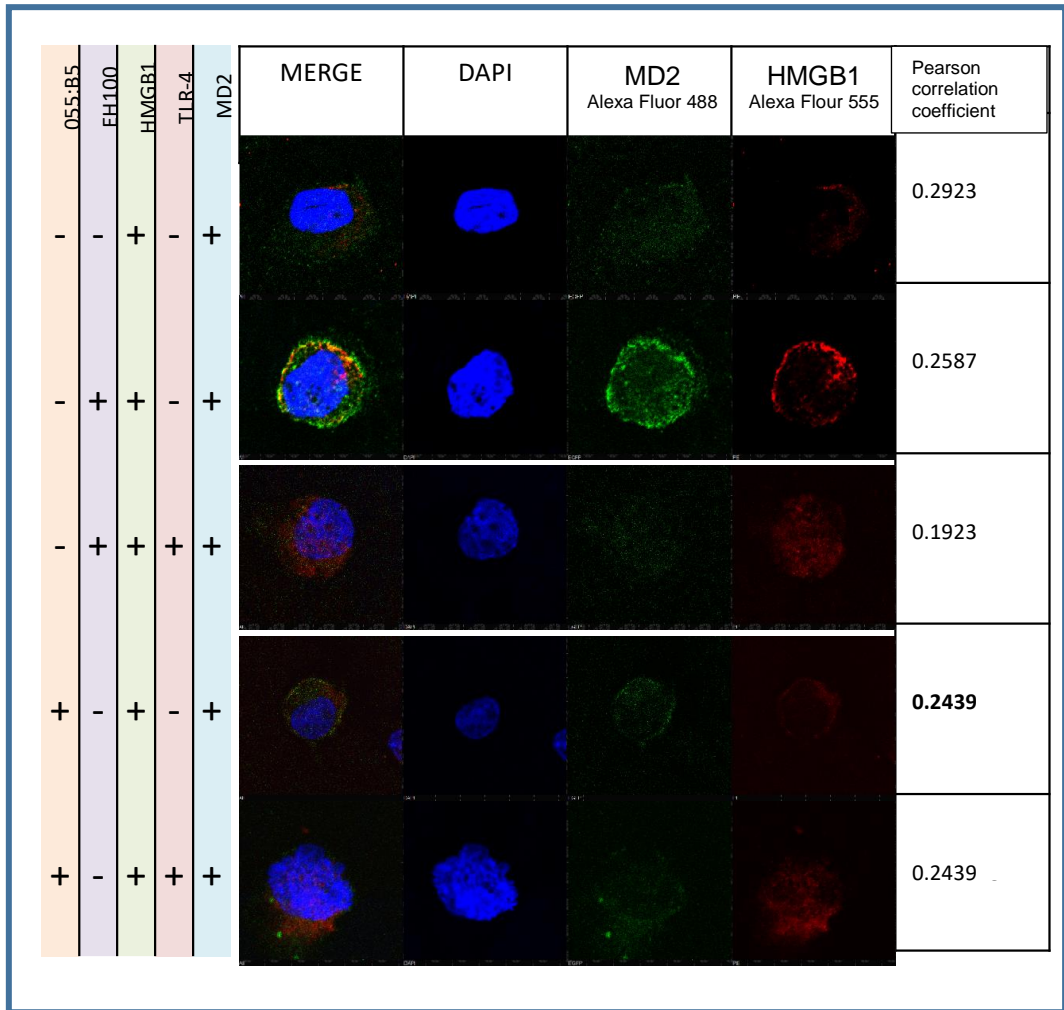


Figure 5-7: Co-localisation of MD2 and HMGB1 on the cell-surface of THP-1 cells for 60 min stimulation with rough EH100 and smooth 055:B5 LPS.

THP-1 cells were cultured on square cover slips 2 cm² at a density of 10 x10⁴ cells per well for 72h. We investigate whether the importance of Myeloid Differentiation2 (MD2) and (HMGB1) in presence and absence of (TLR-4) when treated for (60 min) by rough EH100 and smooth 055:B5 lipopolysaccharides. Isotype representing cells stained with isotype control mouse IgG1 primary and Alexa Fluor 488 and Alexa Fluor 555 secondary antibodies, visualised by using green 488 nm and red 555 nm wavelength lasers to measure non-specific antibody binding. Blue colour shows 4', 6-diamidino-2-phenylindole (DAPI). DAPI stained cell's nuclei. Red and Green shows merged image. Co-localisation of TLR4 and HMGB1, MD2 and HMGB1 on the cell-surface of THP-1 cells are shown. THP-1 cells were double stained with MD2 antibody labelled with Alexa Fluor 488 (green) and with HMGB1 antibody labelled with Alexa Fluor 555 (red). Co-localisation is shown as Yellow/orange; fluorescence shows the potential co-localisation of two antigens, which are the result of merging green and red channels, the images above shown different levels of co-localisation area of MD2 and HMGB1.

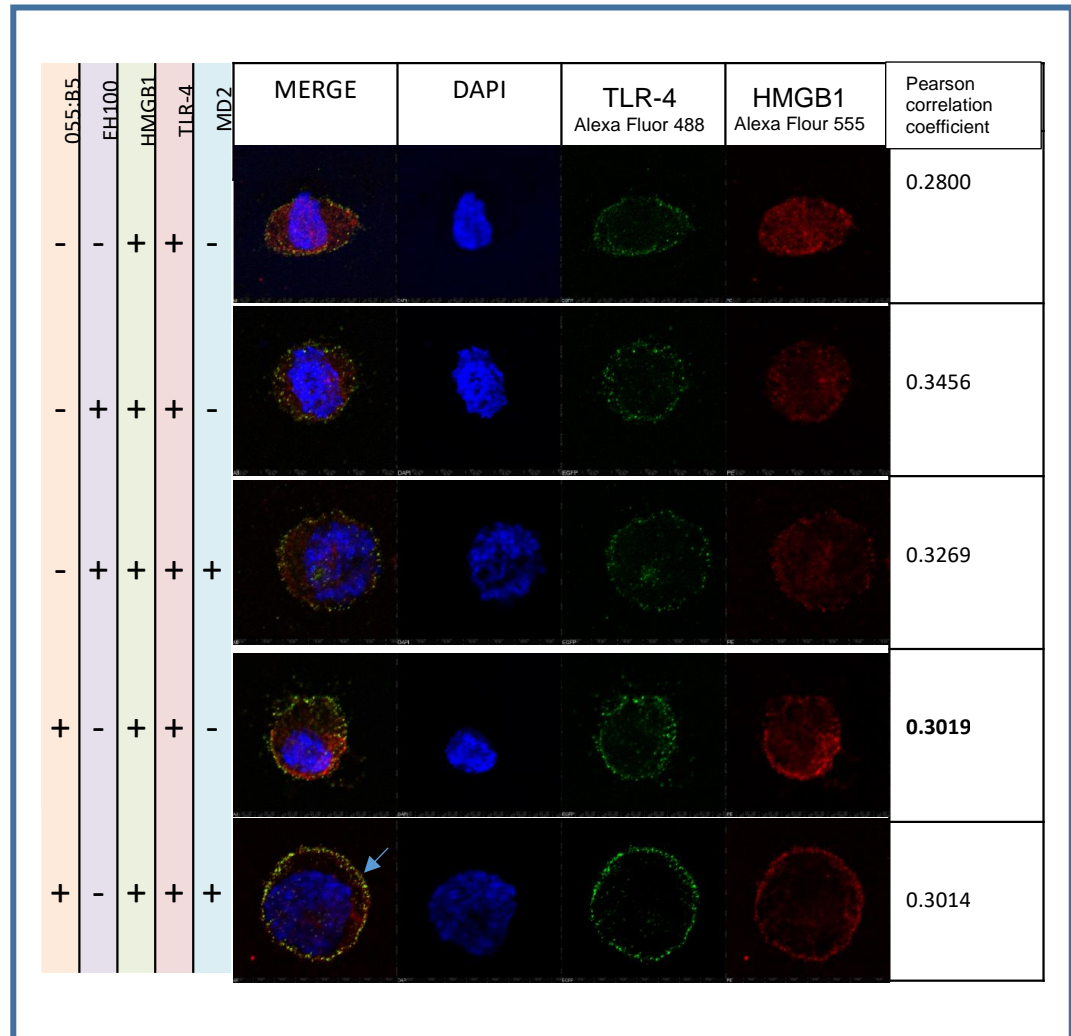


Figure 5-8: Co-localisation of TLR-4 and HMGB1 on the cell-surface of THP-1 cells for 60 min stimulation with rough EH100 and smooth 055:B5 LPS.

THP-1 cells were cultured on square cover slips 2 cm² at a density of 10 x10⁴ cells per well for 72h. We investigate whether the (TLR-4) and (HMGB1) in presence and absence of (MD2) treated for (60 min) by rough EH100 and smooth 055:B5 lipopolysaccharides. Isotype representing cells stained with isotype control mouse IgG1 primary and Alexa Fluor 488 and Alexa Fluor 555 secondary antibodies, visualised by using green 488 nm and red 555 nm wavelength lasers to measure non-specific antibody binding. Blue colour shows 4', 6-diamidino-2-phenylindole (DAPI). DAPI stained cell's nuclei. Red and Green shows merged image. Co-localisation of TLR-4 and HMGB1 on the cell-surface of THP-1 cells are shown. THP-1 cells were double stained with TLR-4 antibody labelled with Alexa Fluor 488 (green) and with HMGB1 antibody labelled with Alexa Fluor 555 (red). Co-localisation is shown as Yellow/orange; fluorescence shows the potential co-localisation of two antigens, which are the result of merging green and red channels, the images above shown different levels of co-localisation area of MD2 and HMGB1.

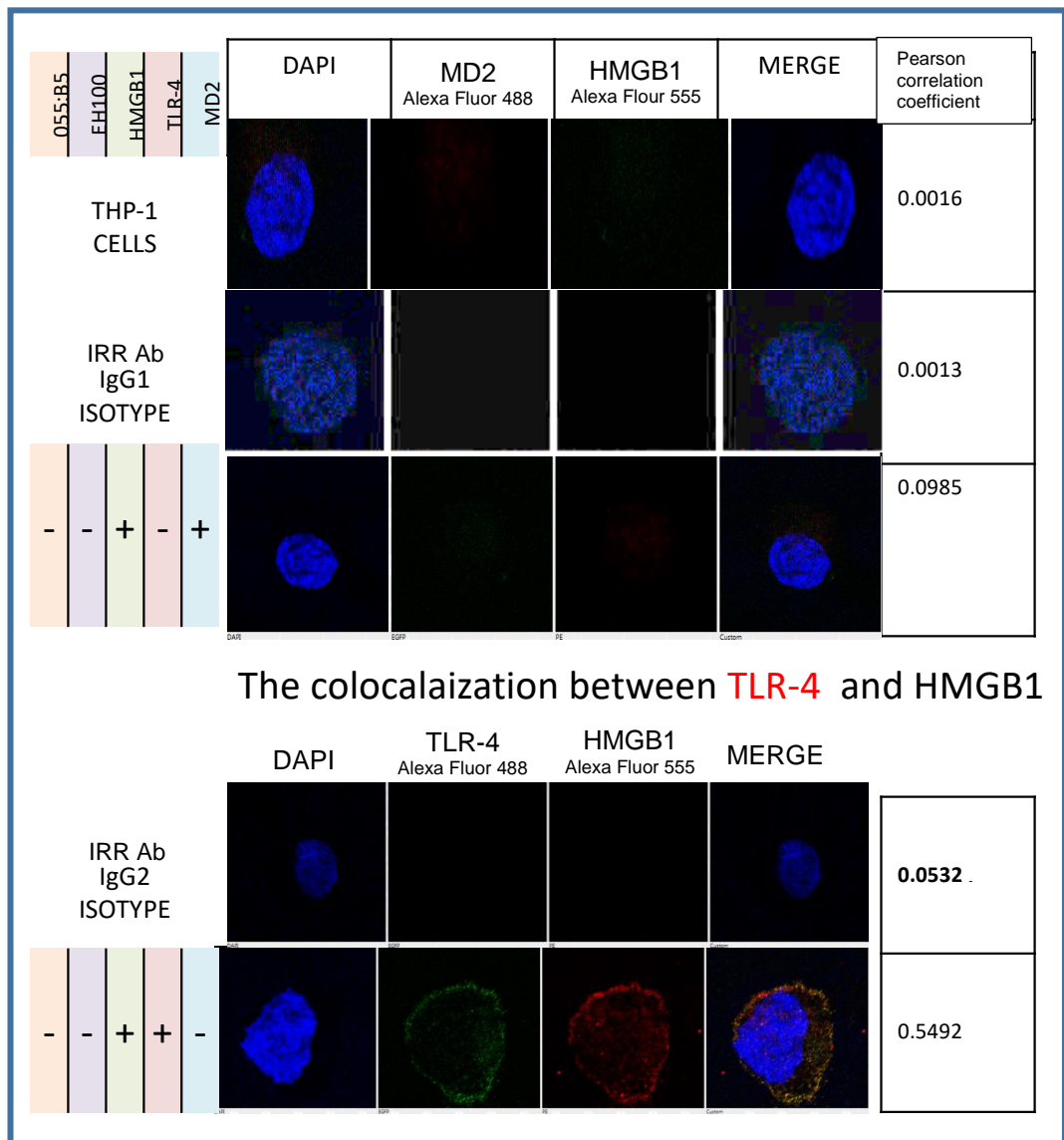


Figure 5-9: Co-localisation of (a) MD2 and HMGB1 and (b) TLR-4 and HMGB1 on the cell-surface of THP-1 cells for 120 min stimulation with rough EH100 and smooth 055:B5 LPS.

THP-1 cells were cultured on square cover slips 2 cm² at a density of 10 x 10⁴ cells per well for 72h. We investigate whether the importance of Myeloid Differentiation2 (MD2), (TLR-4) and (HMGB1) treated for **120 min** by rough EH100 and smooth 055:B5 lipopolysaccharides. Isotype representing cells stained with isotype control mouse IgG1 primary and Alexa Fluor 488 and Alexa Fluor 555 secondary antibodies, visualised by using green 488 nm and red 555 nm wavelength lasers to measure non-specific antibody binding. Blue colour shows 4', 6-diamidino-2-phenylindole (DAPI). DAPI stained cell's nuclei. Red and Green shows merged image. Co-localisation of TLR4 and HMGB1, MD2 and HMGB1 on the cell-surface of THP-1 cells are shown. THP-1 cells were double stained with TLR-4, MD2 primary antibodies labelled with Alexa Fluor 488 (green) and with HMGB1 secondary antibody labelled with Alexa Fluor 555 (red). Co-localisation is shown as Yellow/orange, fluorescence shows the potential co-localisation of two antigens which are the result of merging green and red channels, (a) and (b) shown a controls with no co-localisation as isotype and some co-localised area of TLR4 and HMGB1, MD2 and HMGB1 is shown in specific slides.

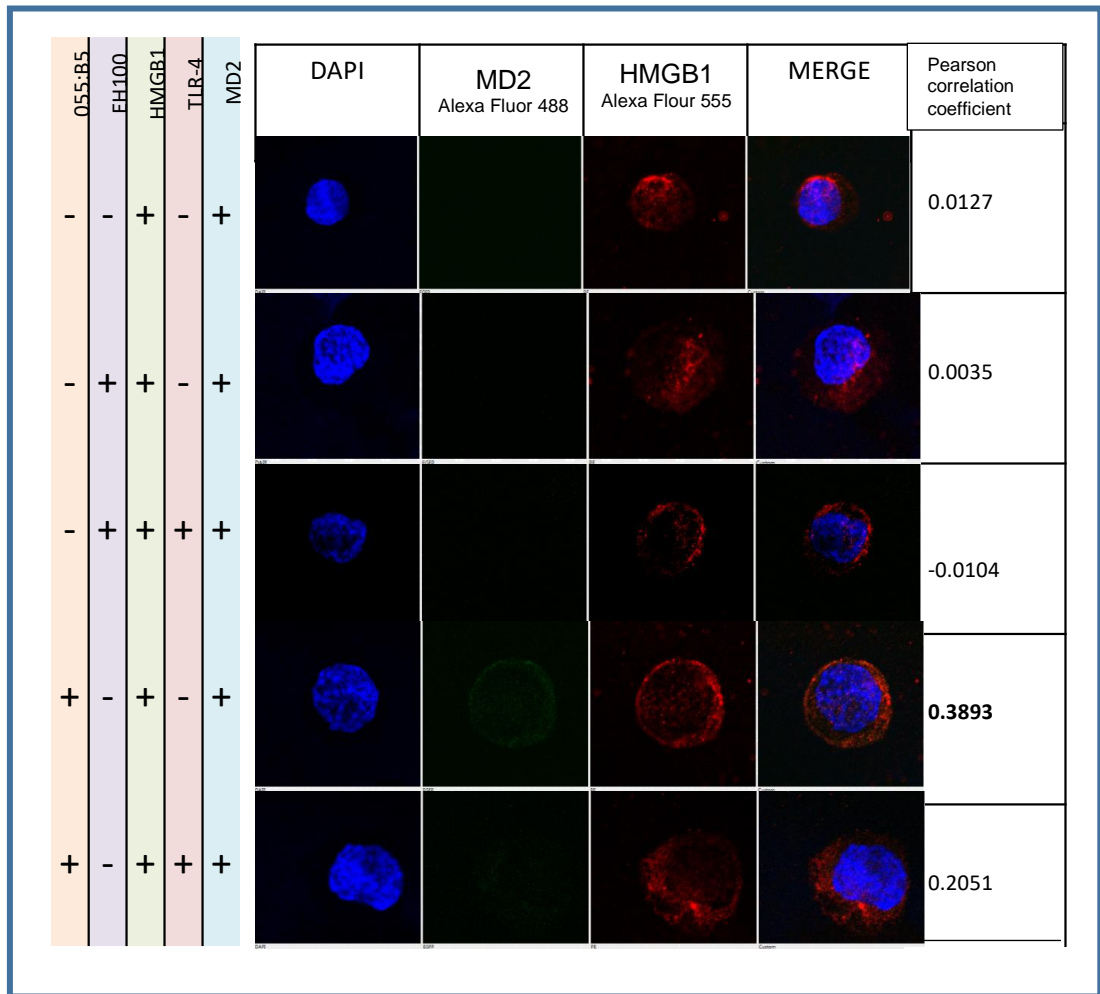


Figure 5-10: Co-localisation of MD2 and HMGB1 on the cell-surface of THP-1 cells for 120 min stimulation with rough EH100 and smooth 055:B5 LPS.

THP-1 cells were cultured on square cover slips 2 cm² at a density of 10 x10⁴ cells per well for 72h. We investigate whether the importance of Myeloid Differentiation2 (MD2) and (HMGB1) in presence and absence of (TLR-4) when treated for (120 min) by rough EH100 and smooth 055:B5 lipopolysaccharides. Isotype representing cells stained with isotype control mouse IgG1 primary and Alexa Fluor 488 and Alexa Fluor 555 secondary antibodies, visualised by using green 488 nm and red 555 nm wavelength lasers to measure non-specific antibody binding. Blue colour shows 4', 6-diamidino-2-phenylindole (DAPI). DAPI stained cell's nuclei. Red and Green shows merged image. Co-localisation of TLR4 and HMGB1, MD2 and HMGB1 on the cell-surface of THP-1 cells are shown. THP-1 cells were double stained with MD2 antibody labelled with Alexa Fluor 488 (green) and with HMGB1 antibody labelled with Alexa Fluor 555 (red). Co-localisation is shown as Yellow/orange; fluorescence shows the potential co-localisation of two antigens, which are the result of merging green and red channels, the images above shown different levels of co-localisation area of MD2 and HMGB1.

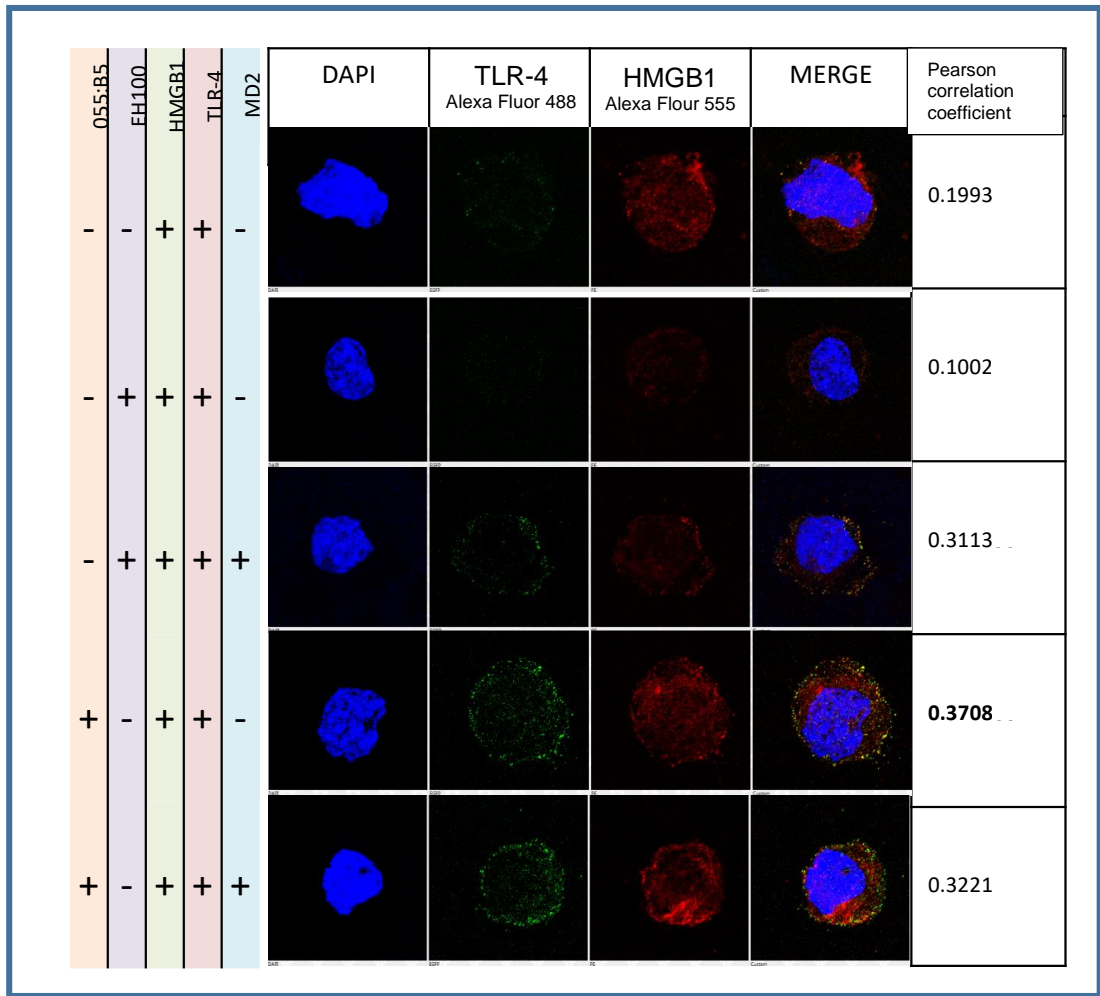


Figure 5-11: Co-localisation between TLR-4 and HMGB1 on the cell-surface of THP-1 cells for 120 min stimulation with rough EH100 and smooth 055:B5 LPS.

THP-1 cells were cultured on square cover slips 2 cm² at a density of 10 x10⁴ cells per well for 72h. We investigate whether the (TLR-4) and (HMGB1) in presence and absence of (MD2) treated for (120 min) by rough EH100 and smooth 055:B5 lipopolysaccharides. Isotype representing cells stained with isotype control mouse IgG1 primary and Alexa Fluor 488 and Alexa Fluor 555 secondary antibodies, visualised by using green 488 nm and red 555 nm wavelength lasers to measure non-specific antibody binding. Blue colour shows 4', 6-diamidino-2-phenylindole (DAPI). DAPI stained cell's nuclei. Red and Green shows merged image. Co-localisation of TLR-4 and HMGB1 on the cell-surface of THP-1 cells are shown. THP-1 cells were double stained with TLR-4 antibody labelled with Alexa Fluor 488 (green) and with HMGB1 antibody labelled with Alexa Fluor 555 (red). Co-localisation is shown as Yellow/orange; fluorescence shows the potential co-localisation of two antigens, which are the result of merging green and red channels, the images above shown a different level of co-localisation area of TLR-4 and HMGB1.

5.3 Conclusions

In this study we found that the smooth LPS (055:B5) work as a motivator of the interaction between TLR-4 and HMGB-1, while the absence of MD2, which translated scientifically that it found another pathway to co-localise together. However in presence of MD2 and treated with Rough LPS (EH100) the co-localization was increased. In the other hand, co-localisation between HMGB-1 and MD2 is shown slightly weak in this study, which approved that the relation between both proteins occurred infrequently, refer to signaling pathway.

The confocal laser scanning microscopy is a scientific technique to show a high resolution cells images in two and three dimensions. Nikon A1si confocal microscope was used. Co-localisation of fluorescent signals from two or more different proteins is an indicator of their association and potential interaction. The co-localisation measures by Pearson correlation coefficient is one of the most common co-localisation measurement method. It has range of -1 to $+1$. Where 1 is total positive linear correlation, 0 is no linear correlation, and -1 is total negative linear correlation. THP-1 cells were cultured on cover slips 2 cm^2 and 0.13 thickness at a density of 25×10^3 cells per well for 72 hours after treated by 5 ng of PMA to be macrophage-like cells as a mature cells. We investigate whether the importance of MD2 and TLR-4 to interact with HMGB1 when treated by rough EH100 and smooth 055:B5 lipopolysaccharides. the cells washed and stained as the samples coverslips with isotype control, mouse IgG1 as primary antibody with Alexa Fluor 488 and mouse IgG2 as primary antibody with Alexa Fluor 555 secondary antibodies, visualised by using green 488 nm and red 555 nm wavelength lasers to measure non-specific antibody binding. Blue colour shows 4', 6-diamidino-2-phenylindole (DAPI). DAPI stained cell's nuclei. Red and Green shows merged image. Co-localisation of TLR-4

with HMGB1 also Co-localisation of MD2 with HMGB1 on the cell-surface of THP-1 cells is shown in treated cells.

**Chapter 6 TNF- α and IL-1 β Detection by Enzyme-linked
Immunosorbent Assays (ELISA)**

6 TNF- α and IL-1 β Detection by Enzyme-linked immunosorbent assays (ELISA)

6.1 Introduction

Cytokines controlled by innate immunity, tumor necrosis factor alpha (TNF- α) and interleukin 1 beta (IL-1 β) in this study were investigated by ELISA test, which is for the quantitative detection of TNF- α , and IL-1 β in supernatant of differentiated THP1-1 cells samples. The cells stimulated with rough LPS (EH100) and smooth LPS (O55:B5) in presence and absence of Myeloid Differentiation 2 (MD2) presence and absence PARP inhibitor PJ34, the cells incubated for four hours.

Tumor necrosis factor alpha (TNF- α) is a pro-inflammatory cytokine that exhibits a wide range of biological effects. TNF is synthesised as a type II transmembrane protein (tmTNF). Upon stimulation, the TNF alpha-converting enzyme ADAM17 cleaves the extracellular domain of tmTNF, which releases the soluble TNF (sTNF). The newly generated membrane-bound moiety of TNF is further cleaved within its intramembrane region by signal peptide peptidase-like 2b (SPPL2b), leading to the generation of an intracellular domain (ICD) of TNF. Soluble TNF signals through two distinct cell surface receptors, TNFR1 and TNFR2. Most of the biological activities of TNF are mediated through TNFR1. Upon binding to TNFR1, the ligand-bound receptor aggregates and serves as a scaffold to recruit adaptor proteins. The activated sub-membranous complex triggers cellular activation via NF κ B and mitogen-activated protein kinases or apoptosis via complex internalisation and activation of apical caspases (Poggi *et al.*, 2013; *Cytokine Frontiers*, 2014; Sedger and McDermott, 2014).

6.2 Materials and methods

ELISA Ready-SET-Go for human TNF- α and IL-1 β was purchased from Ebioscience, UK. 96 wells plates were used and 100 μ l/well of capture antibody applied, sealed and incubated overnight at 4°C, wells aspirated and washed 3 times with 250 μ l/well by Wash Buffer, then 200 μ l/well applied of diluent, and kept for 1 hour, then washed once by wash buffer, after this step, the plate was ready to add 100 μ l/well of the standard dilution and the samples, the top standard concentration of the TNF- α 500 pg/ml and 150 pg/ml in IL-1 β . Plate was Incubated for overnight at 4°C, After wash, 100 μ l/well of detection antibody was added and the plate kept for 1 hour at room temperature, after washed 3-5 times, 100 μ l/well of Avidin was added , and incubated for 30 minutes, then washed 5 times, then 100 μ l/well of TMP (substrate) was added and incubated for 15 min, finally 50 μ l/well was added of stop solution to the wells then FLUOstar Omega plate reader from BMG labtech was used to read the plate at 450 nm.

6.3 Results

Non-differentiated THP-1 cells (2×10^5 cell/ml) grown in RPMI 1640 supplemented with 10 % of FCS. were stimulated with 100 ng/ml of LPS in presence and absence of 10 μ M of PJ34 for 30 minutes then treated by Myeloid Differentiation 2 (MD2) for 30 minutes, The cells stimulated and incubated for 2 hours and 4 hours with rough LPS (EH100) and smooth LPS (O55:B5), supernatant was collected for TNF- α and IL-1 β analysis by ELISA.

The study required to investigate the amount of cytokines which are show clearly a significant different between the differentiated and non-differentiated THP-1 cells which treated with different conditions as mentioned before, and the effect of rough

LPS (EH100) and smooth LPS (O55:B5) was indicated that the TNF- α and IL-1 β levels were significantly changed and the presence and absence of MD2 and PJ34 have a significant effectiveness represented in (Figure 6-6).

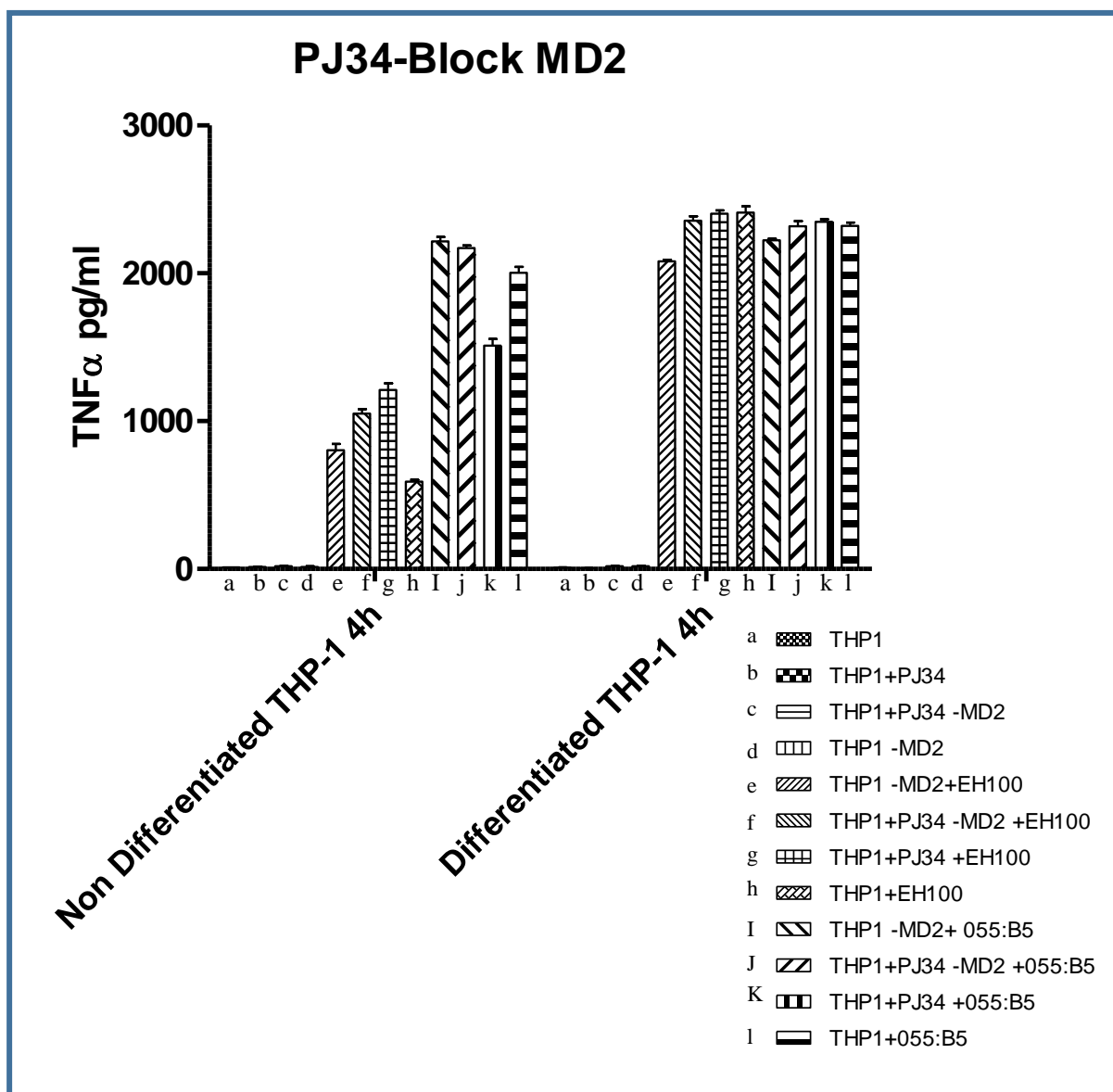


Figure 6-1: TNF- α level in differentiated and non-differentiated THP-1 in presence and absence of (MD2), also presence and PJ34, then stimulated with rough (EH100) and smooth (O55:B5) LPS for four hours.

The bar charts represent a TNF- α level in the tissue culture supernatant of differentiated and non-differentiated THP-1 cells samples. The cells stimulated with rough LPS EH100 and smooth LPS O55:B5 for **four hours** in presence and absence of Myeloid Differentiation 2 (MD2) and PARP inhibitor (PJ34). The first four samples shows nothing secreted of TNF- α , because of no stimulation with (LPS), but the differentiated THP-1 cells as a macrophage-like cells present a high level of receptors around the cell surface and high amount of cytokines released, because of the amount of antibodies was decreased and the LPS still active in the same concentration, but non differentiated THP-1 cells graphs represents a different levels specially the samples effected by EH100.

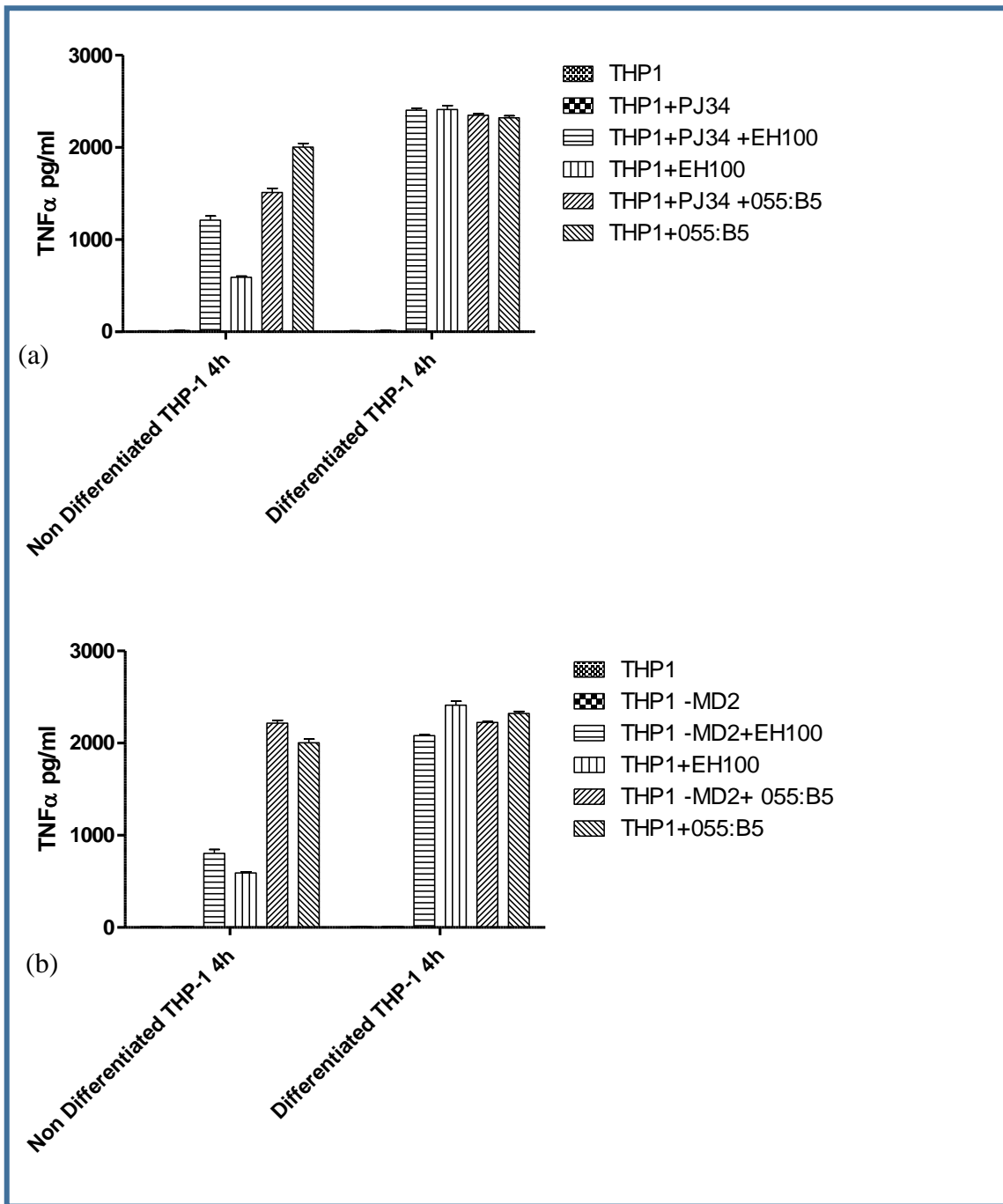


Figure 6-2: TNF- α level in differentiated and non-differentiated THP-1 in presence and absence of PJ34 (a) and presence and absence of (MD2) (b) then stimulated with rough (EH100) and smooth (O55:B5) LPS for four hours.

The bar charts represent a TNF- α level in the tissue culture supernatant of differentiated and non-differentiated THP-1 cells samples. The cells stimulated with rough LPS EH100 and smooth LPS O55:B5 for four hours in (a) presence and absence of PJ34 also (b) presence and absence of (MD2). The differentiated THP-1 cells as a macrophage-like cells present a high level of receptors around the cell surface and high amount of cytokines released, because of the amount of antibodies was decreased and the LPS still active in the same concentration, but non-differentiated THP-1 cells graphs represents a different levels specially the samples treated by EH100.

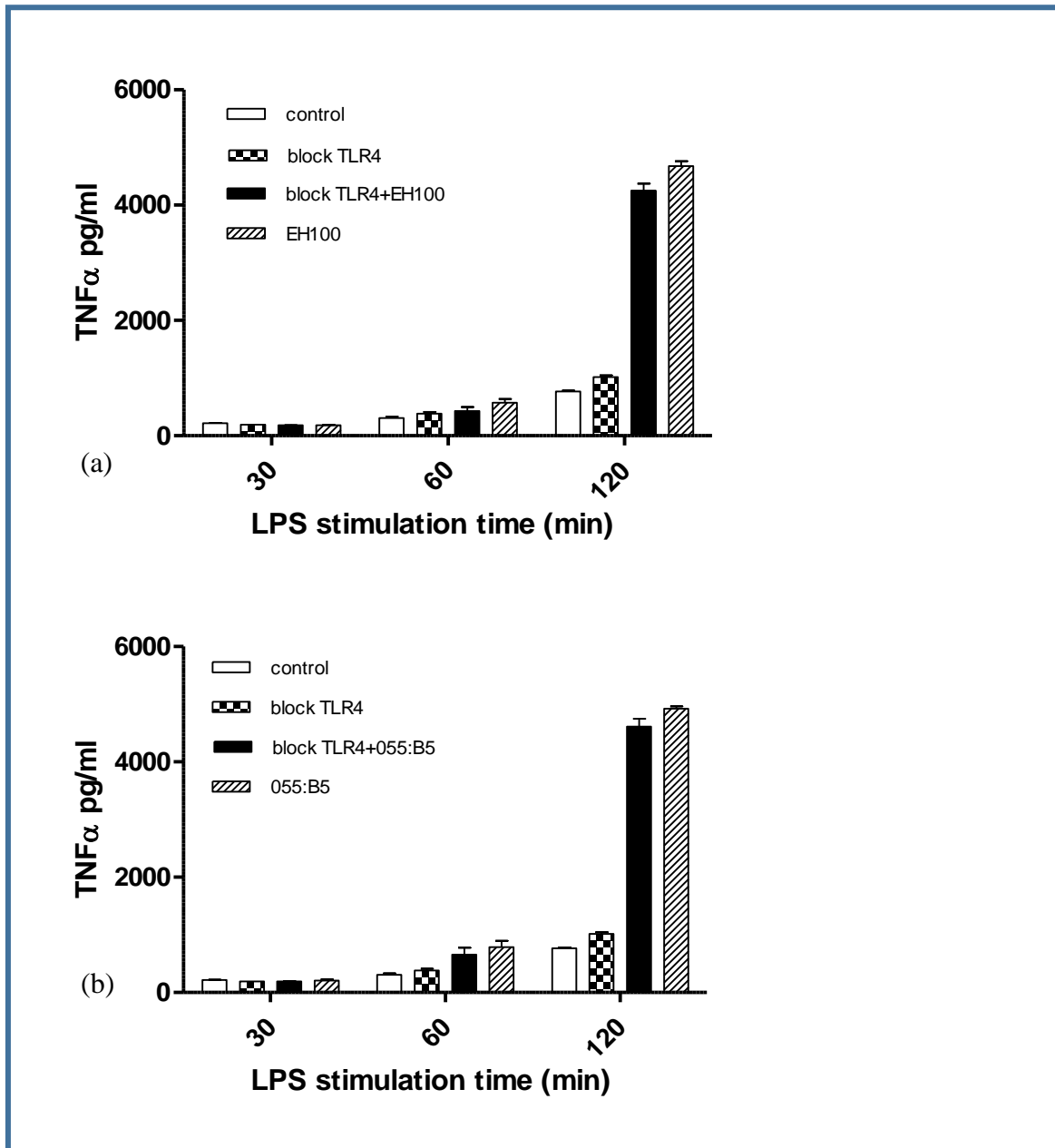


Figure 6-3 : TNF- α level in differentiated THP-1 when TLR-4 was blocked then stimulated with (EH100) LPS (a) and stimulated with (O55:B5) (b) LPS for 30, 60, and 120 minutes.

The bar charts represent a TNF- α level in the tissue culture supernatant of differentiated THP-1 cells samples. The TLR-4 antibody was blocked in specific samples. The cells stimulated with rough LPS EH100 (a) and smooth LPS O55:B5 (b) for 30, 60, and 120 minutes. The differentiated THP-1 cells as a macrophage-like cells represent a similar level of TNF- α except the samples in 60 min stimulated with smooth LPS O55:B5 shows significant increasing than the cells stimulated with rough LPS EH100, and the results increased highly significant in 120 min stimulation with LPS, refer to the degredation happened to amount of TLR-4 and MD2 added at the beginning of the experiments, or there is another signalling pathway managed after this time to increase the TNF- α level.

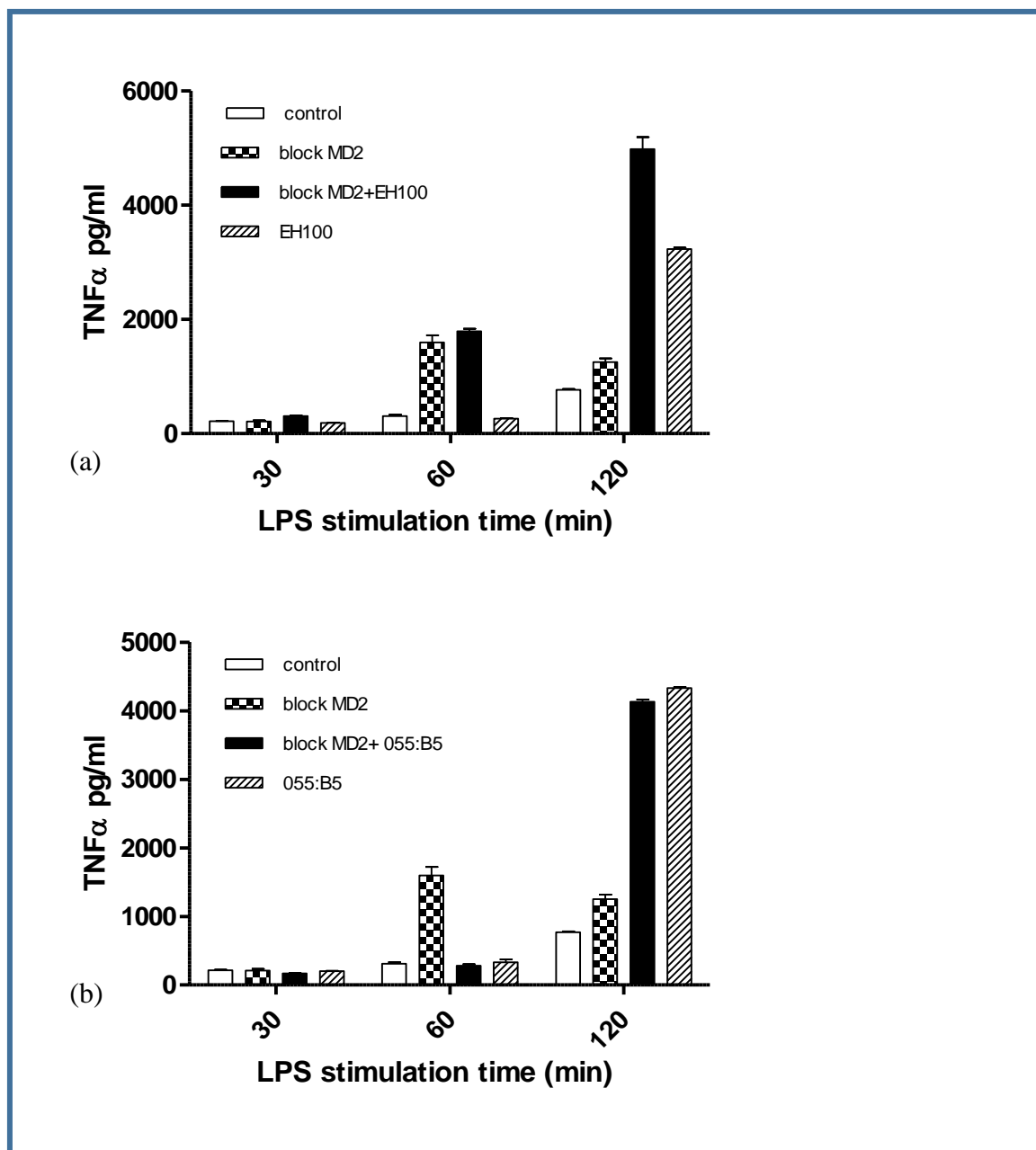


Figure 6-4 : TNF- α level in differentiated THP-1 when MD2 was blocked then stimulated with (EH100) LPS (a) and stimulated with (O55:B5) LPS (b) for 30, 60, and 120 minutes.

The bar charts represent a TNF- α level in the tissue culture supernatant of differentiated THP1-1 cells samples. The MD2 antibody was blocked in specific samples. The cells stimulated with rough LPS EH100 (a) and smooth LPS O55:B5 (b) for 30, 60, and 120 minutes. The differentiated THP-1 cells as a macrophage-like cells represent a similar level of TNF- α except the samples in **60** min stimulation shows significant increasing when MD2 blocked, and the results increased gradually in **120** min stimulation with LPS, refer to the degredation happened to amount of TLR-4 added from the beginning, or there is another signalling pathway managed after this time to increase the TNF- α level.

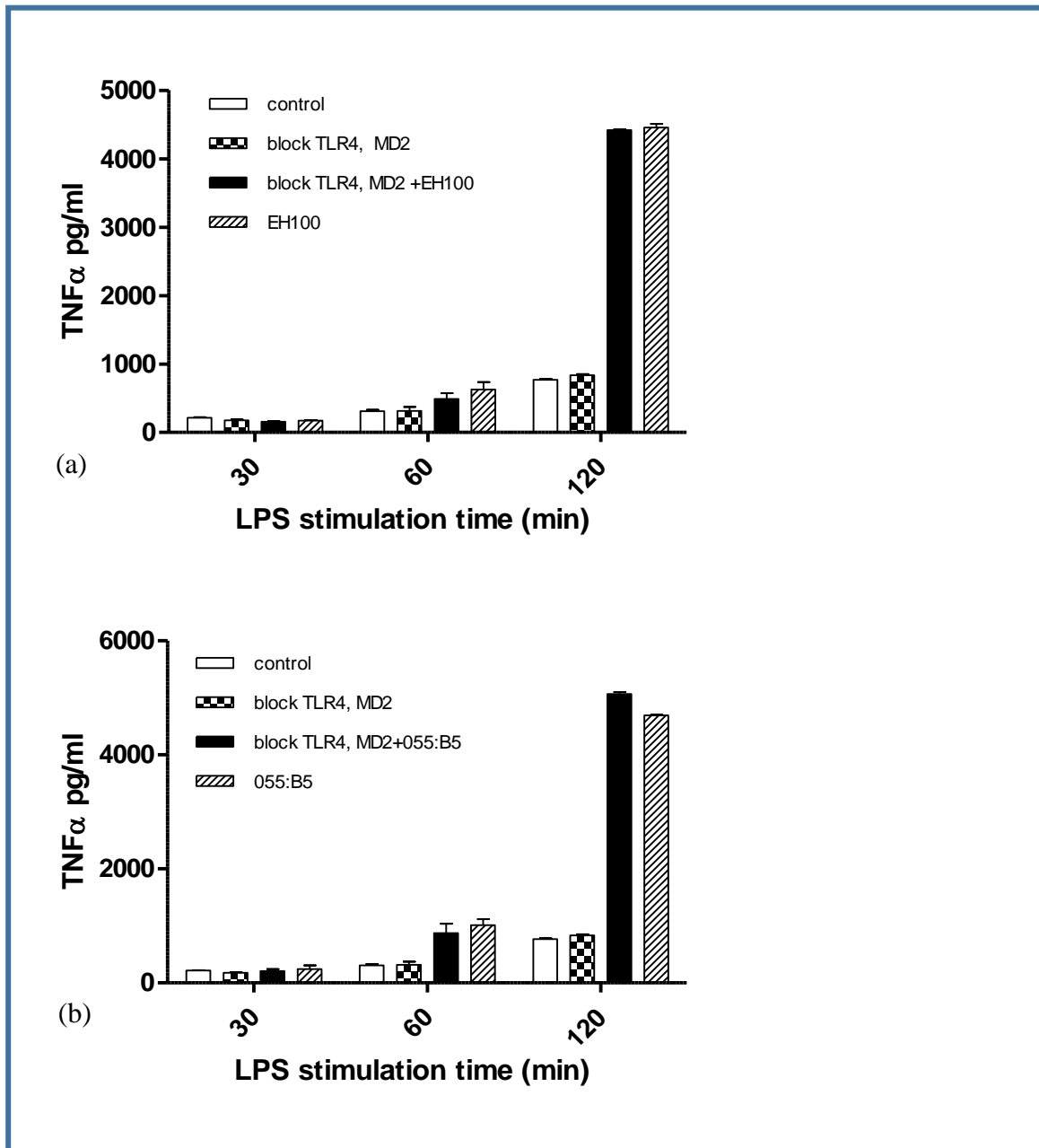


Figure 6-5 : TNF- α level in differentiated THP-1 when TLR-4 and MD2 were blocked then (a)stimulated with rough LPS EH100 and (b) stimulated with smooth LPS O55:B5 for 30, 60, and 120 minutes.

The bar charts represent a TNF- α level in the tissue culture supernatant of differentiated THP-1 cells samples. The TLR-4 and MD2 antibodies were blocked in specific samples. The cells stimulated with rough LPS EH100 (a) and smooth LPS O55:B5 (b) for 30, 60, and 120 minutes. The differentiated THP-1 cells as a macrophage-like cells represent a similar level of TNF- α except the samples in 60 min stimulated with smooth LPS O55:B5 shows significant increasing than the cells stimulated with rough LPS EH100, and the results increased highly significant in 120 min stimulation with LPS, refer to the degredation happened to amount of TLR-4 and MD2 added at the beginning of the experiments, or there is another signalling pathway managed after this time to increase the TNF- α level.

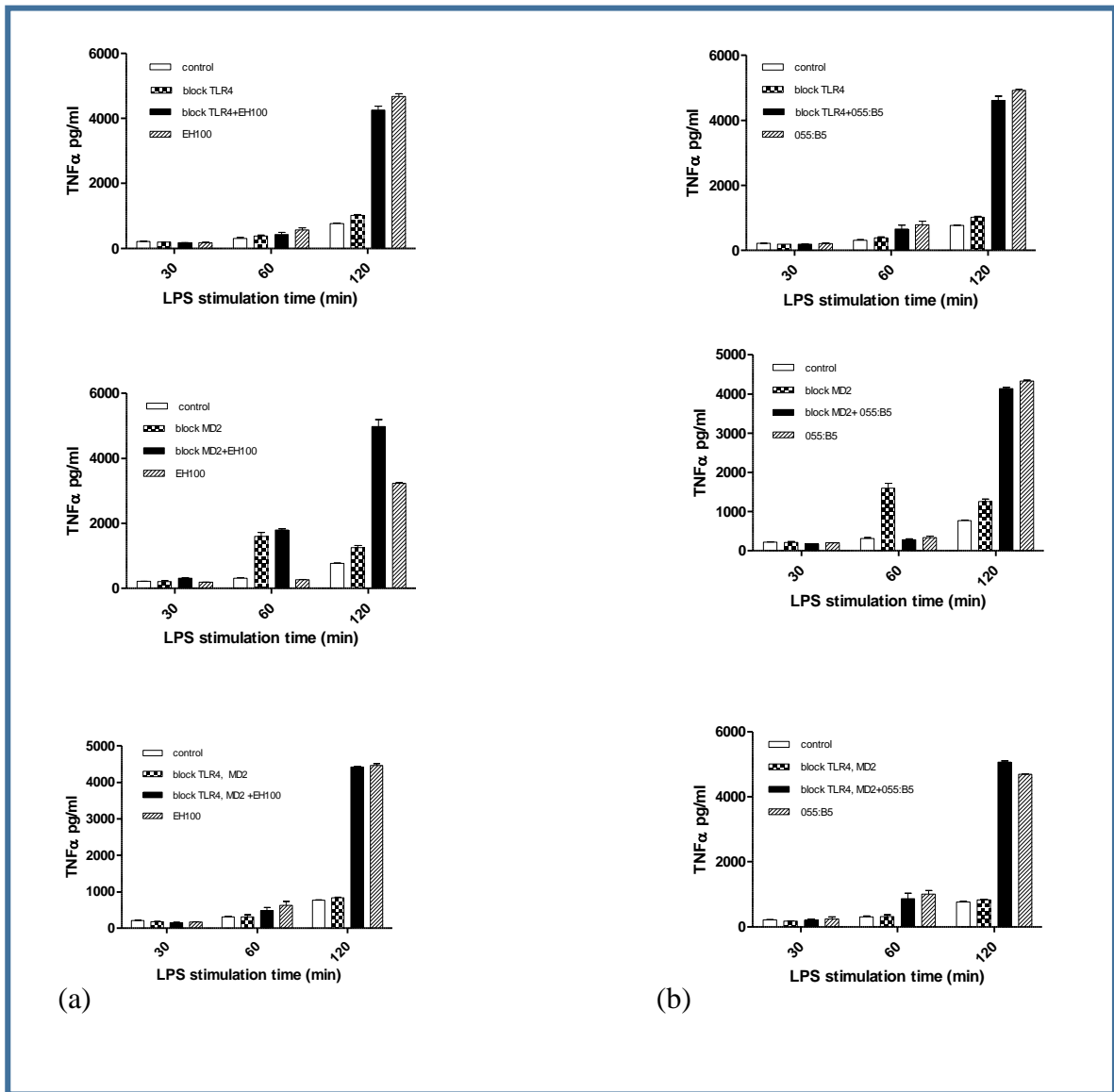


Figure 6-6 : TNF- α level in differentiated THP-1 when TLR-4 and MD2 were blocked then (a) stimulated with EH100 and (b) stimulated with O55:B5 for 30, 60, and 120 minutes.

The bar charts represent a TNF- α level in the tissue culture supernatant of differentiated THP-1 cells samples. The TLR-4 and MD2 antibodies were blocked in specific samples separately and together. The cells stimulated with rough LPS EH100 (a) and smooth LPS O55:B5 (b) for 30, 60, and 120 minutes. The differentiated THP-1 cells as a macrophage-like cells represent a similar level of TNF- α except the samples in 60 min stimulated with rough LPS EH100 and smooth LPS O55:B5 shows significant increasing than the cells stimulated with rough LPS EH100, and the results increased highly significant in 120 min stimulation with LPSs, refer to the degredation happened to amount of TLR-4 and MD2 added at the beginning of the experiments, or there is another signaling pathway managed after this time to increase the TNF- α level.

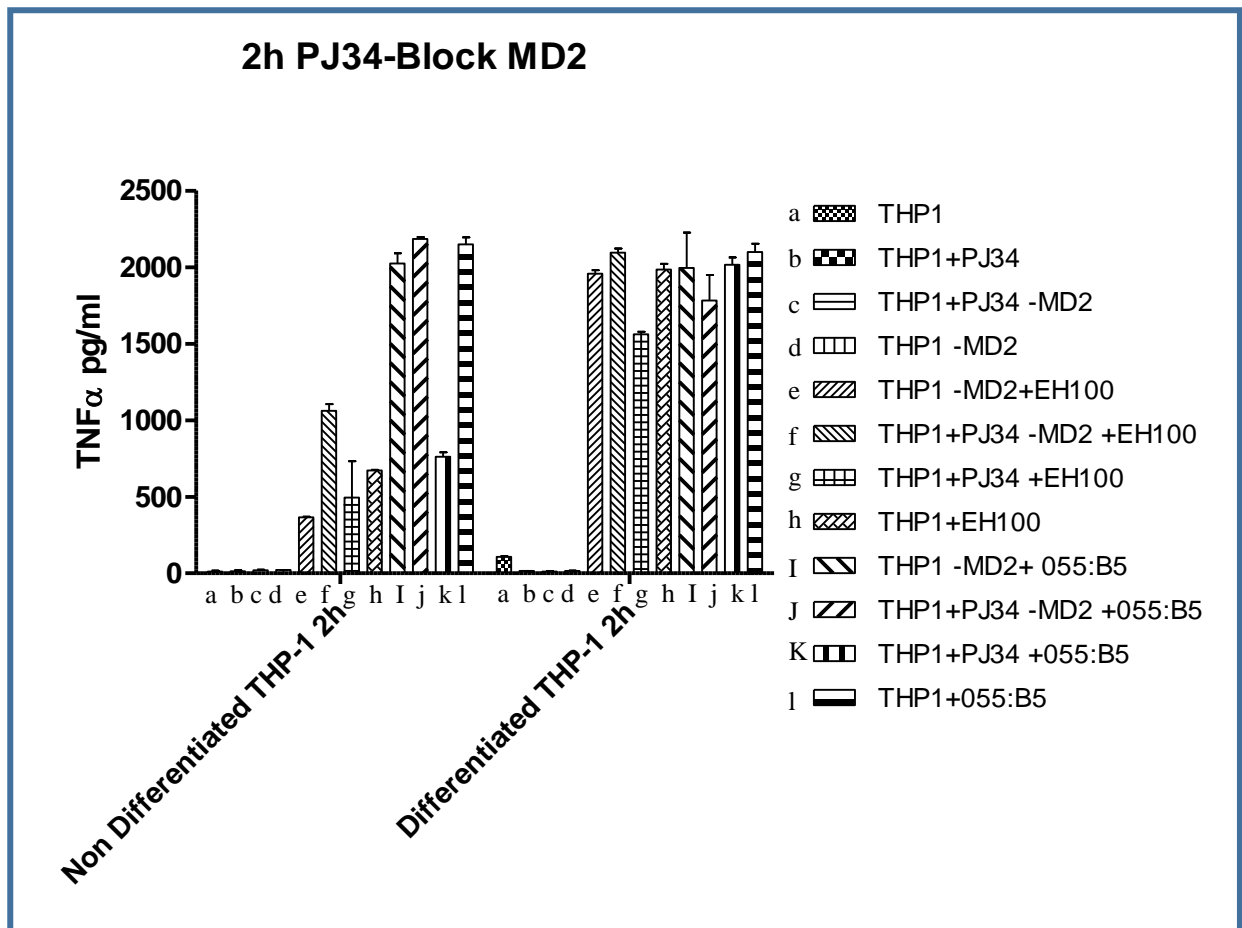


Figure 6-7: TNF- α level in differentiated and non-differentiated THP-1 cells in presence and absence of (MD2), also presence and PJ34, then stimulated with (EH100) (O55:B5) LPS for two hours.

The bar chart represents a TNF- α level in the tissue culture supernatant of differentiated and non-differentiated THP-1 cells samples. The cells stimulated with rough LPS EH100 and smooth LPS O55:B5 for **two hours** in presence and absence of Myeloid Differentiation 2 (MD2) and PARP inhibitor (PJ34). The first four samples show nothing secreted of TNF- α , because of no stimulation with (LPS), but the differentiated THP-1 cells as macrophage-like cells present a high level of receptors around the cell surface and high amount of cytokines released, because of the amount of antibodies was decreased and the LPS still active in the same concentration, but non-differentiated THP-1 cells graphs represent a different level of TNF- α specially the samples effected by EH100. The conditions in order: (a) THP-1, (b) THP-1+PJ34, (c) THP-1+PJ34+MD2, (d) THP-1+MD2, (e) THP-1+MD2 +EH100, (f) THP-1+PJ34+MD2+EH100, (g) THP-1+PJ34+EH100, (h) THP-1+EH100, (i) THP-1+MD2+O55:B5, (j) THP-1+PJ34+MD2+O55:B5, (k) THP-1+PJ34+O55:B5, (l) THP-1+O55:B5.

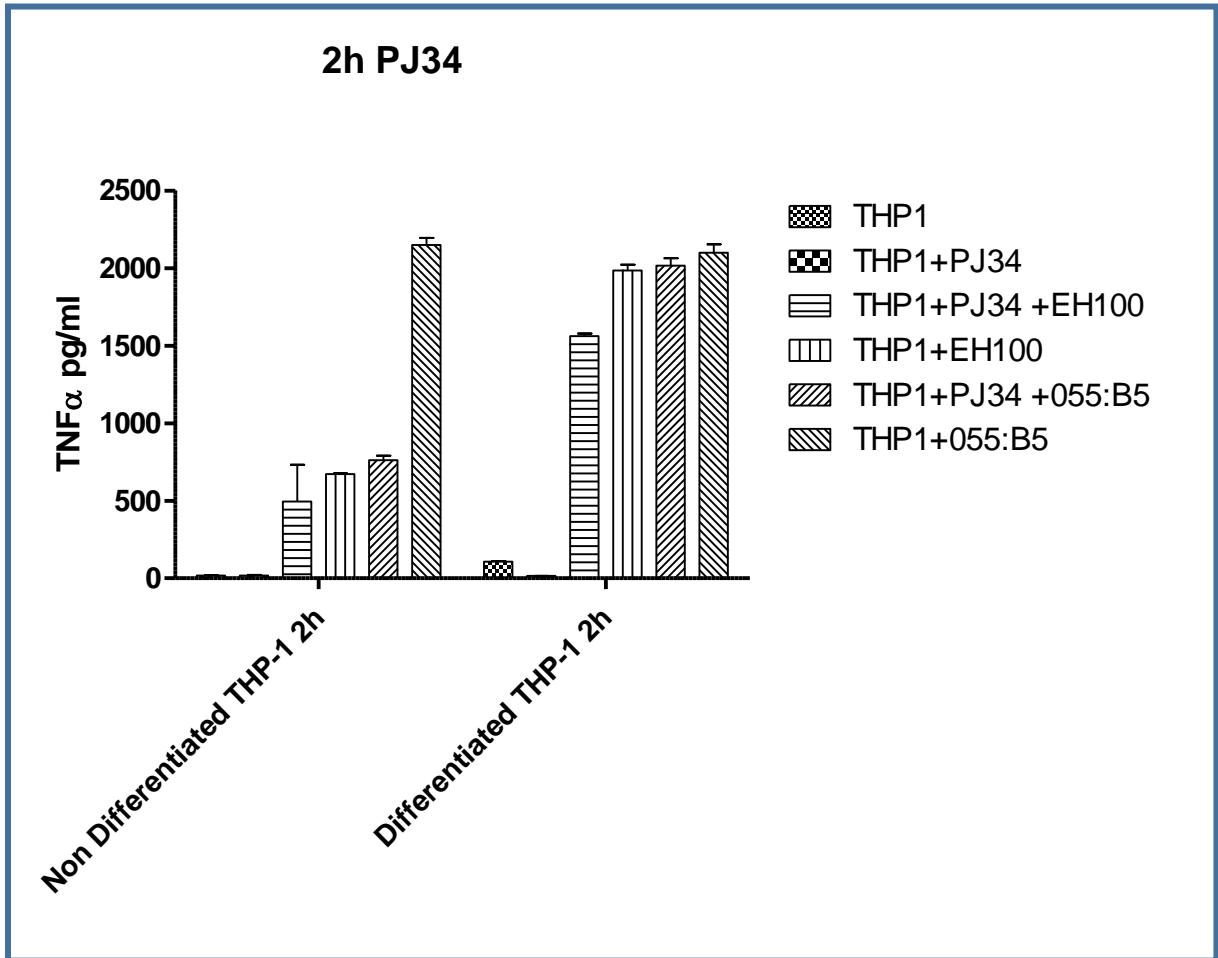


Figure 6-8 : TNF- α level in differentiated and non-differentiated THP-1 in presence and absence of PJ34 then stimulated with EH100 and 055:B5 LPSs for two hours.

The bar chart represents a cytokines TNF- α level in the tissue culture supernatant of differentiated and non- differentiated THP-1 cells samples. The cells stimulated with rough LPS EH100 and smooth LPS 055:B5 for **two hours** in presence and absence of PJ34. The differentiated THP-1 cells as a macrophage-like cells present a high level of receptors around the cell surface and high amount of cytokines (TNF- α) released, because of the amount of antibodies was decreased and the LPS still active in the same concentration, but non-differentiated THP-1 cells graphs represents a different levels of TNF- α and high level the sample treated by smooth LPS O55:B5.

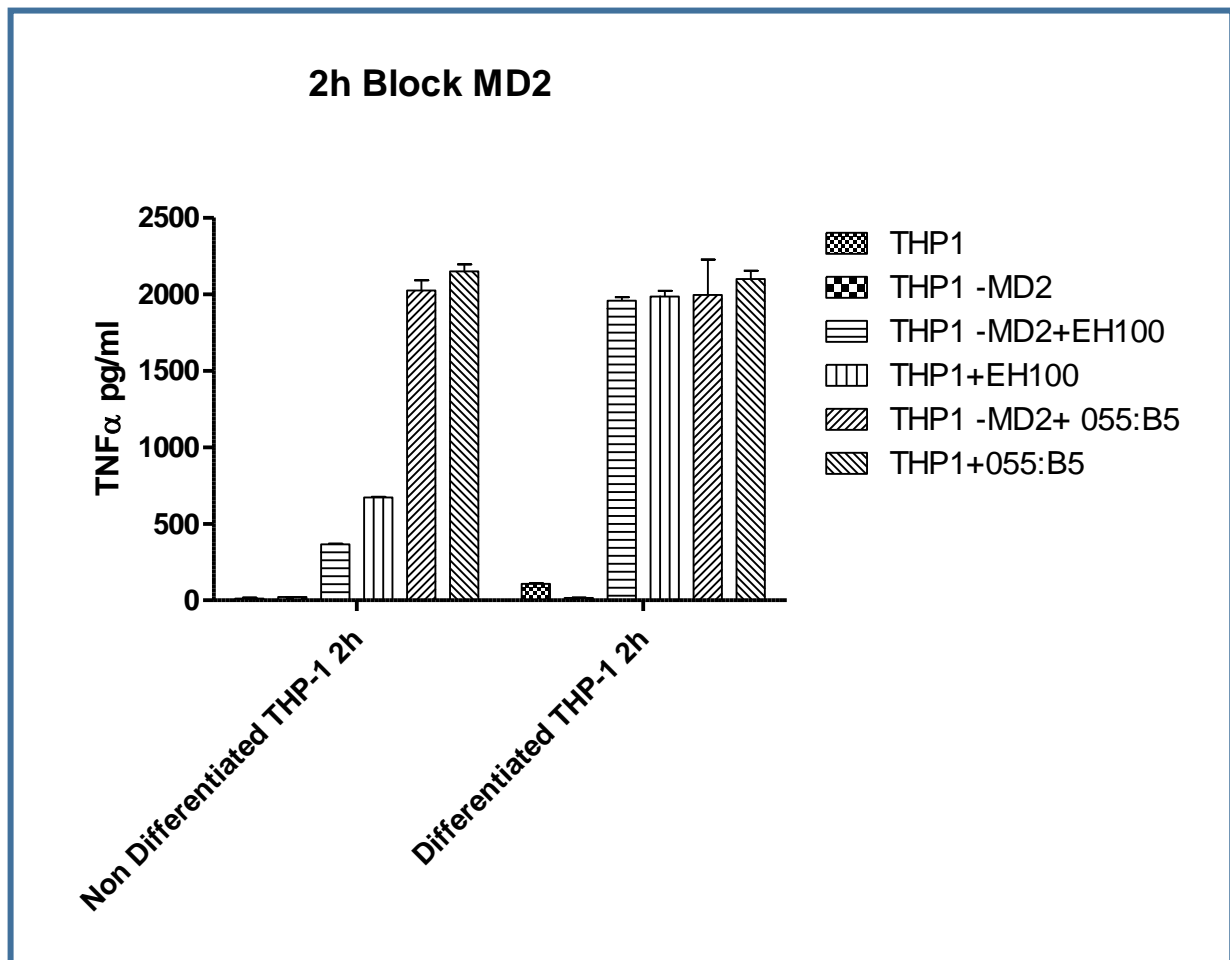


Figure 6-9: TNF- α level in differentiated and non-differentiated THP-1 cells in presence and absence of (MD2), then stimulated with EH100 and O55:B5 LPS for two hours.

The bar chart represents a TNF- α level in the tissue culture supernatant of differentiated and non-differentiated THP-1 cells samples. The cells stimulated with rough LPS EH100 and smooth LPS O55:B5 for **two hours** in presence and absence of Myeloid Differentiation 2 (MD2), the first two samples show nothing significant secreted of TNF- α , because of not stimulated with (LPS), but the differentiated THP-1 cells as a macrophage-like cells present a high level of receptors around the cell surface and high amount of cytokines released, because of the amount of antibodies was decreased and the LPS still active in the same concentration, but non-differentiated THP-1 cells graphs represents a slightly different levels of TNF- α but the samples treated by O55:B5 show a high significant level of TNF- α .

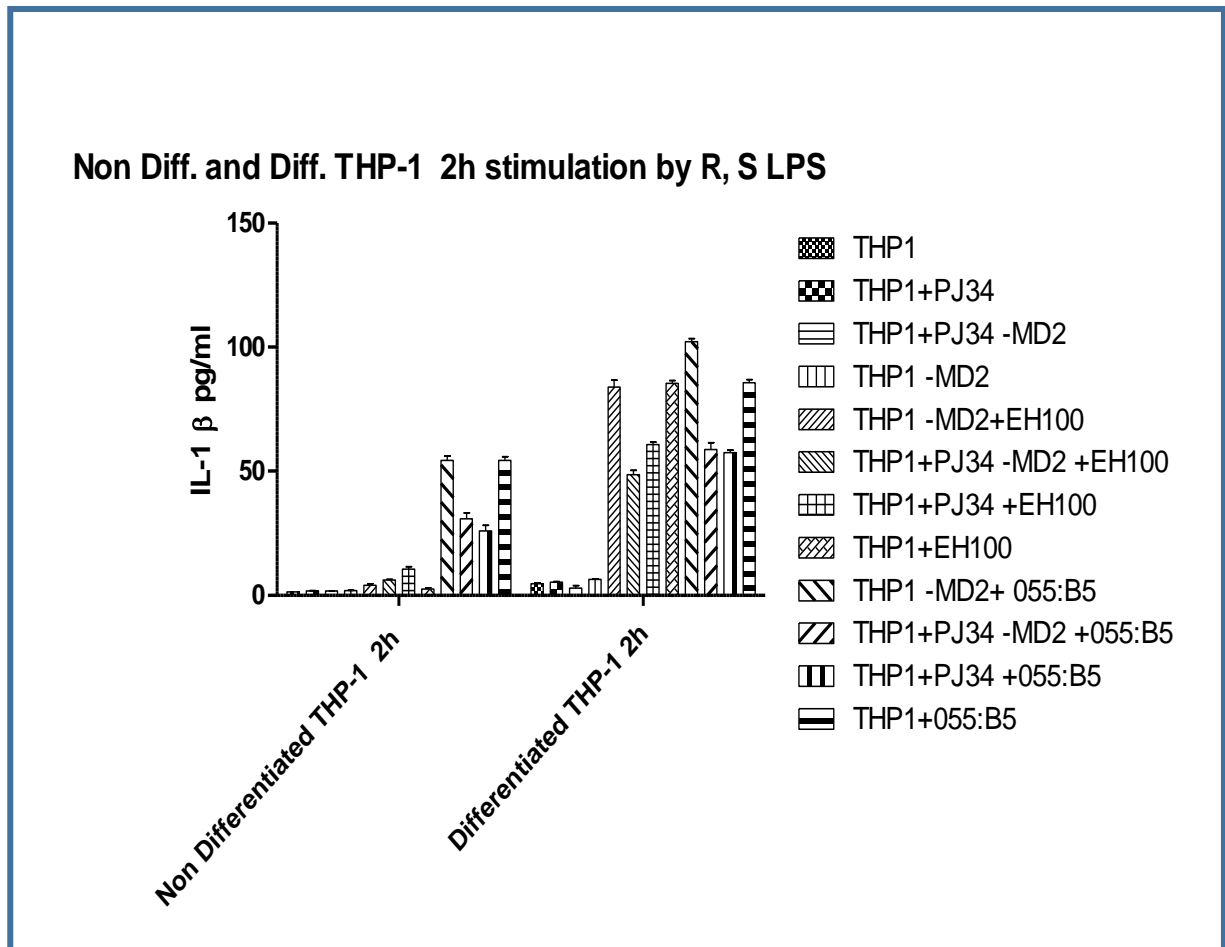


Figure 6-10: IL-1 β level in differentiated and non-differentiated THP-1 cells in presence and absence of (MD2), and (PJ34), then stimulated with EH100 and O55:B5 LPS for two hours.

The bar chart represents an IL-1 β level in the tissue culture supernatant of differentiated and non-differentiated THP-1 cells samples in presence and absence of Myeloid Differentiation 2 (MD2) and PARP inhibitor (PJ34). The cells stimulated with rough LPS EH100 and smooth LPS O55:B5 for **two hours** the first four samples shows nothing secreted of IL-1 β , because of no stimulation with (LPS), but the differentiated THP-1 cells as a macrophage-like cells present a high level of receptors around the cell surface and high amount of cytokines released, also because of the amount of antibodies was decreased and the LPS still active in the same concentration, but non-differentiated THP-1 cells graphs represents a different significant levels of IL-1 β specially the samples effected by EH100 and O55:B5.

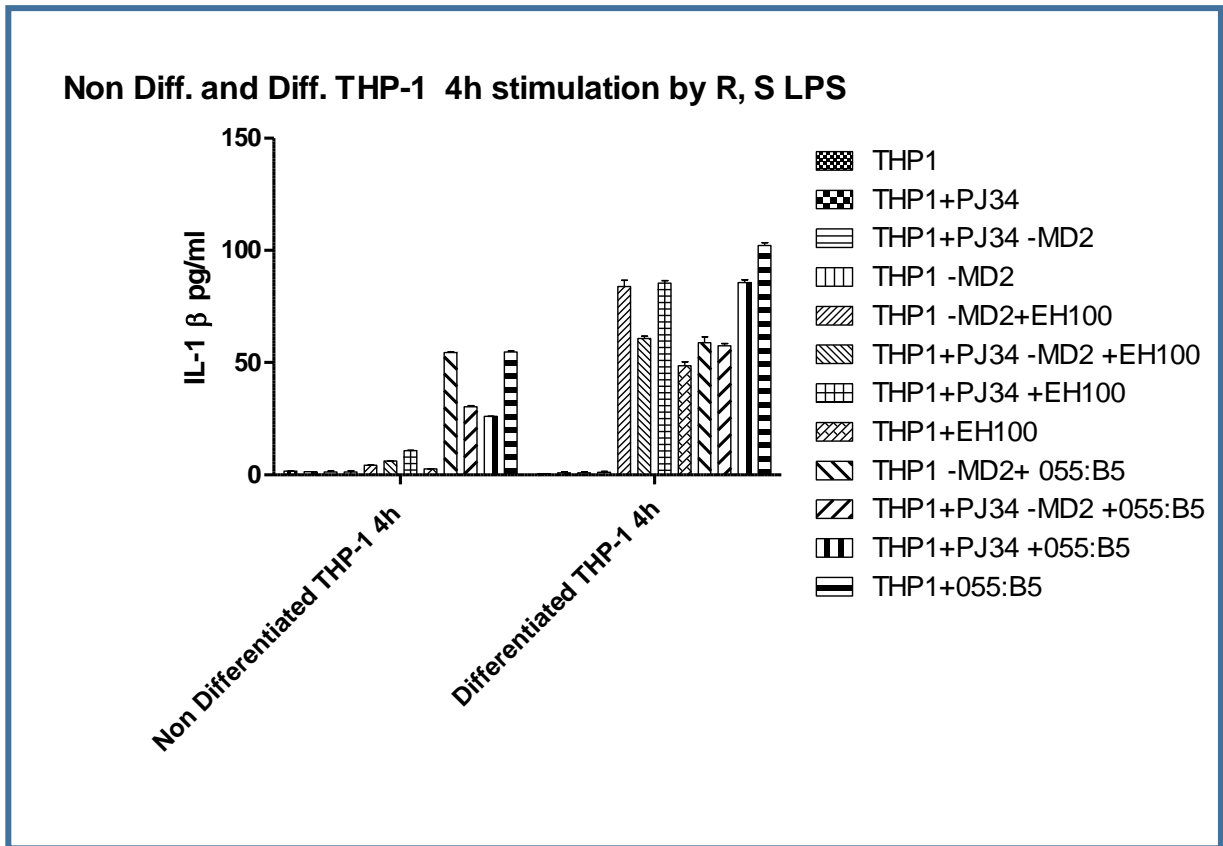


Figure 6-11: IL-1 β level in differentiated and non-differentiated THP-1 cells in presence and absence of (MD2), and (PJ34), then stimulated with EH100 and O55:B5 LPS for four hours.

The bar chart represents an IL-1 β level in the tissue culture supernatant of differentiated and non-differentiated THP-1 cells samples in presence and absence of Myeloid Differentiation 2 (MD2) and PARP inhibitor (PJ34). The cells stimulated with rough LPS EH100 and smooth LPS O55:B5 for **four hours** the first four samples shows nothing secreted of IL-1 β , because of no stimulation with (LPS), but the differentiated THP-1 cells as a macrophage-like cells present a high level of receptors around the cell surface and high amount of cytokines released, also because of the amount of antibodies was decreased and the LPS still active in the same concentration, but non-differentiated THP-1 cells graphs represents a different significant levels of IL-1 β specially the samples effected by EH100 and O55:B5, the similarity with small difference of IL-1 β level in both stimulation time is refer to same effectiveness of the LPSs in two hours and four hours.

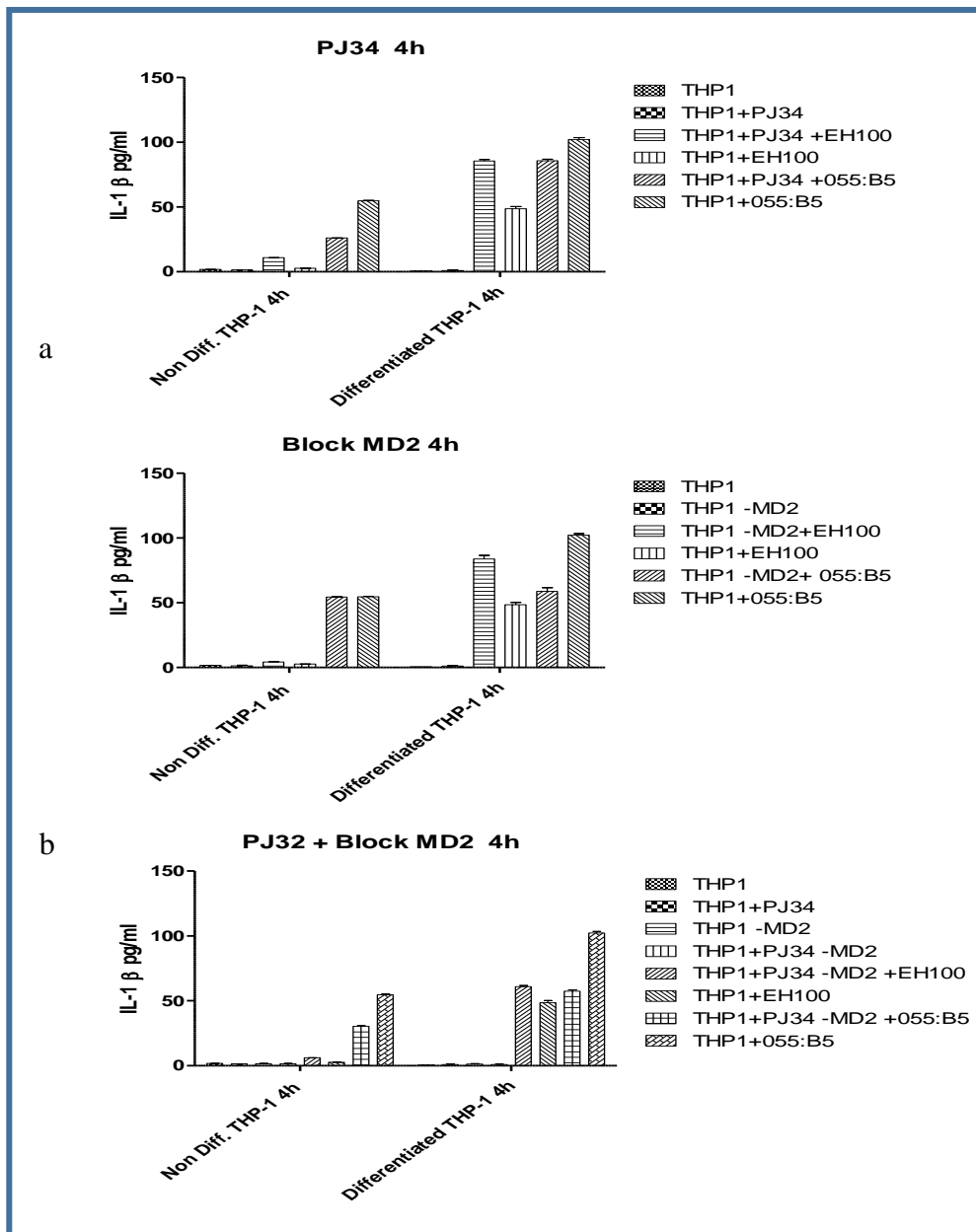


Figure 6-12: The effect of PJ-34 on IL-1 β secretion by non-differentiated and PMA differentiated THP-1 cells in presence and absence of MD2 by response to *E. coli* rough EH100 and smooth 055:B5 LPS.

Non-differentiated THP-1 cells (2×10^5 cell/ml) grown in RPMI 1640 supplemented with 10 % of FCS. were stimulated with 100 ng/ml of LPS in presence and absence of 10 μ M of PJ34 for 30 minutes then treated by Myeloid Differentiation 2 (MD2) for 30 minutes, The cells stimulated and incubated for 4 hours with rough LPS EH100 and smooth LPS O55:B5, supernatant was collected for IL-1 β analysis by ELISA. The graph represents an IL-1 β level in the tissue culture supernatant of differentiated and non-differentiated THP-1 cells samples. The cells stimulated with rough LPS EH100 and smooth LPS O55:B5 for four hours in presence and absence of PJ34 and Myeloid Differentiation 2 (MD2). The differentiated THP-1 cells as macrophage-like cells existing a high level of receptors around the cell surface and high amount of cytokines released. Stimulation by smooth O55:B5 LPS showing a higher level of IL-1 β . Refer to decreasing of the antibodies amount and concentration effectiveness of smooth LPS. The effectiveness of PJ34 is shown significantly in both kinds of cells.

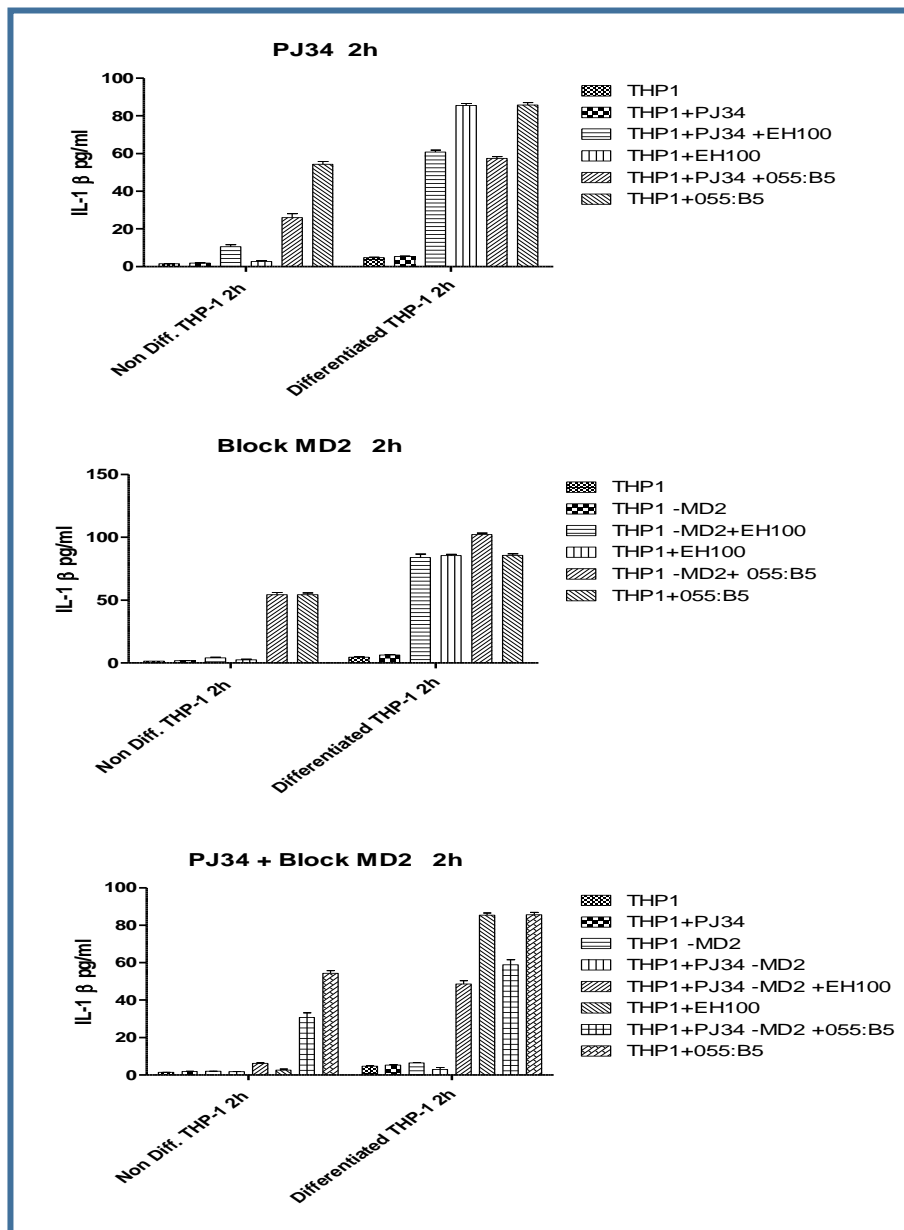


Figure 6-13: The effect of PJ-34 on IL-1 β secretion by non-differentiated and PMA differentiated THP-1 cells in presence and absence of MD2 by response to *E. coli* rough EH100 and smooth 055:B5 LPSs.

Non-differentiated THP-1 cells (2×10^5 cell/ml) grown in RPMI 1640 supplemented with 10 % of FCS. were stimulated with 100 ng/ml of LPS in presence and absence of 10 μ M of PJ34 for 30 minutes then treated by Myeloid Differentiation 2 (MD2) for 30 minutes, The cells stimulated and incubated for 2 hours with rough LPS EH100 and smooth LPS O55:B5, supernatant was collected for IL-1 β analysis by ELISA. The graph represents an IL-1 β level in the tissue culture supernatant of differentiated and non-differentiated THP1-1 cells samples. The cells stimulated with rough LPS EH100 and smooth LPS O55:B5 for four hours in presence and absence of PJ34 and Myeloid Differentiation 2 (MD2). The differentiated THP-1 cells as macrophage-like cells existing a high level of receptors around the cell surface and high amount of cytokines released. Stimulation by showing a higher level of IL-1 β . Refer to decreasing of the antibodies amount and concentration effectiveness of smooth LPS.

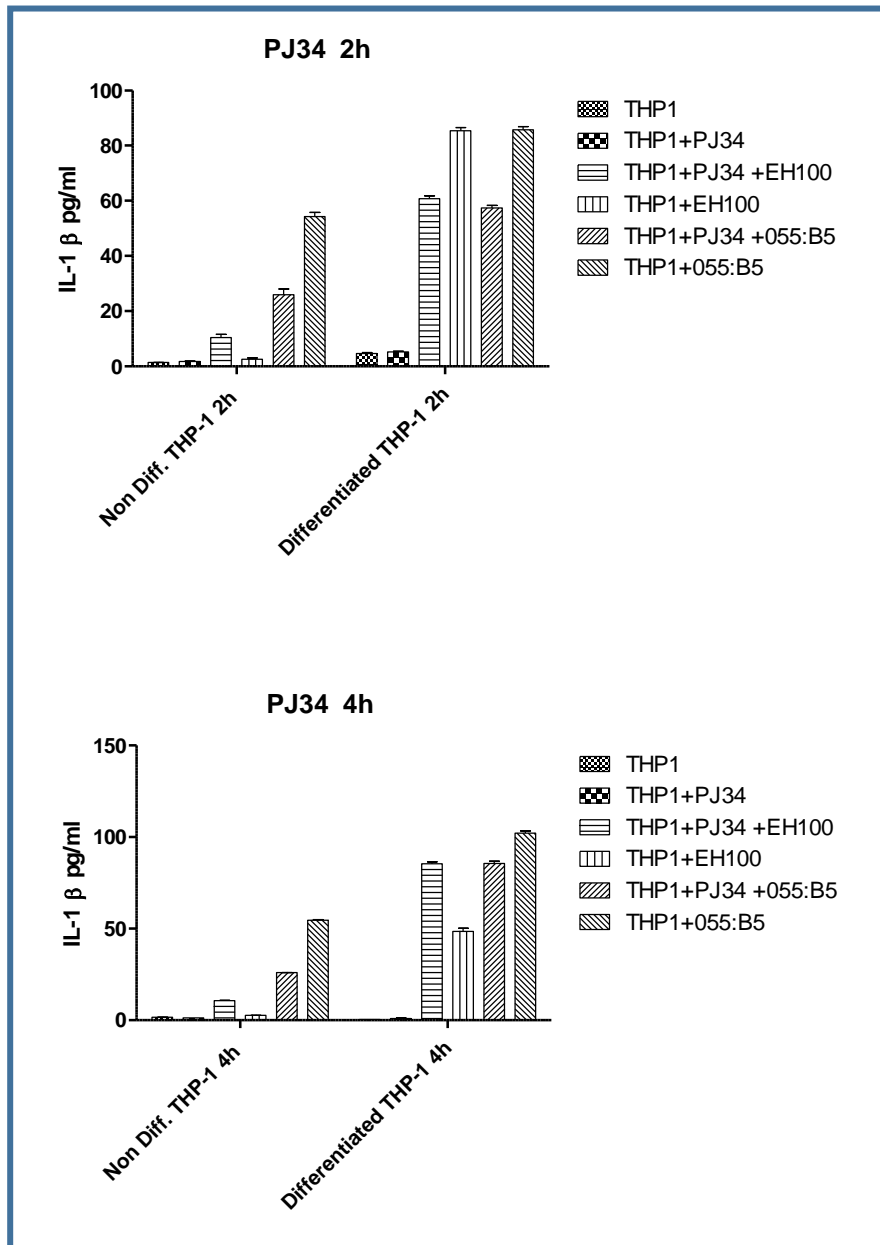


Figure 6-14: IL-1 β level in differentiated and non-differentiated THP-1 cells in presence and absence of PJ34, then stimulated with EH100 and O55:B5 LPSs for two and four hours.

The bar chart represents an IL-1 β level in the tissue culture supernatant of differentiated and non-differentiated THP-1 cells samples. The cells stimulated with rough LPS EH100 and smooth LPS O55:B5 for **two and four hours** in presence and absence of PARP inhibitor (PJ34). The first two samples show nothing secreted of IL-1 β , because of no stimulation with (LPS), but the differentiated THP-1 cells as a macrophage-like cells present a high level of receptors around the cell surface and high amount of cytokines released, because of the amount of antibodies was decreased and the LPS still active in the same concentration, but non-differentiated THP-1 cells graphs represents a different levels of IL-1 β specially the samples effected by EH100.

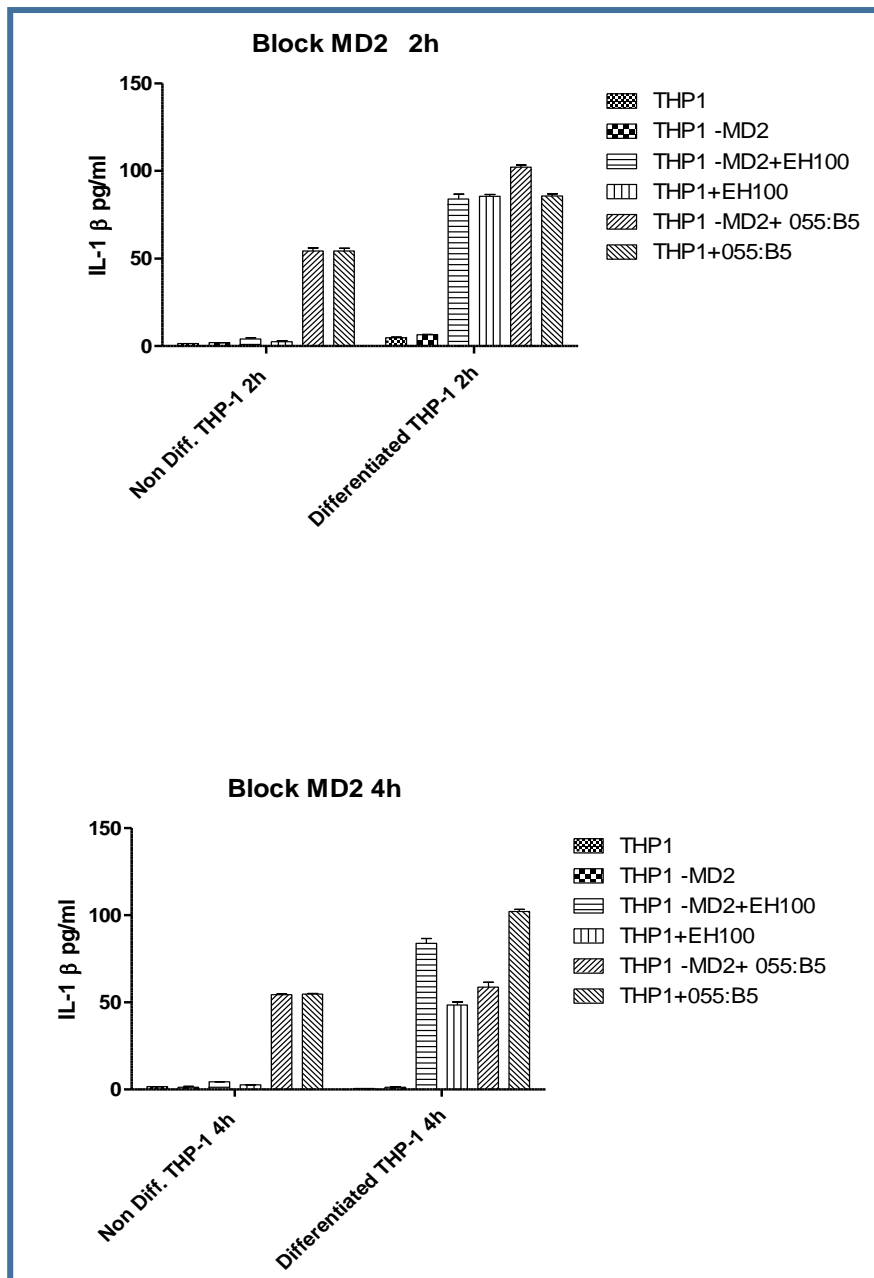


Figure 6-15: IL-1 β level in differentiated and non-differentiated THP-1 cells in presence and absence of MD2, then stimulated with (EH100) (O55:B5) LPS for two and four hours.

The bar chart represents an IL-1 β level in the tissue culture supernatant of differentiated and non-differentiated THP-1 cells samples. The cells stimulated with rough LPS EH100 and smooth LPS O55:B5 for **two and four hours** in presence and absence of Myeloid Differentiation 2 (MD2). The first two samples shows nothing secreted of IL-1 β , because of no stimulation with (LPS), but the differentiated THP-1 cells as a macrophage-like cells present a high level of receptors around the cell surface and high amount of cytokines released, because of the amount of antibodies was decreased and the LPS still active in the same concentration, but non-differentiated THP-1 cells graphs represents a different levels of IL-1 β specially the samples effected by EH100 and similar level for the samples treated with O55:B5.

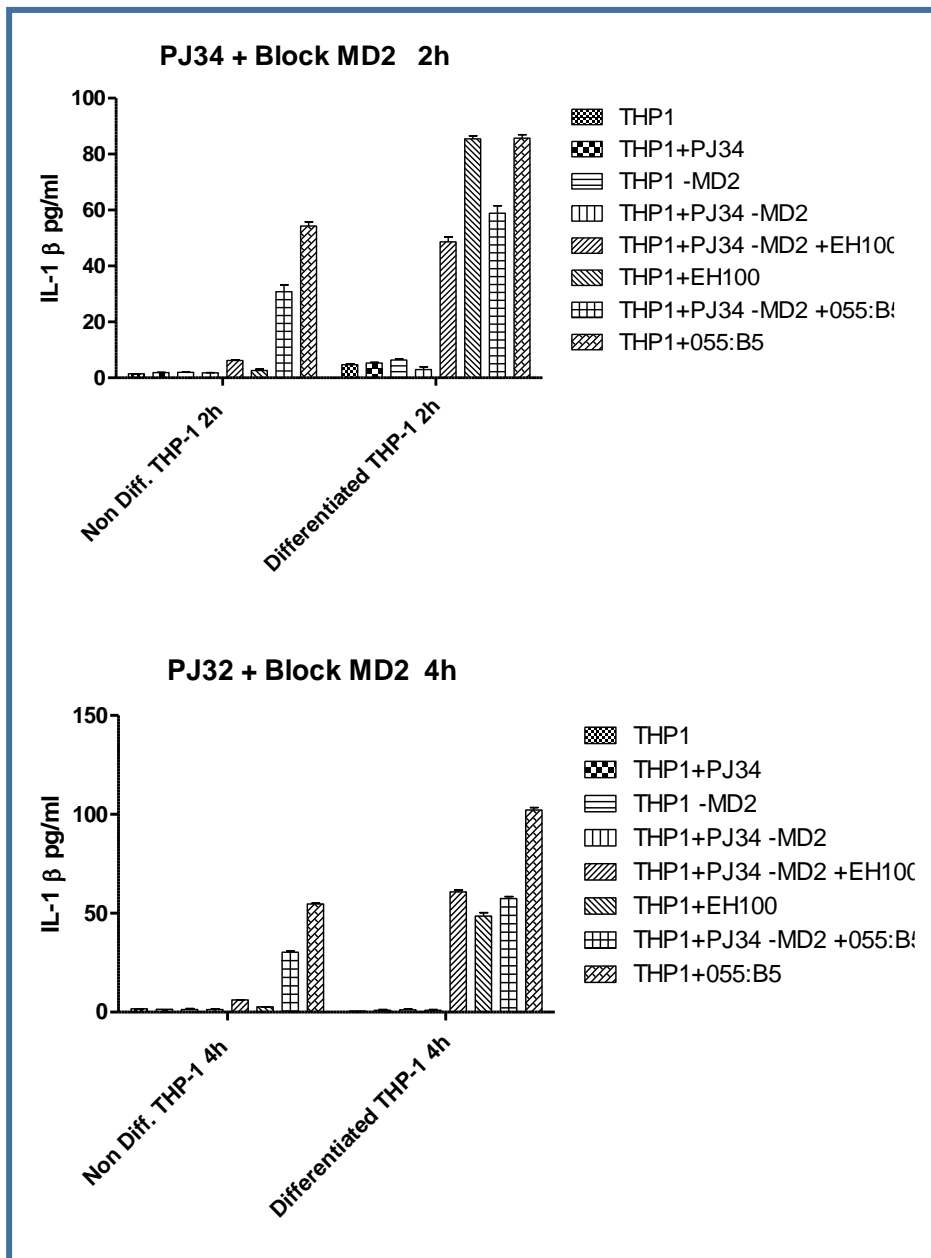


Figure 6-16: IL-1 β level in differentiated and non-differentiated THP-1 cells in presence and absence of (MD2), also presence and PJ34, then stimulated with EH100 and O55:B5 LPSs for two and four hours.

The bar chart represents an IL-1 β level in the tissue culture supernatant of differentiated and non-differentiated THP-1 cells samples. The cells stimulated with rough LPS EH100 and smooth LPS O55:B5 for **two and four hours** in presence and absence of Myeloid Differentiation 2 (MD2) and PARP inhibitor (PJ34).the first four samples shows nothing secreted of IL-1 β , because of not stimulated with (LPS), but the differentiated THP-1 cells as a macrophage-like cells present a high level of receptors around the cell surface and high amount of cytokines released, because of the amount of antibodies was decreased and the LPS still active in the same concentration, but non-differentiated THP-1 cells graphs represents a different levels of IL-1 β specially the samples effected by EH100.

6.4 Conclusions

In current study the model cell was THP-1 cells, four techniques were used, Flow-cytometry, Confocal Microscopy, ELISA and Proteomics. The monocytes cells (non-differentiated) and macrophage-like cells differentiated by 5 ng/ml PMA, investigate the effectiveness of rough LPS (EH100) and smooth LPS (O55:B5) in presence and absence of Myeloid Differentiation 2 (MD2), and presence and absence of PARP inhibitor PJ34.

The differentiated cells as a macrophage-like cells has high level of receptors that's show an increasing of the expression and the level of cytokines released such as TNF- α and IL-1 β , help to show a valuable images of co-localisation between CD14 and TLR4 and help to get a hundreds of proteins spots in the 2D gels.

The effectiveness of rough LPS (EH100) and smooth LPS (O55:B5) shows a different results, the rough LPS (EH100) is more effective than the smooth LPS (O55:B5). We found the importance of the MD2 with CD14 and TLR4 to interact with different LPS chemotype. The confocal laser scanning microscopy is a scientific technique to show a high resolution cells images in 2 and 3 dimensions. Nikon A1si confocal microscope was used. Co-localisation of fluorescent signals from two or more different proteins is an indicator of their association and potential interaction. The co-localisation measures by Pearson correlation coefficient is one of the most common co-localisation measurement method. It has range of -1 to +1 (Adler and Parmryd, 2010; Zhu, Welsch and Matsudaira, 2016). Where 1 is total positive linear correlation, 0 is no linear correlation, and -1 is total negative linear correlation.

THP-1 cells were cultured on cover slips 2 cm² and 0.13 thickness at a density of 25 x10³ cells per well for 72 hours after treated by 5 ng of PMA to be macrophage-like cells as a mature cells. We investigate whether the importance of MD2 and TLR-4 to

interact with HMGB1 when treated by rough EH100 and smooth O55:B5 lipopolysaccharides. the cells washed and stained as the samples coverslips with isotype control, mouse IgG1 as primary antibody with Alexa Fluor 488 and mouse IgG2 as primary antibody with Alexa Fluor 555 secondary antibodies, visualised by using green 488 nm and red 555 nm wavelength lasers to measure non-specific antibody binding. Blue colour shows 4', 6-diamidino-2-phenylindole (DAPI). DAPI stained cell's nuclei. Red and Green shows merged image. Co-localisation of TLR4 with HMGB1 also Co-localisation of MD2 with HMGB1 on the cell-surface of THP-1 cells is shown in treated cells.

To clarify the results as the LPS incubation time, when the TLR-4 and MD2 antibodies were blocked in specific samples separately and together. The cells stimulated with rough LPS EH100 and smooth LPS O55:B5 for 30, 60, and 120 minutes. The differentiated THP-1 cells as a macrophage-like cells represent a similar level of TNF- α except the samples in 60 min stimulated with rough LPS EH100 and smooth LPS O55:B5 shows significant increasing than the cells stimulated with rough LPS EH100, and the results increased highly significant in 120 min stimulation with LPSs, refer to the degregation happened to amount of TLR-4 and MD2 added at the beginning of the experiments, or there is another signalling pathway managed after this time to increase the TNF- α level.

The cells stimulated with rough LPS EH100 and smooth LPS O55:B5 for four hours in presence and absence of Myeloid Differentiation 2 (MD2) and PARP inhibitor (PJ34). The first four samples shows nothing secreted of TNF- α , because of no stimulation with (LPS), but the differentiated THP-1 cells as a macrophage-like cells present a high level of receptors around the cell surface and high amount of cytokines released, because of the amount of antibodies was decreased and the LPS still active

in the same concentration, but non differentiated THP-1 cells graphs represents a different levels specially the samples effected by EH100.

The other cytokine have been investigated is IL-1 β , at the same conditions of differentiated and non-differentiated THP-1 cells samples in presence and absence of Myeloid Differentiation 2 (MD2) and PARP inhibitor (PJ34). The cells stimulated with rough LPS EH100 and smooth LPS O55:B5 for two hours the first four samples shows nothing secreted of IL-1 β , because of no stimulation with (LPS), but the differentiated THP-1 cells as a macrophage-like cells present a high level of receptors around the cell surface and high amount of cytokines released, also because of the amount of antibodies was decreased and the LPS still active in the same concentration, but non-differentiated THP-1 cells graphs represents a different significant levels of IL-1 β specially the samples effected by EH100 and O55:B5.

Chapter 7 General Discussion

7 General Discussion

A range of techniques such as 2-D gel proteomics, Flow cytometry, ELISA, and Confocal laser Microscopy were used to investigate the effect of LPS on the model cell line THP-1. This cell line offers a unique model system to examine the properties of cells under *in vitro* treatment. The cells belong to a myelomonocytic lineage derived from a patient suffering from Leukaemia. The cells resemble the properties of monocytes/macrophages and thus are useful to gather first line information. The monocytes cells (non-differentiated) were induced to differentiate by incubating the cells with 5 ng/ml PMA. This dose of LPS is known as the highest as present in human pathogenic component present in Gram-negative bacteria. In addition, 10 µg/ml rough LPS (EH100) and 10 µg/ml smooth LPS (O55:B5) were employed to investigate in the presence or absence of TLR-4 and MD2 and presence of (HMGB1). The PARP inhibitor PJ34 was also used in order to show whether inhibiting PARP has any effect on the properties of THP-1.

The differentiated THP-1 cells as macrophage-like cells display a high level of receptors and show an increase in the expression and levels of cytokines released. These include TNF- α . Co-localisation between TLR4 and HMGB1 also MD2 and HMGB1 was also observed suggesting these associations have a functional role, which is consistent with Maxwell et al., (2015) studies.

The effectiveness of smooth LPS (O55:B5) is clearly significant in most of the triplicate results in all techniques refer this to the chemotype of the smooth LPS which contains the first level of the sugar chain, so it has the high efficiency as the rough LPS, and concentration that was used is 10 µg/ml. The importance of MD2, TLR4 with HMGB1 to interact with different LPS chemotypes, which represents how is LPS

effects the reaction of the THP-1 cells in the immune level by the CD14 and TLR-4 in the flow cytometry results, and the expression by CD14 in differentiated and non-differentiated THP-1 cells. High amount of the mCD14 and sCD14 receptors on the surface and around the cells, especially on differentiated THP-1 cells because they were macrophage-like cells and less effect on the non-differentiated THP-1 cells were observed. .

MD2 is the main co-receptor to TLR-4; the results were clearly significant when MD2 antibody was blocked suggesting the importance of the complex receptors TLR-4 and MD2. The twelve conditions of 2-D gels were analysed by loaded in Prognosis Same Spot software, exposed a massive number of polypeptides expressed with presence and absence of MD2 and PARP inhibitor (PJ34), all done when THP-1 cells stimulated by rough (EH100) and smooth (055:B5) LPS for 24 hours. Some spots were not present in samples stimulated with smooth (055:B5) even treated by PJ-34 for 30 minutes in specific samples as approved with Selleckchem, (2014) which indicate that the smooth LPS is more effective than the rough LPS. Also, found that PJ-34 PARP inhibitor imparts a protective effect, allowing sustained cell survival after LPS was targeted. Further study of the polypeptide proteins found to be differentially expressed is now necessary in order to establish their role in sepsis and to assess the role of PJ-34 in cell survival during LPS-induced toxemia.

The most exciting results, which represent by the confocal laser scanning microscopy, one of the scientific technique can demonstrate high-resolution cells images in two dimensions and three dimensions. Nikon A1si confocal microscope was used. Co-localisation of fluorescent signals from two different proteins CD14 with TLR-4, TLR-4 with MD2, MD2 with HMGB1, and TLR-4 with HMGB1, the indicator of

their association and potential interaction, by showing yellow areas around the cell surfaces as the overlap between dual colour fluorescence images from green and red channels as cited by Cao et al., (2018). The co-localisation can be measured by Pearson correlation coefficient, one of the most common co-localisation measurement methods. It has a range of -1 to $+1$. Where 1 is a total positive linear correlation, 0 is no linear correlation, and -1 is a total negative linear correlation.

We found that the samples, which were treated with Rough LPS (EH100) show a high co-localisation between CD14 and TLR-4 but less when, treated with smooth LPS. In other experiments, the smooth LPS (O55:B5) work as a motivator to the interaction between TLR-4 and HMGB-1 while the absence of MD2, which translated scientifically that it found another pathway to co-localise together. However in the presence of MD2 and treated with Rough LPS (EH100) the co-localization was increased. On the other hand, co-localisation between HMGB-1 and MD2 were shown slightly weak in this study, which approved that the relation between both proteins occurred infrequently refer to signalling pathway as Obara et al., (2013) stated this results.

The ELISA test support the observations in this study. The differentiated cells as a macrophage-like cells has high level of receptors that's show an increasing of the expression and the level of cytokines released such as TNF- α and IL-1 β , help to show a valuable images of co-localisation between CD14 and TLR4 and help to get a hundreds of proteins spots in the 2D gels. The effectiveness of rough LPS (EH100) and smooth LPS (O55:B5) shows different results, EH100 is more effective as a rough LPS than (O55:B5) the smooth LPS. The importance of the MD2 with CD14 and TLR4, to be interact with different LPS chemotype.

The future plan proposed as part of this study to follow the intracellular pathway of the effect of LPS in all chemotype produced and available to use, to explore the effect of rough LPS on each component such as (Ra, Rb, Rc, Rd and Re) and the smooth LPS with different level of sugar chain on the same model of cell line (THP-1) and PBMC.

8 References

Reference

- Abbas Abul K., Lichtman, A. H. and Pillai, S. (2014) *Cellular and Molecular Immunology*. In Elsevier. Chapter 15, Chapter 21.
- Aderem, A. and Ulevitch, R. J. (2000) 'Toll-like receptors in the induction of the innate immune response.', *Nature*, 406(6797), pp. 782–7. doi: 10.1038/35021228.
- Adler, J. and Parmryd, I. (2010) 'Quantifying colocalization by correlation: The Pearson correlation coefficient is superior to the Mander's overlap coefficient', *Cytometry Part A*, 77(8), pp. 733–742. doi: 10.1002/cyto.a.20896.
- Agita, A. and Alsagaff, M. T. (2017) 'Inflammation, Immunity, and Hypertension', *Acta medica Indonesiana*. doi: 10.1161/HYPERTENSIONAHA.110.163576.
- Annane, D., Bellissant, E. and Cavaillon, J.-M. (2005) 'Septic shock.', *Lancet*, 365(9453), pp. 63–78. doi: 10.1016/S0140-6736(04)17667-8.
- Anwar, M. A. and Choi, S. (2014) 'Gram-negative marine bacteria: Structural features of lipopolysaccharides and their relevance for economically important diseases', *Marine Drugs*. doi: 10.3390/md12052485.
- Bolte, S. and Cordelières, F. P. (2006) 'A guided tour into subcellular colocalisation analysis in light microscopy', *Journal of Microscopy*, 224(3), pp. 13–232. doi: 10.1111/j.1365-2818.2006.01706.x.
- Cao, C. *et al.* (2018) 'Toll-like receptor 4 deficiency increases resistance in sepsis-induced immune dysfunction', *International Immunopharmacology*. doi: 10.1016/j.intimp.2017.11.006.
- Caroff, M. and Karibian, D. (2003) 'Structure of bacterial lipopolysaccharides', *Carbohydrate Research*, pp. 2431–2447. doi: 10.1016/j.carres.2003.07.010.
- Cecconi, M. *et al.* (2018) 'Sepsis and septic shock', *The Lancet*. doi: 10.1016/S0140-6736(18)30696-2.

- Chen, G. (2004) 'Bacterial endotoxin stimulates macrophages to release HMGB1 partly through CD14- and TNF-dependent mechanisms', *Journal of Leukocyte Biology*, 76(5), pp. 994–1001. doi: 10.1189/jlb.0404242.
- Crotzer, V. L. and Blum, J. S. (2010) 'Autophagy and adaptive immunity', *Immunology*, pp. 9–17. doi: 10.1111/j.1365-2567.2010.03321.x.
- Cytokine Frontiers* (2014) *Cytokine Frontiers*. doi: 10.1007/978-4-431-54442-5.
- Dantzer, R. (2004) 'Cytokine-induced sickness behaviour: A neuroimmune response to activation of innate immunity', *European Journal of Pharmacology*. doi: 10.1016/j.ejphar.2004.07.040.
- Geyer, P. E. *et al.* (2016) 'Plasma Proteome Profiling to Assess Human Health and Disease', *Cell Systems*. doi: 10.1016/j.cels.2016.02.015.
- Harris, H. E., Andersson, U. and Pisetsky, D. S. (2012) 'HMGB1: A multifunctional alarmin driving autoimmune and inflammatory disease', *Nature Reviews Rheumatology*, pp. 195–202. doi: 10.1038/nrrheum.2011.222.
- Hosakote, Y. M. *et al.* (2016) 'Respiratory Syncytial Virus Infection Triggers Epithelial HMGB1 Release as a Damage-Associated Molecular Pattern Promoting a Monocytic Inflammatory Response', *Journal of Virology*. doi: 10.1128/jvi.01279-16.
- Huang, S. H. *et al.* (2008) 'PJ34, an inhibitor of PARP-1, suppresses cell growth and enhances the suppressive effects of cisplatin in liver cancer cells', *Oncology Reports*. doi: 10.3892/or_00000043.
- Janetzki, S. and Britten, C. M. (2012) 'The impact of harmonization on ELISPOT assay performance', *Methods in Molecular Biology*. doi: 10.1007/978-1-61779-325-7_2.
- Jonkman, J., Brown, C. M. and Cole, R. W. (2014) 'Quantitative confocal microscopy: Beyond a pretty picture', *Methods in Cell Biology*. Academic Press, 123, pp. 113–134. doi: 10.1016/B978-0-12-420138-5.00007-0.
- Kitchens, R. (2000) 'Role of CD14 in cellular recognition of bacterial lipopolysaccharides', *Chemical Immunology and Allergy*, 74, pp. 61–82.

- Kolodziejczyk, A. A. *et al.* (2015) 'The Technology and Biology of Single-Cell RNA Sequencing', *Molecular Cell*. doi: 10.1016/j.molcel.2015.04.005.
- Lachmanovich, E. *et al.* (2003) 'Co-localization analysis of complex formation among membrane proteins by computerized fluorescence microscopy: Application to immunofluorescence co-patching studies', *Journal of Microscopy*, 212(2), pp. 122–131. doi: 10.1046/j.1365-2818.2003.01239.x.
- Laganowsky, A. *et al.* (2014) 'Membrane proteins bind lipids selectively to modulate their structure and function', *Nature*. doi: 10.1038/nature13419.
- LaRock, C. N. *et al.* (2016) 'IL-1b is an innate immune sensor of microbial proteolysis', *Science Immunology*. doi: 10.1126/sciimmunol.aah3539.
- Lemcke, H. *et al.* (2013) 'Neuronal differentiation requires a biphasic modulation of gap junctional intercellular communication caused by dynamic changes of connexin43 expression', *European Journal of Neuroscience*. doi: 10.1111/ejn.12219.
- Leonard, F. *et al.* (2017) 'Thioaptamer targeted discoidal microparticles increase self immunity and reduce Mycobacterium tuberculosis burden in mice', *Journal of Controlled Release*. Elsevier, 266, pp. 238–247. doi: 10.1016/J.JCONREL.2017.09.038.
- Lu, Y. C., Yeh, W. C. and Ohashi, P. S. (2008) 'LPS/TLR4 signal transduction pathway', *Cytokine*. doi: 10.1016/j.cyto.2008.01.006.
- Manders, E. M. M. (1997) 'Chromatic shift in multicolour confocal microscopy', *Journal of Microscopy*, 185(3), pp. 321–328. doi: 10.1046/j.1365-2818.1997.d01-625.x.
- Masters, S. L. *et al.* (2009) '*Horror Autoinflammaticus*: The Molecular Pathophysiology of Autoinflammatory Disease', *Annual Review of Immunology*, 27(1), pp. 621–668. doi: 10.1146/annurev.immunol.25.022106.141627.
- Maxwell, L. J. *et al.* (2015) 'TNF-alpha inhibitors for ankylosing spondylitis', *Cochrane Database of Systematic Reviews*. doi: 10.1002/14651858.CD005468.pub2.
- McCluskey, A. G. *et al.* (2012) 'Inhibition of poly(ADP-ribose) polymerase enhances

the toxicity of 131I-metaiodobenzylguanidine/topotecan combination therapy to cells and xenografts that express the noradrenaline transporter', *Journal of Nuclear Medicine*. doi: 10.2967/jnumed.111.095943.

McMaster, W. G. *et al.* (2015) 'Inflammation, Immunity, and Hypertensive End-Organ Damage', *Circulation Research*. doi: 10.1161/CIRCRESAHA.116.303697.

Medzhitov, R. and Janeway, C. a (1997) 'Innate immunity: impact on the adaptive immune response Ruslan Medzhitov and Charles A Janeway Jr', *Current Opinion in Immunology*, 9(1), pp. 4–9.

Microscopy, V. *et al.* (2003) 'Co-localization analysis of complex formation among membrane proteins by computerized uorescence microscopy: application to immuno uorescence co-patching studies', *Journal of Microscopy*.

Mukherjee, S., Karmakar, S. and Babu, S. P. S. (2016) 'TLR2 and TLR4 mediated host immune responses in major infectious diseases: A review', *Brazilian Journal of Infectious Diseases*. doi: 10.1016/j.bjid.2015.10.011.

Murdock, J. L. and Núñez, G. (2016) 'TLR4: The Winding Road to the Discovery of the LPS Receptor', *The Journal of Immunology*. doi: 10.4049/jimmunol.1601400.

NCBI (2017) *IL-1 beta*. Available at:

<https://www.ncbi.nlm.nih.gov/gene?Db=gene&Cmd=ShowDetailView&TermToSearch=3553>.

Obara, B. *et al.* (2013) 'A novel method for quantified, superresolved, three-dimensional colocalisation of isotropic, fluorescent particles', *Histochemistry and Cell Biology*. doi: 10.1007/s00418-012-1068-3.

Oliver, F. J. *et al.* (1999) 'Resistance to endotoxic shock as a consequence of defective NF- κ B activation in poly (ADP-ribose) polymerase-1 deficient mice', *EMBO Journal*, 18(16), pp. 4446–4454. doi: 10.1093/emboj/18.16.4446.

Ong, S. E. and Mann, M. (2005) 'Mass Spectrometry–Based Proteomics Turns Quantitative', *Nature Chemical Biology*. doi: 10.1038/nchembio736.

Park, J. S. *et al.* (2004) 'Involvement of Toll-like Receptors 2 and 4 in Cellular

Activation by High Mobility Group Box 1 Protein', *Journal of Biological Chemistry*, 279(9), pp. 7370–7377. doi: 10.1074/jbc.M306793200.

Parkin, J. and Cohen, B. (2001) 'An overview of the immune system', *Lancet*, pp. 1777–1789. doi: 10.1016/S0140-6736(00)04904-7.

Peri, F. and Piazza, M. (2012) 'Therapeutic targeting of innate immunity with Toll-like receptor 4 (TLR4) antagonists', *Biotechnology Advances*. doi: 10.1016/j.biotechadv.2011.05.014.

Poggi, M. *et al.* (2013) 'Palmitoylation of TNF alpha is involved in the regulation of TNF receptor 1 signalling', *Biochimica et Biophysica Acta - Molecular Cell Research*, 1833(3), pp. 602–612. doi: 10.1016/j.bbamcr.2012.11.009.

Rachal Pugh, C. *et al.* (2001) 'The immune system and memory consolidation: A role for the cytokine IL-1 β ', *Neuroscience and Biobehavioral Reviews*, pp. 29–41. doi: 10.1016/S0149-7634(00)00048-8.

Ren, K. and Torres, R. (2009) 'Role of interleukin-1beta during pain and inflammation', *Brain Research Reviews*, pp. 57–64. doi: 10.1016/j.brainresrev.2008.12.020.

Rizk, A. *et al.* (2014) 'Segmentation and quantification of subcellular structures in fluorescence microscopy images using Squassh', *Nature Protocols*, 9(3), pp. 586–596. doi: 10.1038/nprot.2014.037.

Rock, F. L. *et al.* (1998) 'A family of human receptors structurally related to Drosophila Toll', *Proceedings of the National Academy of Sciences*, 95(2), pp. 588–593. doi: 10.1073/pnas.95.2.588.

Rogowska-Wrzesinska, A. *et al.* (2013) '2D gels still have a niche in proteomics', *Journal of Proteomics*. doi: 10.1016/j.jprot.2013.01.010.

Scaffidi, P., Misteli, T. and Bianchi, M. E. (2002) 'Release of chromatin protein HMGB1 by necrotic cells triggers inflammation', *Nature*, 418(6894), pp. 191–195. doi: 10.1038/nature00858.

Scalia, M. *et al.* (2013) 'PARP-1 inhibitors DPQ and PJ-34 negatively modulate

proinflammatory commitment of human glioblastoma cells', *Neurochemical Research*. doi: 10.1007/s11064-012-0887-x.

Schumann, R. *et al.* (1990) 'Structure and function of lipopolysaccharide binding protein', *Science*, 249(4975), pp. 1429–1431. doi: 10.1126/science.2402637.

Sedger, L. M. and McDermott, M. F. (2014) 'TNF and TNF-receptors: From mediators of cell death and inflammation to therapeutic giants - past, present and future', *Cytokine and Growth Factor Reviews*. doi: 10.1016/j.cytogfr.2014.07.016.

Selleckchem (2014) 'Inhibitors of Signaling Pathways', *Catalogue*.

Setoguchi, M. *et al.* (1989) 'Mouse and human CD14 (myeloid cell-specific leucine-rich glycoprotein) primary structure deduced from cDNA clones', *BBA - Gene Structure and Expression*, 1008(2), pp. 213–222. doi: 10.1016/0167-4781(80)90012-3.

Shibutani, S. T. *et al.* (2015) 'Autophagy and autophagy-related proteins in the immune system', *Nature Immunology*. doi: 10.1038/ni.3273.

Shimazu, R. *et al.* (1999) 'MD-2, a molecule that confers lipopolysaccharide responsiveness on toll-like receptor 4', *Journal of Experimental Medicine*. doi: 10.1084/jem.189.11.1777.

Shiu, J. and Gaspari, A. A. (2017) 'Toll-like receptors', in *Clinical and Basic Immunodermatology: Second Edition*. doi: 10.1007/978-3-319-29785-9_2.

Singh, B. P. Chauhan, R. S. and Singhal, L. k. (2003) 'No TitleToll like receptors and their role in innate immunity', *J. curr. Sci.*, 85(8), pp. 1156–1164.

Solomon, M. A. (2017) 'Determination of the subcellular distribution of liposomes using confocal microscopy', in *Methods in Molecular Biology*. doi: 10.1007/978-1-4939-6591-5_10.

Stasi, A. *et al.* (2017) 'Emerging role of Lipopolysaccharide binding protein in sepsis-induced acute kidney injury', *Nephrology Dialysis Transplantation*. doi: 10.1093/ndt/gfw250.

Steimle, A., Autenrieth, I. B. and Frick, J. S. (2016) 'Structure and function: Lipid A modifications in commensals and pathogens', *International Journal of Medical Microbiology*. doi: 10.1016/j.ijmm.2016.03.001.

Szabo, C. (2002) 'PARP as a Drug Target for the Therapy of Diabetic Cardiovascular Dysfunction.', *Drug news & perspectives*, 15(4), pp. 197–205. doi: 10.1358/dnp.2002.15.4.840052.

Tapping, R., T. P. (2000) 'Soluble CD14-mediated cellular responses to lipopolysaccharide', *Chemical Immunology and Allergy*, 74, pp. 108–21.

Thorsell, A. G. *et al.* (2017) 'Structural Basis for Potency and Promiscuity in Poly(ADP-ribose) Polymerase (PARP) and Tankyrase Inhibitors', *Journal of Medicinal Chemistry*. doi: 10.1021/acs.jmedchem.6b00990.

Tribbick, G. (2002) 'Multipin peptide libraries for antibody and receptor epitope screening and characterization', *Journal of Immunological Methods*. doi: 10.1016/S0022-1759(02)00138-2.

Tsung, A. *et al.* (2005) 'The nuclear factor HMGB1 mediates hepatic injury after murine liver ischemia-reperfusion', *The Journal of Experimental Medicine*, 201(7), pp. 1135–1143. doi: 10.1084/jem.20042614.

Wang, X. and Quinn, P. J. (2010) 'Lipopolysaccharide: Biosynthetic pathway and structure modification', *Progress in Lipid Research*, pp. 97–107. doi: 10.1016/j.plipres.2009.06.002.

Wilkinson, S. G. (1996) 'Bacterial lipopolysaccharides - Themes and variations', *Progress in Lipid Research*, 35(3), pp. 283–343. doi: 10.1016/S0163-7827(96)00004-5.

Yan, W. and Chen, S. S. (2005) 'Mass spectrometry-based quantitative proteomic profiling', *Brief Funct Genomic Proteomic*, 4(1), pp. 27–38.

Zhang, W. *et al.* (2015) 'Necrotic myocardial cells release Damage-Associated Molecular Patterns that provoke fibroblast activation in vitro and trigger myocardial inflammation and fibrosis in vivo', *Journal of the American Heart Association*. doi:

10.1161/JAHA.115.001993.

Zhou, Y. *et al.* (2014) 'Inflammation in intracerebral hemorrhage: From mechanisms to clinical translation', *Progress in Neurobiology*. doi: 10.1016/j.pneurobio.2013.11.003.

Zhu, S., Welsch, R. E. and Matsudaira, P. T. (2016) 'A method to quantify co-localization in biological images', in *Proceedings of the Annual International Conference of the IEEE Engineering in Medicine and Biology Society, EMBS*. doi: 10.1109/EMBC.2016.7591577.

Appendix

Appendix

A.1 Chemicals

Accutase Sigma-Aldrich Dorset, UK

Acrylamide 30% BIO-RAD, UK

Agarose Invitrogen, UK

CHAPS AppliChem, Darmstadt Chloroform Merck, Darmstadt

Ethanol Fisher Scientific, UK

Lipopolysaccharide Sigma-Aldrich, Steinheim

Magnesium sulfate Sigma-Aldrich, Steinheim

Methanol Fisher Scientific, UK

Paraformaldehyde Sigma, Germany

Potassium chloride Fisher Scientific, UK

Sodium acetate Roth, Karlsruhe

Sodium carbonate Roth, Karlsruhe

Sodium chloride Sigma-Aldrich, Steinheim

Sodium citrate Merck, Darmstadt

Sodium dodecyl sulfate Merck, Darmstadt

Sodium periodate Sigma-Aldrich, Steinheim

Sodium thiosulfate Roth, Karlsruhe

Sodium thiosulfate Roth, Karlsruhe

Tris (hydroxymethyl) aminomethane Roth, Karlsruhe

Triton X-100 Sigma-Aldrich, UK

Trypan blue Gibco, USA

Tween-20 Roth, Karlsruhe

Urea Merck, Darmstadt

Experiments done with unsatisfied results and not preferred to include them in the main body of the thesis because they are first experiments and the results not satisfied.

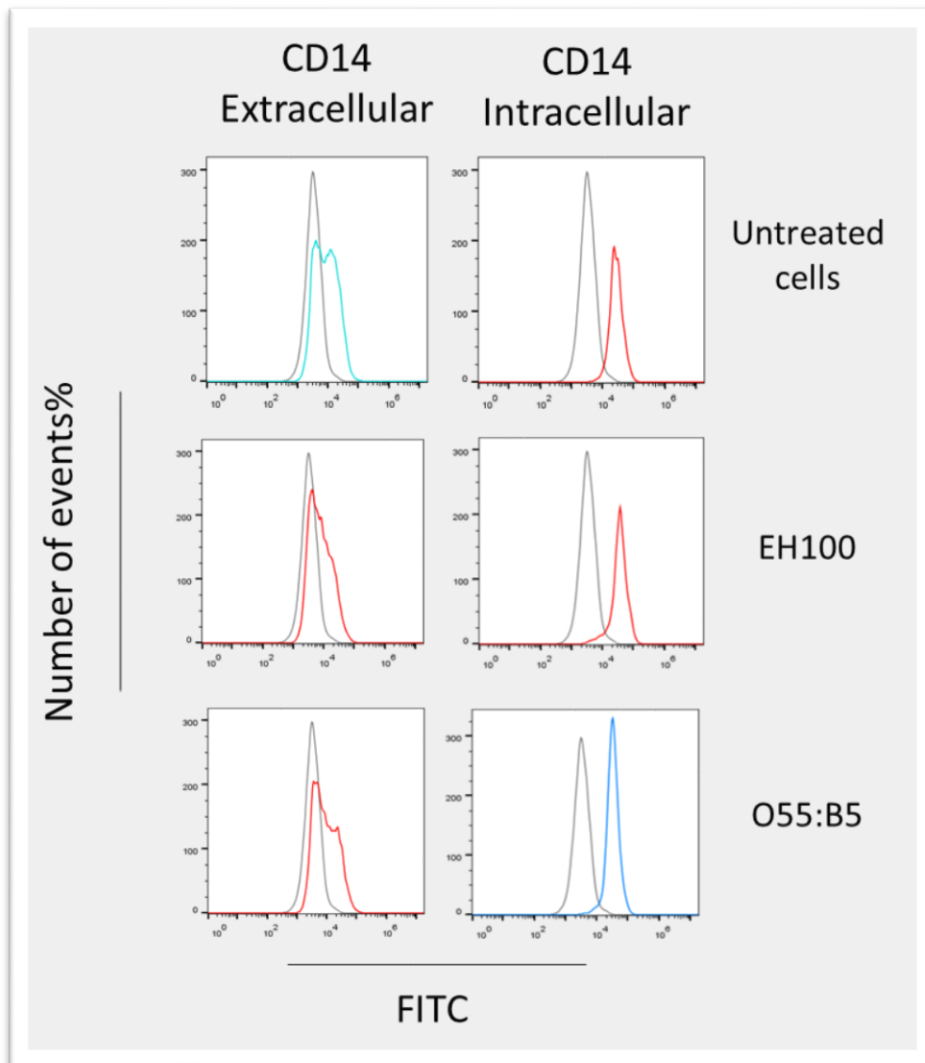


Figure A1: Extracellular and intracellular expression of CD14 in THP-1 cell lines.

The cells were incubated in RPMI 1640 supplemented with 10 % of FCS with EH100 and O55:B5 or with media alone. The grey histogram represents the cells treated only with secondary antibody as negative control. However, the red histogram represents cell surface or intracellular expression of CD14 in non-treated THP-1 cells or rough chemotype of LPS (EH100) and smooth serotype of LPS (O55:B5).

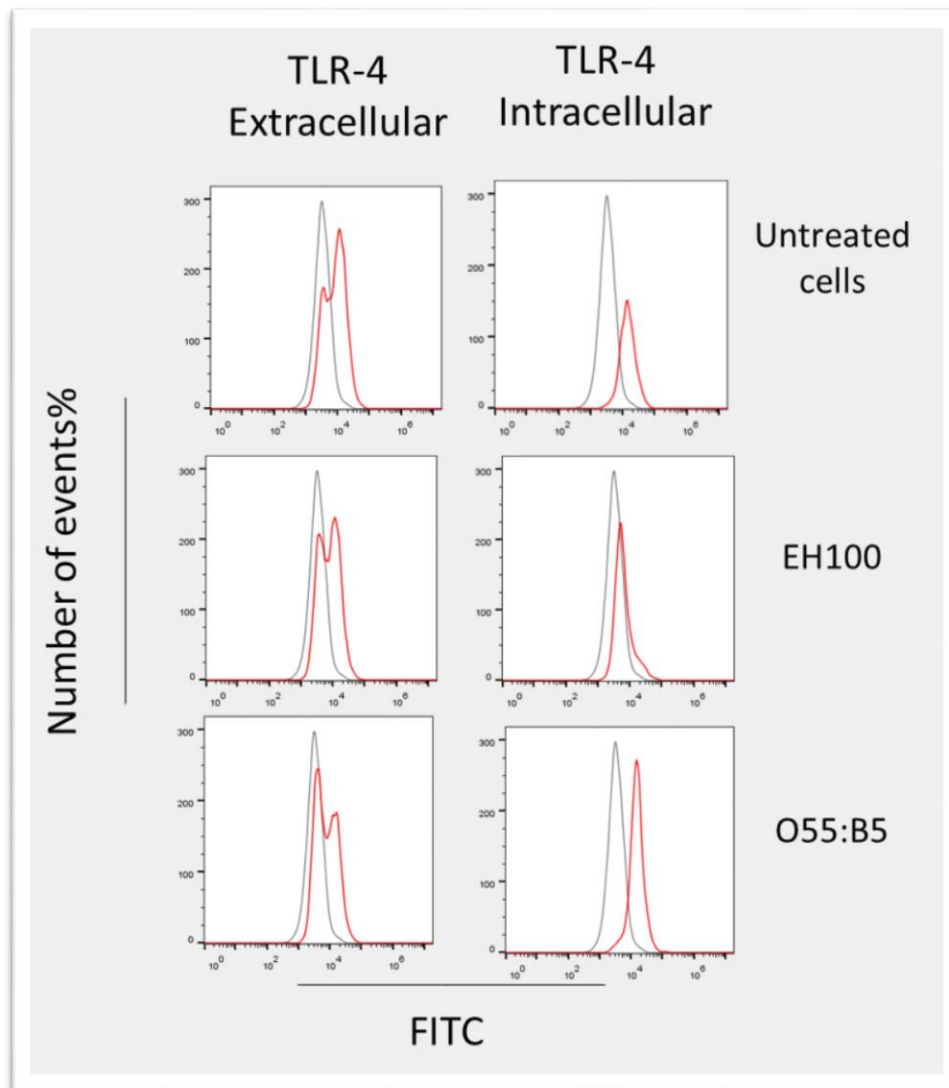


Figure A2 : Extracellular and intracellular expression of TLR-4 in THP-1 cell lines.

The cells were incubated in RPMI supplemented with 10 % of FCS with EH100 and O55:B5 or with media alone. The grey histogram represents the cells treated only with secondary antibody as negative control. However, the red histogram represents cell surface or intracellular expression of TLR-4 in non-treated THP-1 cells or rough chemotype of LPS (EH100) and smooth serotype of LPS (O55:B5).

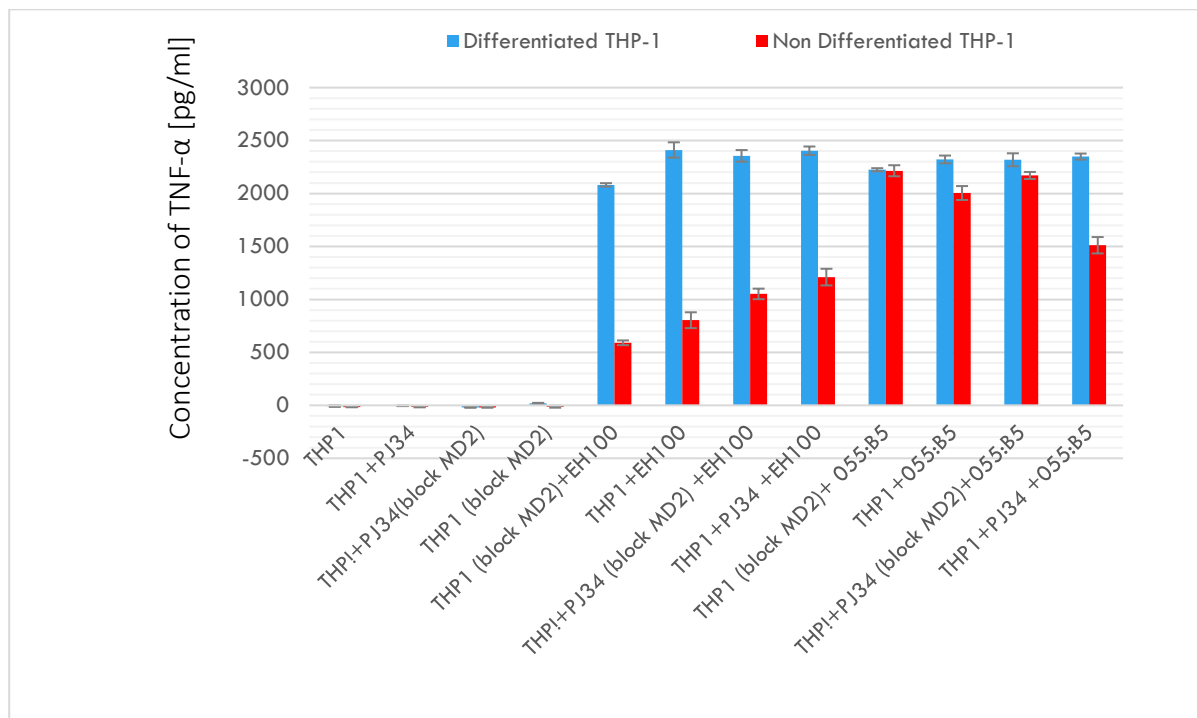


Figure A3 : TNF- α Detection by (ELISA)

The graph represents TNF- α level in the tissue culture supernatant of differentiated and non- differentiated THP-1 cells, with rough and smooth LPS stimulation.

Those results were for the first experiments of flowcytometry and ELISA techniques which have some mistakes because the test is sensitive and it need to follow the supervisor and manufacturer instructions.

Some results such as control samples represents values below zero, refer to contamination or calculated mistakes done during the washing steps or standard curve equation.

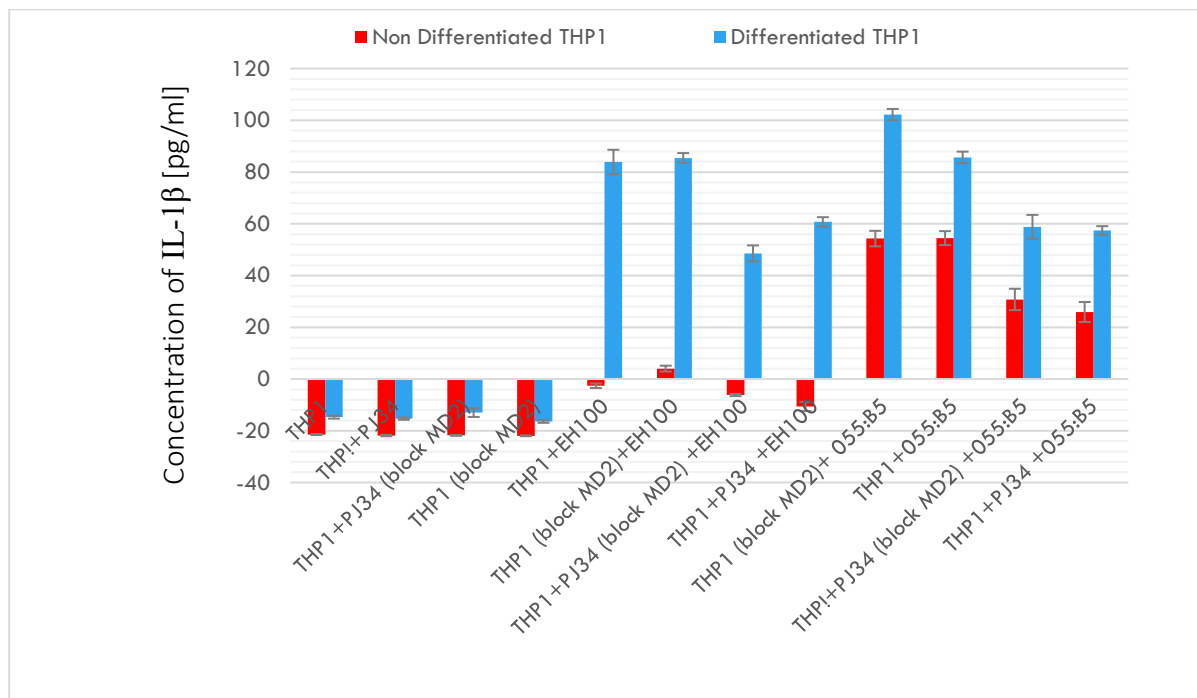


Figure A4 : IL-1 β Detection by (ELISA)

The graph represents IL-1 β level in the tissue culture supernatant of differentiated and non-differentiated THP-1 cells with rough and smooth LPS stimulation.

Those results were for the first experiments of flowcytometry and ELISA techniques which have some mistakes because the test is sensitive and it need to follow the supervisor and manufacturer instructions.

Some results such as control samples represents values below zero, refer to contamination or calculated mistakes done during the washing steps or standard curve equation.



Figure A5: ELISA micro plate reader

FLUOstar Omega
The software: Omega



Figure A6 : NIKON Confocal laser microscope A1

The software: NIS Elements



Figure A7 : Accuri C6 Flowcytometer
Software: BD Accuri 6

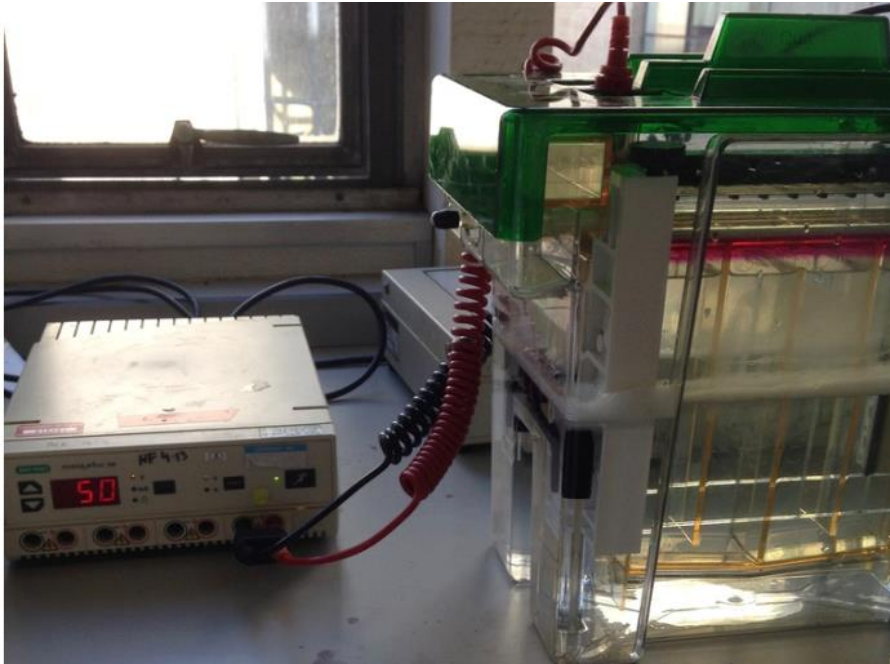
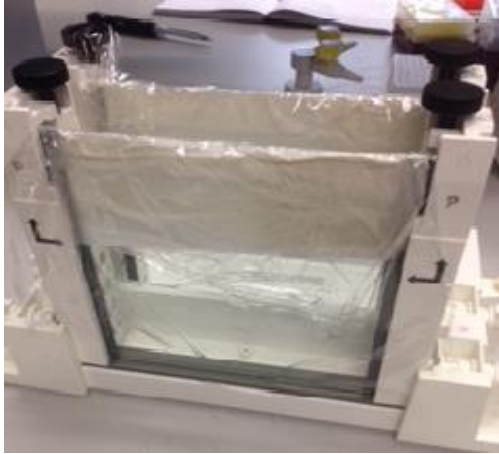
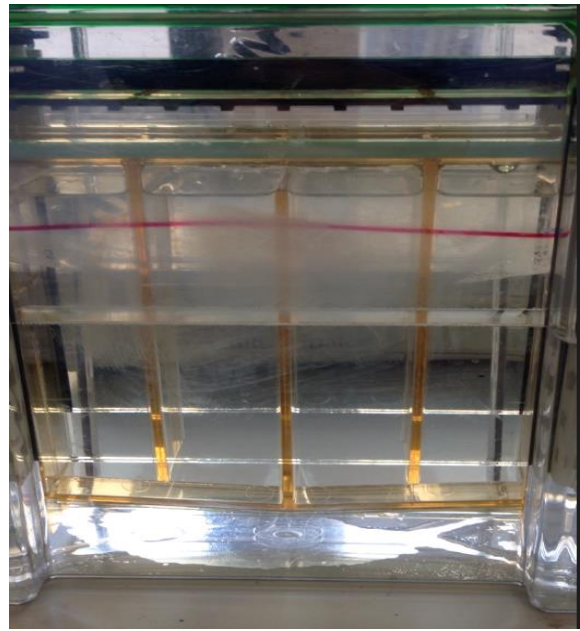


Figure A8 BIO-RAD PROTEAN II System

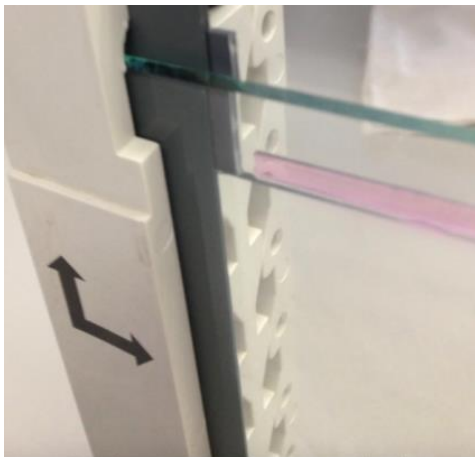
This instrument and accessories used for SDS-PAGE Gel preparation. (Khayat, B. 2015, BS, Essex University)



(a)



(b)



(c)

Figure A9 : 2D gel preparation for electrophoresis system

- a) Cover the double glass gel holder by wet paper and cling film to save it for several days.
- b) The IPG strips placed on the top of the gel and leave 5 mm space for protein marker.
- c) The electrophoresis tank has the gel and run the system and the red bromophenol dye shown moving. **(Khayyat, B. 2015, BS, Essex University)**



Figure A 10 : Place the gels on the glass of Epson image scanner III.

One of the important step, remove the air bubbles by smooth glass stick, before scanning. (Khayyat, B. 2015, BS, Essex University)

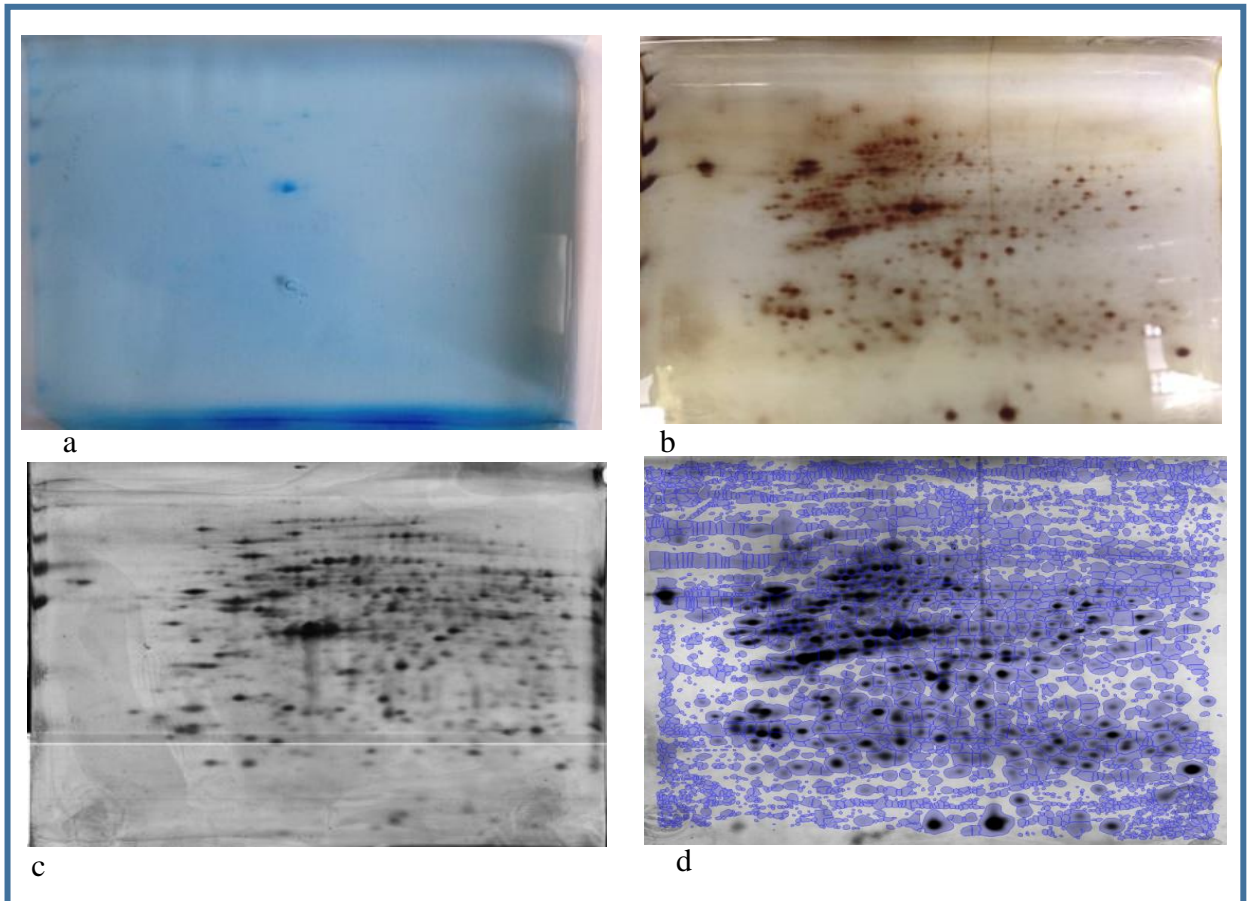


Figure A11 : Sensitivity of instant blue and silver nitrate for the detection of 2-D gel separated polypeptide spots.

The images above explain the best stain to use to highlight the protein spots in the gels, by using silver nitrate stain. (a) the gel stained by Instant blue, (b) the gel stained by silver nitrate, (c) the image taken by Sam spot software, (d) the software analyse the represent a huge amount of countable spots by using Epson image scanner III to analyse.



Figure A12 : General Electric Healthcare Bio-sciences AB. Etan IPG Phor3
Used for first dimension gel electrophoresis



(a)



(b)

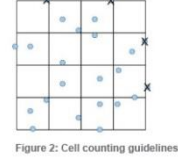
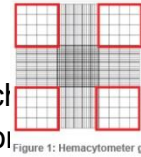
Figure A 13 : Kinds of pipettes used in this study.

(a) Ovation Vista Lab ergonomic automated pipettes single and multi-channels form 20-1000 μl , (b) Mechanical Single channel pipettes form 0.1-20 μl .

Date / /20

Bioimaging experiments protocol form

- 1- Take the cell culture flask from the incubator
- 2- Check the cells condition and quality by microscope
- 3- Count the cells in the flask by using hemacytometer
- 4- 140 cells the total in 2 grids use the following equation

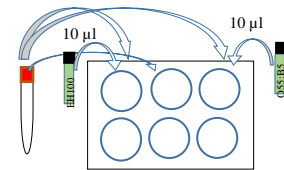


$$X / 4 \times 10^4 = Y \quad \text{cells in 1 ml}$$

- 5- if I need in my experiment 10 ml with 25,000 cells/ 1 ml I'll go with the following equation

$$\frac{25,000 \times 10}{Y} = Z \quad \text{ml cells}$$

- 6- Add Z + ml of the RPMI media to complete the size to ml Using 10 ml tube.



- 7- Bring 2 X 6 wells culture plates.
- 8- Put the cells in 15ml tube
- 9- Add 0.5 µl/ml of Phorbol 12-myristate 13-acetate (PMA) to differentiate the cells cover slips.

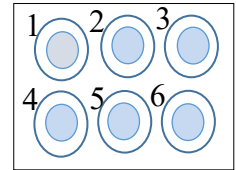
- 10- Apply 1 ml of the suspension media in the 6 well plates.

- 11- Incubate for 72h.

- 12- Refresh the media by vacuum the wells carefully.

- 13- After 24 hours.

- 14- We will block the MD2 by adding 1 µl anti MD2 to mentioned wells.



- 15- We will use the PJ34 to mentioned wells.

- 16- Incubate for 30 min.

- 17- The LPS chemotypes that we were used are (Rough [EH100] and Smooth [O55:B5])

- 18- Add 10 µl/ml of (R and S) LPS in every noticed well.

- 19- Incubate in 37°C for 2 hours.

- 20- Wash by adding 1ml of (PBS) 0.1% to the wall of each well. (X 2)

- 21- Apply the Fixing solution 50-100 µl in each well.

- 22- Add 1ml of blocking buffer 2% to the wall of each well for 1hour.

- 23- Centrifuge then remove the supernatant.

- 24- Add the 1 µl primary antibodies as mentions on the following table. Irrelevant, CD14 and TLR4

- 25- Be sure that the CD14 tagged with mouse anti human or goat anti mouse (red)

- 26- Incubate at 8°C for 1h.

- 27- Wash by adding 1ml of (PBS) 0.1% to the wall of each well. (X 2)

- 28- Add the primary TLR-4 to the CD14 WELLS.

29-Incubate at 8C for 1h.

30-Wash by adding 1ml of (PBS) 0.1% to the wall of each well. (X 1)

31-Add the secondary antibody (FITC)

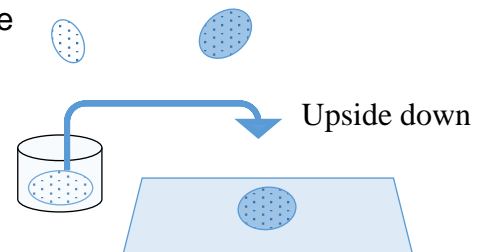
32-Wait for 1h

33-Wash by 1ml (PBS 0.1%) to the wall of each well.

34-Remove the cover slips to the numeric slides upside-down using mounting media hard set to save the cells in a good condition

35- Avoid the light source because its effect the fluorescent tagged the cells.

36-Slides are ready.



To avoid any complicated better to separate the tubes to add the cells as the following:

	Cells	PJ34	Anti MD2	EH100	O55:B5	irrelevant Ab	CD14	GREEN	TLR-4	RED
1	X									
2	X					X		X		X
3	X						X	X	X	X
4	X	X					X	X	X	X
5	X		X 1 μ l				X	X	X	X
6	X	X	X 1 μ l				X	X	X	X
7	X	X	X 1 μ l	X			X	X	X	X
8	X		X 1 μ l	X			X	X	X	X
9	X	X		X			X	X	X	X
10	X			X			X	X	X	X
11	X	X	X 1 μ l		X		X	X	X	X
12	X		X 1 μ l		X		X	X	X	X
13	X	X			X		X	X	X	X
14	X				X		X	X	X	X

- Note:**1- Prepare Phosphate Buffered Saline (PBS)0.1% [How to prepare it ?] = 1gm/1000ml
2- Prepare the blocking buffer 2%. 2g of Bovine Serum Albumin (BSA) to 100 ml of PBS. 2gm/100ml
3-Prepare the LPS that we want to treat the cells with (we divide it in advance to 10 μ l) and add 990 μ l media, to be 10 μ g/ml.

Comments:

Date / /20

Flow-Cytometer Protocol Form In tissue culture lab

- 1- Take the cell culture flask from the incubator
- 2- Check the cells condition and quality under the microscope.
- 3- Count the cells in the flask by using hemocytometer chamber.
- 4- X cells the total in 4 grids use the following equation
$$\frac{X}{4} \times 10^4 = Y$$
 cells in 1 ml

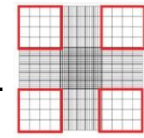


Figure 1: Hemacytometer grid

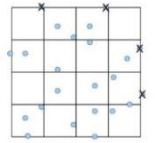
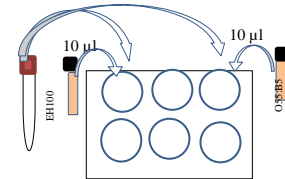


Figure 2: Cell counting guidelines

- 5- If we need in our experiment 15 ml with 200,000 cells in each sample, we'll follow with the following equation:

$$\frac{\text{---} \times 10^5 \times \text{---} \text{ ml} = Z}{\text{---} Y} \text{ ml cells}$$



- 6- Add Z + ml of the RPMI media to complete the size to 20 ml Using 45 ml tube.
- 7-
- 8- Bring 12 wells culture plates
- 9- Apply 500 µl of the suspension media in the 12 wells.
- 10- Prepare the LPS that we want to treat the cells with (we divide it in advance to 10µl) and add 990 µl media, to be
- 11- we will block the MD2, by adding anti MD2 before stimulate the cells by LPS by adding 1.5 µl/ml to mentioned wells we want to treat with LPS, incubate for 30 min. we used 1500 µl cells so I add 4.5µl MD2 from : ----> : incubation
- 12- To know the effect of adding PARP inhibitor PJ34 to specific samples, incubate for 30 min. we add 10 µl pj34/1 ml so we have 1.5ml so we add 15 µl PJ34 from : ----> : incubation
- 13- The LPS chemotypes that we are use is (Rough [EH100] and Smooth [O55:B5])
- 14- Add 10 µl/ml of every LPS samples in every noticed well. So we add 15 µl of each LPS
- 15- Incubate in 37°C for 2 hours. : ----> :
- 16- Prepare Phosphate Buffered Saline (PBS) [How to prepare it?]

Note: prepare the Blocking buffer by applying 140 mg of Bovine Serum Albumin (BSA) to 140 ml of PBS.

In the bench laboratory

- 17- Prepare 25 tubes by serial number from 1-25
- 18- Apply 1000 µl of the cells with media to every tube.

To avoid any complicated better to separate the tubes to add the cells as the following:

	Cells	PJ34	Anti MD2	EH100	O55:B5	CD14	irrelevant Ab mouse IgG1	FITC
1	X							X
2	X						X	X
3	X					X		X
4	X	X				X		X
5	X		X			X		X
6	X	X	X			X		X
7	X	X	X	X		X		X
8	X	X		X		X		X
9	X			X		X		X
10	X	X	X		X	X		X
11	X	X			X	X		X
12	X		X		X	X		X
13	X				X	X		X

	Cells	PJ34	Anti MD2	EH100	O55:B5	TLR-4	irrelevant Ab mouse IgG2	FITC
14	X						X	X
15	X					X		X
16	X	X				X		X
17	X		X			X		X
18	X	X	X			X		X
19	X	X	X	X		X		X
20	X	X		X		X		X
21	X			X		X		X
22	X	X	X		X	X		X
23	X	X			X	X		X
24	X		X		X	X		X
25					X	X		X

- 19-Centrifuge them for 1:30 min at 1200 rpm.
 - 20-Save the supernatant for ELIZA TEST.
 - 21-add 1000 µl of PBS to each Eppendorf tube 2 times to wash and remove all the media around the cells
 - 22-Add 50-100µl fixing solution (9ml PBS + 1ml formaldehyde and sodium hydroxide) to the pellets to all eppendorff tubes while they are on ice bath for 30min.
 - 23-Add 1000 µl blocking buffer.
 - 24-centrifuge the tubes 1:30 min at 1200 rpm, then discard the supernatant
 - 25-Be careful when discard the supernatant do avoid lose the cells.
 - 26-Apply the primary (monoclonal) antibody 2 µl (CD14, TLR4) to each sample in group.
 - 27-Vortex them,
 - 28- Overnight cold incubation is recommended also.
 - 29-Then Add 1000 µl blocking buffer then centrifuge the tubes (1:30 min) 90 sec at 1200 rpm, then discard the supernatant, to remove all extra anti-bodies on the cell surfaces.
 - 30-add the secondary antibody(fluorescence tagged)
 - 31-Keep the tubes at 4°C for 30min
 - 32-Then Add 1000 µl blocking buffer then centrifuge the tubes 1:30 min at 1200 rpm, then discard the supernatant, to remove all extra anti-bodies on the cell surfaces.
 - 33-Then Add 400 µl BPS.
 - 34-The samples ready to test by the (Flowcytometer).
- Note:** Don't forget to book the time 2 days in advance.

Note: we should take the file from accuri 6 then open it on flowJO application to analyze it.

Note:To enlarge the amount of the anti-body [every sample need 2 µl so we should add 8 µl blocking buffer to use 10 µl of the anti-body].
 Each Primary Ab 22 µl+88 µl bb
 secondary 50 µl +200 µl bb



